Imperial College of Science, Technology and Medicine

Energy Packet Network with Negligible Service Time: A Modelling and Performance Analysis Approach to Wireless Sensor Networks

by

Yasin Murat Kadioglu

June 4, 2018

A thesis submitted in fulfilment of requirements for the degree of

Doctor of Philosophy of The Imperial College of Science, Technology and Medicine

Supervised by Prof. Erol Gelenbe

Intelligent Systems and Networks Group

Department of Electrical and Electronic Engineering

Imperial College of Science, Technology and Medicine

Abstract

Autonomous self-organising systems have gained much attention to manage complex tasks without any human interaction. Similarly, simpler systems are also required for the applications of Internet of Things, such as smart home services, wearables, smart cities and connected health systems. These simpler systems provide autonomous stand-alone devices for remote sensing, processing and transmission of information. However, such devices may not have a reliable connections to power mains or may not be convenient for regular battery replacements. Therefore, local energy capturing from ambient intermittent sources such as vibration, electromagnetic waves, heat or light through harvesting could be of great interest for such devices.

This thesis researches mathematical modelling and performance analysis of such autonomous digital devices operating with energy harvesting from intermittent sources. The approach used in this research is based on the Energy Packet Network paradigm where the arrivals of data and energy at devices are considered as discrete random processes. The devices operate by consuming harvested energy in a discrete manner in order to process, store and transmit data (wired or wireless) in a negligible time interval, such that the operation or the workload of the devices is also modelled as a discrete random process.

Probability models based on random walks and Markov chains are investigated in this study to predict effective rates at which such devices operate well for different energy consumption scenarios, and to obtain closed-form formulas for stationary probability distributions and to make further analysis on the other quantities of interest. Consequently, a "product form solution" of a cascade network of N nodes where state transitions involve simultaneous state changes in multiple nodes, due to data packets that flow through several nodes consuming energy packets is proposed. A modelling approach to evaluate the effect of several battery attacks on such devices is studied. Finally, optimum placement of wireless nodes into a region where there is a spatial continuous distribution of energy and data traffic is presented for different transmission schemes, and optimisation objectives.

Acknowledgements

First and foremost, I would like to express my sincere appreciation to my supervisor, Professor Erol Gelenbe, for his invaluable academic guidance and supervision without which this work would not have been possible. It has been a real privilege and an honour for me to share his tremendous scientific knowledge and deep insights. His wisdom and guidance have taught me well beyond the academic world, and significantly contributed to shaping my future life. I also wish to thank my examiners, Professor Helena Szczerbicka and Professor William Knottenbelt, for their thorough reading and helpful comments, and all my colleagues at the Intelligent Systems and Networks Group for the warm and friendly atmosphere they created.

Nobody has been more helpful, understanding and careful to me in the pursuit of this thesis than Elif Tugce Ceran, Burak Simsek, Yasin Tumtas, Osman Gucluturk and Cihad Oge. Their precious guidance, reassuring companionship, and recuperative comments help me to carry out this tough process. I appreciate every single moment that we share together.

I would also like to acknowledge some precious friends: Baha, Ridvan, Ahmet Kerim, Alper, Tugrul, Ulvi, Melih, Elif Parlak, Elif Genc, Ipek, Anil, Oner, Eymen, Mustafa, Beril, Nilufer, Cuneyt, Seza, Emre, Ece, Can, Zaid, Mihajlo, Omar, Murteza, Lan, Paul, Basil, Olivier, Yonghua, Huibo, Olumide, Yuanchen, Kiarash, Patrick, Joan and Sarah for their invaluable support throughout my postgraduate studies. I must also thank Cagatay, Asim Burak, Mucahit, Istemihan, Serdar, Burak, Miray, Deniz, Tugce Erkilic, Tugce Tasci, Ozlem, Gamze, Sedef, Emre, Fatih for always being there for me since my childhood.

Last but not least, I wish to thank my beloved parents, Sedat Kadioglu and Adalet Kadioglu for their endless love and support. Father, thank you for all that you have done and sacrificed to provide me with the best possible life and education despite all the poverty and hardship we suffered from. I have always been proud of having such a father like you, and I hope the person I became and my academic success make you feel the same. Mother, no words can describe how grateful I am to you. I have always known living apart is unbearably sorrowful for you, but your compassion has allowed me to pursue my academic dream. You are the source of every achievement and happiness in my entire life. Enormous thanks to you for holding on to life and not leaving me alone.

Copyright

Declaration of Originality

I, Yasin Murat Kadioglu, declare that this thesis titled, 'Energy Packet Network with Negligible Service Time: A Modelling and Performance Analysis Approach to Wireless Sensor Networks' and the work presented in it are my own. I confirm that:

- This work was done wholly or mainly while in candidature for a research degree at Imperial College of Science, Technology and Medicine.
- Where I have consulted the published work of others, this is always clearly attributed.
- Where I have quoted from the work of others, the source is always given. With the exception of such quotations, this thesis is entirely my own work.
- I have acknowledged all main sources of help.
- Where the thesis is based on work done by myself jointly with others, I have made clear exactly what was done by others and what I have contributed myself.

Yasin Murat Kadioglu

Date: 04/06/2018

Contents

List of Figures

Abbreviations

IoT	Internet of Things
RFID	Radio Frequency Identification Devices
WSN	Wireless Sensor Network
EPN	Energy Packet Network
DP	Data Packet
EP	Energy Packet
EN	Energy Network
FCFS	First Come First Serve
LCFS	Last Come First Serve
SIRO	Service In Random Order
DTMC	Discrete Time Markov Chain
CTMC	Continuous Time Markov Chain
EHWSN	Energy Harvesting Wireless Sensor Node
QoS	Quality of Service
PFS	The Product Form Solution
EDF	Energy Data Flow
BPSK	Binary Phase Shift Keying

Dedicated to my beloved parents, Adalet & Sedat Kadioglu...

Chapter 1

Introduction

1.1 Introduction

The energy needs of devices in the wired backbone of mobile networks, the Internet, and the Internet of Things (IoT) [1–3], together with the need to power them even when they are not plugged into permanent electricity sources [4], and the inconvenience of changing batteries, has motivated research into systems which are powered with harvested energy sources [5, 6]. Efficient analytical techniques to analyse the behaviour of multiple interconnected units, provided each unit operates with unlimited energy, have been available since the mid-sixties thanks to Jackson's Theorem [7] and its generalisations [8]. However, a new and major challenge is to model systems with intermittent sources of energy, since energy flow is random and not always available. Consequently, the processing of jobs or forwarding of data packets (DPs) is interrupted when energy is not available at a unit. While DPs and jobs are represented as discrete entities, it is convenient to model the flow of energy in terms of discrete energy packets (EPs). Moreover, a battery can be viewed as a "buffer or queue" of EPs.

As harvested energy is generally intermittent, the Quality of Service (QoS) of systems that operate with harvested energy will critically depend on the releationship between the amount of energy that is harvested and stored in each device, and the workload or traffic that the device processes or forwards [9, 10]. In these systems, mathematical performance models are needed to combine the effect of both the arrival of energy (EPs) and the flow of DPs when the service units are network nodes, or jobs when the service units are computer servers. Advancement in such analytical models has always progressed in steps. Moreover, the general results in Jackson's Theorem [7] were preceded by an earlier solution technique that only considered tandem queuing systems [11]. These earlier models did not consider the issue of intermittent energy sources. Models in which

work is conducted in parallel sub-systems and then synchronised [12–14], as well as Petri Nets with synchronisation constraints [15] have also been considered. In [16] a PFS was proven for the flow of work and of control signals in a system of interconnected service units. This was subsequently extended to Petri Nets in [17]. In addition, these techniques have been used to model Gene Regulatory Networks [18] and Cloud Computing systems [19].

The term IoT was first proposed in late-nineties by indicating its usage for determining the characteristics of objects. In the first stage of IoT, people believed IoT only stood on the radio frequency identification devices (RFID) to understand the interconnection of objects [20]. Later, Melon Steven stated that IoT devices with RFID bring computers autonomous ability of identification, tracking, monitoring and managing [21]. However, the first formal concept of IoT was only mentioned in 2005 by International Telecommunication Union. According to the Union, the IoT concept demonstrates the interaction of people and things by communicating over short-distance mobile transceivers. Although there is still no standard definition of IoT, it can be considered as a focus on object identification and interconnection, as well as the communication network [22].

Over the last few years much work has been carried out into IoT [23–25]. This is because it is a promising paradigm of wired and wireless communication systems, as well as the identification, tracking and monitoring technologies, and smart distributed network devices. IoT has been providing significant contributions to develop self-organised or autonomic industrial systems and applications by improving radio frequency identification and wireless sensor network (WSN) [1]. The core concept of IoT is that there are objects with identifying, sensing, processing, and networking potentials that allows them to communicate with other devices and services over the internet for providing convenient objectives [2]. The usage of IoT has increased and has spread over several areas including [26]: environmental monitoring (water quality, atmospheric and soil conditions) [27, 28], infrastructure management (monitoring bridges, railway tracks) [24], manufacturing (real time optimisation, dynamic response) [29, 30], agriculture (monitoring temperature, humidity, rainfall) [31], energy management (changing lighting conditions) [32], medical and healthcare (wearable heart monitors) [33], and transportation (smart traffic control) [34]. According to CISCO, there will be 50 billion IoT devices all over the world by 2020, compared to 0.5 billion in 2003 [3].

WSNs are one of the fundamental parts of IoT and play several crucial roles for many IoT applications. WSNs are composed of several wireless sensor nodes cooperatively communicating with each other by passing data through the network. Thus, a user can monitor physical or environmental information via internet or mobile communication systems. WSNs exhibit some differences from traditional networks with respect to source

and design needs. Source needs can be considered as communication range, amount of energy, limited storages or buffers and limited processing mechanism for each node. Design needs basically depend on the application and the environment within which the WSN is used. The environment is also one of the most important parameters in order to determine the size of WSNs and the network topology. For example, while a few nodes could be enough for indoor environments, much more nodes could be needed for outdoor environments to provide reliable operation.

There exist several different types of sensors that are able to sense a wide variety of conditions such as noise level, humidity, temperature, pressure and movement [35]. This variety results in several application areas for WSNs such as military applications (intelligence, surveillance, targeting) [36], environmental applications (animal monitoring, forest fire detection, flood detection) [37–39], health applications (drug administrations) [40, 41], and home applications (home automation) [42]. Moreover, it results in an increasing number of wireless sensing points all over the world. This was 4 million in 2011 and would be expected as more than 25 million in 2018 [43]. In addition, the WSN market is expected to increase from 0.5 billion in 2012 to 2 billion in 2022 [44].

However, finite battery capacity is a major limitation for WSNs, as sensor nodes are only able to operate as long as there is an unfinished battery [45, 46]. Battery depletion results in interruption of applications and requires the regular change of batteries or connection to the mains. The use of large batteries for longer life-times can be seen as a solution; however, it will lead to increased size, weight and cost. In order to achieve a longer operation life-time of battery-powered sensors, some techniques have been developed such as energy-aware MAC protocols [47], power aware storage protocols [48], and adaptive sensing rate [49]. These techniques try to optimise energy usage or maximise life-time of a sensor, but they are not a complete solution for finite operation time. Energy harvesting is an alternative technique that avoids inconvenient and costly services and addresses the problem of finite operation time of a sensor node [5, 6, 50].

Energy harvesting is the process by which energy is harvested from the environment in the form of solar, thermal, light and magnetic energy. These energies are then converted into electrical energy. Therefore, energy harvesting is of particular interest for several applications [51–54], especially remote sensing and security applications [53–55]. Some recent systems have also been designed to harvest energy from vibrations where the vibrations themselves are being sensed [56]. A roadside sensing equipment counts passing vehicles, and transmits this information by using the harvested energy from the vibrations created by the vehicles. Moreover, when energy is harvested for exploitation and scheduled for transmission both the harvesting process and the communication needs must be taken into account [57]. Thus, recent research has addressed new technologies

based on energy harvesting and on optimisation of harvesting nodes, with the aim of minimising energy consumption for a given communication task [58, 59].

Several authors have proposed dynamic control policies for traffic flow in networks with energy harvesting nodes. For example, a mobile base station with a single rechargeable battery has been considered and dynamic policies were studied to share power from the same battery in discrete successive time slots to distinct channels having different traffic rates [60]. Here the power allocation affects the actual transmitted data rate and the overall performance metric to be optimised was found to be a function of these effective data rates. In other work, a control theoretic approach was developed to manage the flow of packets [61]. This was based on the full knowledge of the topology of a multihop wireless network that does not vary over time. It also assumed that the traffic flows were not affected by interference or noise. In addition, this work assumed that the amount of energy and data packets in all nodes was known, that the arrival processes of data and energy were time-independent (stationary), and that the information about the backlog of data in a node could be shared with nodes upstream by creating back pressure. In reference [62], discrete time control models were introduced to maximise the amount of data sensed and forwarded by a sensor network. The used energy was harvested and dynamically allocated to forwarding the data, assuming that the data-forwarding rate depends on the allocated power.

The link between system workload and energy has been recently analysed in [63]. The availability of harvested and stored energy was represented *together with* the queue length of DPs in a single node ($N = 1$) system. In this approach energy was discretised in EPs, so that the amount of energy stored in the node's battery was represented as a discrete number of EPs. Thus in the "Energy Packet Network" (EPN) abstraction, a battery is seen as a "buffer queue" for energy, and a network node is represented by two coupled queues, one for DPs and the other for EPs. This approach has been generalised to systems with finite DP and EP storage [64], while a two hop ($N = 2$) feed-forward network has been also studied in [65]. An additional approach uses the theory of G-Networks to model the flow of energy as the enabler of service being rendered at a Cloud server [19].

The throughput and power consumption in EPs/sec for a single node with transmission errors due to noise and interference, was derived when multiple EPs were needed to transmit a single DP has been considered in [66]. Other work [67, 68] addressed a single node that consumes energy both for data transmission and for processing jobs.

1.2 Thesis Contribution

In this thesis, a model for energy harvesting sensor nodes where a DP can be successfully transmitted by consuming EPs has been assumed. The number of EPs consumed for DP transmission may vary according to transmission power level needed for successful communication. We first assume data transmission occurs via a perfect transmitter. In a perfect transmitter, there is no energy waste for node electronics and energy is only consumed to transmit DPs. The state transition behaviour of the models can be represented by random walks and Markov chains. Closed-form formulas for the stationary probability distributions and the other quantities of interests have been obtained. Next, more realistic scenarios assuming the occurrence of DP transmissions via an imperfect transmitter have been investigated. In an imperfect transmitter, energy is consumed not only for DP transmission but also for node electronics such as DP receiving, processing and storing in the node. Different solution methods using linear algebra techniques have been proposed to obtain stationary probability distributions and other quantities. Alternatively, a network model of sensors has been studied, where a cascade connection of nodes with intermittent sources exhibiting a product form solution under certain assumptions. Also, simple battery depletion attacks have been modelled and their effects on the sensor life-time analysed. Finally, optimum sensor placement in an area where a spatial continuous distribution of energy and density of data traffic has been studied.

1.2.1 Summary of Contributions

The contributions of this thesis can be divided into the following categories: (a) packet transmission via perfect and imperfect transmitter, (b) product-form solution of cascade networks, (c) energy life-time of wireless nodes under energy depletion attacks, and (d) optimum sensor placement in an area where spatial data and energy arrivals exist.

(a) **Packet transmission via perfect and imperfect transmitter**

- (i) Developed a mathematical model for both perfect and imperfect transmitters where data transmission occurs by consuming either a single EP or several (K) EPs. Thus, four different system models have been considered for analysis.
- (ii) Obtained the closed-form solutions for stationary probability distributions by using random walk and Markov chain representations. In addition, companion matrices and linear algebra techniques were used to reduce the computational complexities.
- (iii) Studied data and energy losses due to finite capacity buffers, optimum energy efficiency of the transmission and the system stability.

(iv) Extended the mathematical model to unlimited capacity data and energy buffers with transmission errors and re-obtained closed-form solutions for steady state distributions.

(v) Analysed the transmission errors and linked them to the system parameters for negligible data and energy leakage rates.

(vi) Modelled to noise and interference, and presented several numerical examples to understand effects of system parameters on transmission.

(b) **Product-form solution of cascade networks**

(i) Developed a mathematical model for a cascaded N-hop model assuming data transmission can occur with a single EP via perfect transmitter.

(ii) Obtained a product-form solution for the network under some equilibrium conditions on energy and data flows, and the other system transitions rates.

(iii) Studied the backlog of DPs and showed some numerical examples illustrating the effects of network size and the other parameters on the average waiting time.

(c) **Energy life-time of wireless nodes under energy depletion attacks**

(i) Developed a model to evaluate the effect of energy attacks on battery life-time of nodes for both renewable and replaceable batteries.

(ii) Studied two different types of simple energy attacks: the attacks considered are those that force the node to transmit additional traffic, and those that create electromagnetic noise that induces errors and hence packet retransmissions.

(iii) Proposed a method to mitigate against attacks that imposes a forced loss on incoming traffic, so that the total arrival rate of data packets cannot exceed some value, which may be selected in order that the average energy life-time has a pre-specified life-time value.

(d) **Optimum sensor placement**

(i) Studied a model where sensor nodes can directly communicate with the base-station or cluster head, and optimum placement of sensors to provide full area coverage while minimising the backlog of DPs.

(ii) Studied a multi-hop communication model and optimum node placement to maximise the throughput.

1.3 Thesis Outline

This thesis is organised as follows. In Chapter 2, the background provides the basic information related to queuing theory and networks, and reviews work related to energy packet networks and energy networks. In Chapter 3, a model and study for a perfect transmitter is presented. In Chapter 4, the model is investigated for an imperfect transmitter and an alternative solution is provided. In Chapter 5, a network model in which several nodes are cascaded to each other is analysed and a product form solution obtained. In Chapter 6, energy depletion attacks have been modelled for wireless nodes and their effects on battery life-time are presented. In Chapter 7, optimum sensor placement, for single and multi-hop communication with different optimisation objectives are studied. Chapter 8 provides a summary of the results and points out some future research directions. In addition, Appendix A and Appendix B provides the proof of theorems stated in Chapter 5 and Chapter 7, respectively.

1.4 Publications

- E. Gelenbe and Y.-M. Kadioglu. "Energy loss through standby and leakage in energy harvesting wireless sensors." In Computer Aided Modelling and Design of Communication Links and Networks (CAMAD), 2015 IEEE 20th International Workshop on, pp. 231-236. IEEE, 2015, [69].

- E. Gelenbe and Y.-M. Kadioglu. "Performance of an autonomous energy harvesting wireless sensor." In Information Sciences and Systems 2015, pp. 35-43. Springer, Cham, 2016, [70].

  - [69, 70] present a performance model for the energy harvesting wireless sensor nodes in which data and energy are collected as discrete packet forms. The harvested energy can be stored in a battery or a capacitor, and it is consumed for data transmission. Energy will leak from the energy storage in the standby mode. In addition, there will be energy overflows due to the finite capacity of the energy storage unit. Thus, these papers propose a mathematical model to analyse the performance of such systems in the presence of a random source of energy as well as a random source of data by using Markov chain representation. The equilibrium between random energy, random data and random energy leakage results in an interesting performance analysis of these small but ubiquitous systems as a whole. A discussion is also provided about an infinite capacity model which operates in the presence of transmission errors

due to channel noise and interference. The material from these papers appears in Section 3.2.

- Y.-M. Kadioglu and E. Gelenbe. "Packet transmission with K energy packets in an energy harvesting sensor." In Proceedings of the 2nd International Workshop on Energy-Aware Simulation, p. 1. ACM, 2016, [66].

  – [66] discusses a two-dimensional random walk for modelling a data transmission system with energy harvesting that represents a remotely operating wireless sensor node. If a wireless sensor node gathers enough energy, it transmits a DP by consuming at least $K > 1$ EPs. The stationary probability distribution of this model to compute the performance metrics for a wireless sensor node with energy harvesting is derived by generalising the previous results (for the case $K = 1$) that were obtained in [69, 70]. Then, the probability that a packet is correctly received by a receiver that operates in the presence of N identical wireless sensors, each operating at the power level K, is computed in the presence of noise and of interference. The material from this paper appears in Section 3.3.

- Y.-M. Kadioglu. "Energy consumption model for data processing and transmission in energy harvesting wireless sensors." In International Symposium on Computer and Information Sciences, pp. 117-125. Springer International Publishing, 2016, [67].

  – [67] studies an energy consumption model for data processing and transmission in energy harvesting wireless sensors with the Energy Network (EN) paradigm. A wireless sensor node consumes $K_e = 1$ EP for the node electronics (data sensing and processing), and $K_t = 1$ EP for the data transmission. The assumption of single EP consumptions results in a one-dimensional random walk modelling for the system. The stationary probability distributions are obtained as closed-form solutions, and the other quantities of interest are studied. The material from this paper appears in Section 4.2.

- Y.-M. Kadioglu and E. Gelenbe. "Wireless sensor with data and Energy Packets." 2017 IEEE International Conference on Communications Workshops (ICC Workshops), Paris, pp. 564-569. IEEE, 2017, [68].

  – [68] develops a mathematical model to determine the balance between the energy input and the data sensing in a wireless sensing node by considering generalised values of $K_e > 1$ EPs and $K_t > 1$ EPs. The node's energy and data flows are modelled by a two-dimensional random walk which represents the

backlog of the DPs and EPs. Then, the model is simplified by using companion matrices and matrix algebra techniques that allow us to obtain a closed-form solution for the stationary probability distribution. This leads us to compute important performance measures, including the energy consumption by the node, and its throughput. The model also evaluates the effect of ambient noise and the needs for data retransmissions, including for the case where M sensors operate in proximity and create interference for each other. The material from this paper appears in Section 4.3.

- Y.-M. Kadioglu. "Finite Capacity Energy Packet Networks." Probability in the Engineering and Informational Sciences: 1-28, 2017, [64].

  – [64] surveys the previous studies related to the Energy Packet Network and the Energy Network. The material from this paper appears in Chapter 3 and Chapter 4.

- O.Brun, Y.Yin, Y.-M. Kadioglu, E. Gelenbe. "Deep Learning with Dense Random Neural Networks for Detecting Attacks against IoT-connected Home Environments" In International Symposium on Computer and Information Sciences, Security Workshop. Springer International Publishing, 2018, [71].

  – [71] analyses the network attacks against IoT gateways and proposes a detection technique by using a dense random neural network. In this paper, the identification of the relevant metrics to detect the attacks and the explanation of how they can be computed from packet captures are presented. No material from this paper is used in this thesis.

- E. Gelenbe and Y.-M. Kadioglu. "Battery Attacks on Sensors" In International Symposium on Computer and Information Sciences, Security Workshop. Springer International Publishing, 2018, [72].

- E. Gelenbe and Y.-M. Kadioglu. "Energy Life-Time of Wireless Nodes with Network Attacks and Mitigation." 2018 IEEE International Conference on Communications Workshops (ICC Workshops), Kansas City, USA, IEEE, 2018, [73].

  – [72, 73] first briefly survey the types of attacks which aim at the nodes' energy provisioning systems. Then, these papers analyses the effect of such attacks on the energy lifetime of a wireless node with a renewable or a replaceable battery. In addition, a simple mitigation technique is proposed to provide a certain minimum life-time. This technique forces sensor nodes to drop a certain fraction of the traffic so as to offer a desired energy life-time to the node. The material from these papers appears in Chapter 6.

- Y.-M. Kadioglu and E. Gelenbe. "Product Form Solution to Cascade Networks with Intermittent Energy." In IEEE Systems Journal, 2018 (accepted), [74].

  – [74] develops a new product form solution for the joint probability distribution of energy availability and the job queue length for an N-node tandem system. Results obtained in this paper enable the diligent computation of all the performance metrics for such systems operating with intermittent energy. The material from this paper appears in Chapter 5.

- Y.-M. Kadioglu. "Tandem Networks with Intermittent Energy." In International Symposium on Computer and Information Sciences, Poznan, Poland. Springer International Publishing, 2018 (submitted), [75].

  – [75] investigates the generalised model of the tandem network studied in [74] by considering the external data arrivals for each unit in the cascaded network. A product form solution for the joint distribution is presented. The material from this paper appears in Section 7.5.

Chapter 2

Background

2.1 Introduction

This chapter explains brief but comprehensive background topics which provide a fundamental basis of theoretical aspects of this work. Thus, this chapter first presents the analytical frameworks of the basic queuing theory. Secondly, some queuing networks and the EPN paradigm that was proposed in some previous related works are reviewed. Finally, Markov Chain review is presented. This is used for modelling the state transitions and obtaining the stationary probability distributions of the states for subsequent chapters. The chapter is organized as follows: In Section 2.2 and Section 2.3, the basic theory of queuing systems and networks, and literature review on the EPN paradigm are examined along with the further assumptions related to this thesis. In Section 2.4, a review of the Markov Chain including its basics and properties, and mathematical extensions are presented. The chapter concludes in Section 2.5.

2.2 Basic Queuing Theory

Queuing theory is a part of applied mathematics that models and analyses the characteristics of waiting in the lines. In a basic queuing system, a customer arrives to be served, waits for the service, and leaves after being served. This section presents a brief explanation of the queuing theory formulation along with the its basics and applications.

2.2.1 Exponential and Poisson Probability Distributions

To understand the basic queuing theory, some knowledge about the exponential and Poisson probability distributions is needed.

The exponential distribution with parameter λ is given by:

$$f(t;\lambda) = \begin{cases} \lambda e^{-\lambda t} & t \geq 0 \\ 0 & t < 0 \end{cases} \tag{2.1}$$

Thus, if T is a random variable representing the inter-arrival times with the exponential distribution, then $P(T \leq t) = 1 - e^{-\lambda t}$.

Exponential distribution is used to model customer inter-arrival times and service times due to its specific properties. The first one is the fact that the exponential distribution has the memoryless property. This property implies that the time duration until the next arrival does not depend on how much time has already passed. As the activities of customers are independent of each other, choosing a memoryless distribution to model the customer arrivals makes sense. The other property of the exponential distribution is being strictly decreasing function of t. This suggests that the waiting time of the next arrival is more likely to be smaller after an arrival has occurred.

On the other hand, the Poisson distribution expresses the probability of a certain number of events (or arrivals) in a given time interval. The Poisson distribution with parameter λ is given by:

$$\frac{(\lambda t)^n e^{-\lambda t}}{n!}, \tag{2.2}$$

where n is the number of events in time interval t. If we set $n = 0$, it gives us $e^{-\lambda t}$. Conversely, if an event occurs during t (i.e, $n = 1$), then it gives us $1 - e^{-\lambda t}$. In fact, the results are equal to $P(T > t)$ and $P(T \leq t)$ from the exponential distribution.

In other words, let t_i be the time when i^{th} customer arrives, and T_i be the i^{th} inter-arrival time such that $T_i = t_{i+1} - t_i$ for i>0. If the customer arrivals are assumed to be Poisson process with a parameter λ, then it can be shown that T_i's has exponential distribution with the parameter λ. In addition, the exponentially distributed random variable T satisfies:

$$P(T > t + s | T > s) = P(T > t). \tag{2.3}$$

This result reflects the memoryless property of the exponential distribution, which is important for modelling inter-arrival times of customers.

Furthermore, it is assumed that the service times for different customers are exponentially distributed independent random variables with a parameter μ. The parameter μ can also be seen as the service rate of the queuing system. However, a customer sometimes requires several phases to be served. Therefore, modelling service times with the

exponential distribution does not always give the accurate results. Another probability distribution that can be considered to model service times is the Erlang probability distribution with a rate parameter R and a shape parameter k, and it is given by:

$$\frac{R(Rt)^{k-1}e^{-Rt}}{(k-1)!}, \tag{2.4}$$

where k can be thought of the number of different phases of the service.

2.2.2 Queuing Disciplines

One can easily think that when an arrival occurs in a queuing system, it is placed at the end of the line and waited until all the other customers ahead of it being served in the order they arrived. Although it is convenient to model a service discipline in this way, there are some other existing rules for choosing the next customer to serve. The most commonly used queue disciplines are:

- FCFS - First Come First Serve: Customer arrives earlier, leaves earlier
- LCFS - Last Come First Serve: Customer arrives later, leaves earlier
- SIRO - Service In Random Order: Customer leaves randomly
- Priority: Customer with the higher priority leaves earlier.

The waiting times of particular customers are significantly affected by the selection of a different queuing discipline: for example, no customer would want to arrive early at a queue with LCFS discipline.

2.2.3 Kendall-Lee Notation

In order to describe all of the characteristics of a queuing system, a simple notation (Kendall-Lee notation) can be used [76]. Let us denote a system by the following series of symbols:

$$A/B/m/K/n/D$$

where

- A: the distribution function of the inter-arrival times
- B: the distribution function of the service times

- m: number of servers working together
- K: capacity of the system, maximum number of customers allowed in the system
- n: capacity of the customer sources (i.e. customer population size)
- D: queuing disciplines

For instance, exponentially distributed random variables are denoted by M, indicating Markovian or memoryless. Furthermore, D stands for deterministic, G stands for general distribution, and E stands for the Erlang distribution. Hence, $M/M/1$ represents a single server queuing system with Poisson arrivals and exponentially distributed service time.

2.2.4 Little's Queuing Formula

It is helpful to have some knowledge about waiting times and number of customers in a queuing system to evaluate the behaviour of the system. Let N_q and N_s be the average number of customers waiting in the queue and being occupied in the service when the system has reached to steady-state, respectively. As a customer can only be either in the queue or in the service, the total average number of customer in the system is $N = N_q + N_s$.

In a similar way, let us define W_q and W_s, in steady-state, to be the average amount of time spent in the queue and in the service, respectively. Thus, the total average amount of time spent for a customer is $W = W_q + W_s$. Hence, Little's formula states the following [77]:

$$N_q = \lambda W_q, \tag{2.5}$$

$$N_s = \lambda W_s, \tag{2.6}$$

$$N = \lambda W, \tag{2.7}$$

where λ is the number of customers arriving at the queuing system per unit time.

2.2.5 M/M/1/∞/∞/FCFS Queuing System

An M/M/1/∞/∞/FCFS is one of the simplest queuing systems with a single server and infinite buffer capacity. Let λ and μ be the Poisson distributed customer arrival rate and the exponentially distributed service rate, respectively. After a long operating time, the queuing system might converge to a stable point. Thus, the stationary distributions of

the system are given by:

$$\pi_0 = 1 - \rho \tag{2.8}$$

$$\pi_n = \rho^n(1 - \rho) \tag{2.9}$$

where $\rho = \frac{\lambda}{\mu}$. In order to guarantee stability, the condition $\lambda < \mu$ (or $\rho < 1$) must be satisfied. In addition, some of the important metrics for this queuing system can be calculated as follows:

- **Utilization** is the fraction of time during which the server is operating or busy, and it is given by:

$$U = 1 - \rho_0. \tag{2.10}$$

- **Total average number of customers** in the queuing system is:

$$\bar{N} = E[N] = \sum_{n=0}^{\infty} n\pi^n = \frac{\rho}{1 - \rho}. \tag{2.11}$$

- **Total average waiting time** in the queuing system is by Little's theorem:

$$T = \frac{N}{\lambda} = \frac{1}{\lambda - \mu}. \tag{2.12}$$

2.3 Queuing Networks

A queuing network consists of several interconnected units such that when a customer is served in a queuing unit, it can either enter another queue or leave the network. Queuing networks can roughly be categorized into four groups:

- **Open network:** Customers arrive from outside, then they leave the network or enter another unit after being served.
- **Closed network:** Fixed number of customers is served by the network. There is no external customer arrivals at the units and no customer departures from the network.
- **Loss network:** Customers can arrive from outside if there is available space in the units' buffers. They can also depart after the service.
- **Mixed network:** Any combination of networks mentioned above.

2.3.1 Jackson Network

The traditional method for analysing interconnected service systems with N nodes or units (i.e. computer networks or distributed computer systems) where energy availability is unlimited at the nodes (i.e. all connected to a permanent source of electricity) is as a queueing network. This network includes Poisson external arrivals of packets to each node i with rate λ_i, and exponential service times with parameter μ_i. Moreover, the movement of data packets is represented by a Markov chain with transition probabilities $p_{ij},\ i,j = 1,\ ...\ N$, where p_{ij} is the probability that a packet that leaves node i then enters node j. Such a network is also characterised by the probability $d_i = 1 - \sum_j^N p_{ij}$ that a packet departs from the network after being served at node i. In this model, packets entering a node, are queued to wait for service and are served in First-In-First-Out order. This is known as "Jackson's Network" and is widely used as a simple and effective model for multi-hop backbone networks [7, 78]. The product form solution (PFS) of Jackson's Network states that the joint probability distribution of the N queue lengths of packets at the nodes in steady-state is rigorously expressed as the product (multiplication) of the probability distributions of each individual queue length. Moreover, the probability distribution of the queue length at node i depends only on the queue's total packet arrival rate Λ_i, and its service rate μ_i such that:

$$\pi_i(n) = \rho_i^n(1 - \rho_i) \tag{2.13}$$

where

$$\rho_i = \frac{\Lambda_i}{\mu_i}. \tag{2.14}$$

and

$$\Lambda_i = \lambda_i + \sum_{j=1}^{N} \Lambda_j p_{ji}, \tag{2.15}$$

In addition, the equilibrium state probability distribution for state $(n_1, n_2, \cdots, n_N)$ is given by:

$$\pi(n_1, n_2, \cdots, n_N) = \prod_{i=1}^{N} \pi_i(n_i) = \prod_{i=1}^{N} \rho_i^{n_i}(1 - \rho_i). \tag{2.16}$$

The wide-spread use of this model, and its generalisations to both BCMP networks [8, 79] and G-Networks [80] is due to the rigorous "product form solution" (PFS).

2.3.2 G-Networks

Neural networks was the initial inspiration behind the G-networks. In the random neural network model studied in [81], signals can be either positive or negative. The positive signals represent the excitatory spikes, while the negative signals represent the inhibitory spikes. The potential of a neuron increases by one when a positive spike arrives, and it decreases by one when a negative spike arrives only if the initial neuron potential is positive. Otherwise, when the neuron potential is zero, negative spike has no effect on the neuron's potential. A neuron can transmit both positive and negative signals when its potential is positive, and each transmission reduces the neuron potential by one. It was proved that this random neural network model has a PFS in steady-state.

G-Networks are extension of the random neural network model into the packet queuing networks [82]. A neuron can be seen as a node in the queuing network analogy. In addition, positive and negative spikes represent positive and negative customers. In a similar manner, positive and negative customers increase and decrease the queue length by one, respectively.

The simplest model of G-Networks studied an open network of N queuing nodes. In this network, i.i.d. exponentially distributed service times $(\mu_1, \mu_2, \cdots, \mu_N)$ and inter-arrival times were assumed for each node. In addition, there are two types of customer arrivals: external positive customer arrivals with a rate λ_i^+ and external negative customer arrivals with a rate λ_i^- to the i^{th} node. When a positive customer arrives at a node, it increases the queue size by one and waits to be served. On the other hand, when a negative customer arrives at a queue, it reduces the queue size by one and disappears. If the queue is empty, the negative customer will have no effect on the node and it will directly disappear. In addition, the probability that a positive customer leaves the node i and joins the node j as a positive customer is p_{ij}^+, and as a negative customer is p_{ij}^-. Furthermore, the probability that a customer leaves the network after being served in the node i is d_i. Thus, we can write the following:

$$\sum_{j=1}^{N} p_{ij}^+ + p_{ij}^- + d_i = 1. \tag{2.17}$$

Furthermore, the traffic equations are given by:

$$\Lambda_i^+ = \lambda_i^+ + \sum_{j=1}^{N} q_j \mu_j p_{ij}^+, \tag{2.18}$$

$$\Lambda_i^- = \lambda_i^- + \sum_{j=1}^{N} q_j \mu_j p_{ij}^-, \tag{2.19}$$

$$\tag{2.20}$$

where

$$q_i = \frac{\Lambda_i^+}{\mu_i + \Lambda_i^-}. \tag{2.21}$$

In steady-state, it was proved that [82] this network has a PFS such that:

$$\pi(n_1, n_2, \cdots, n_N) = \prod_{i=1}^{N} \pi_i(n_i) = \prod_{i=1}^{N} q_i^{n_i}(1 - q_i). \tag{2.22}$$

2.3.2.1 Energy Packet Network

The EPN developed by Gelenbe [83] is a queueing network approach based on G-networks theory [84–87] and has been used to model data processing or transmission network that can store and consume harvested energy as discrete units. The analogy that drives this approach is based on the fact that computer jobs and DPs are discrete entities that are queued and then processed in the system. However, Gelenbe proposed [88] that it is also possible to discretise the amount of energy used. He also suggested that electrical batteries or capacitors can also be viewed as storing discrete units of energy. A similar concept in which power is used in a discrete manner has been introduced and feasibility of the 'power packets' dispatching system at the physical layer hase been verified in [89, 90].

In EPNs, EPs and DPs can be considered as regular and negative customers, respectively. In addition, energy storage has a queue role in the system so that the EPNs can be studied as queueing networks. An EPN study in which the surges in energy demand on smart grids were suppressed has been previously presented in [91]. The grid contains both steady energy sources that meet the energy requirements in a grid most of the time and renewable energy sources that are mainly used when the energy demand exceeds a particular energy need. A similar model related to energy management for the cloud computing servers was studied in [92] where energy consumption centres can be considered as cloud computing centres. The general idea in [91, 92] is obtaining the steady state probabilities of the nodes in the EPN by using G-Network theory and adjusting the parameters

to satisfy energy needs of consumption or cloud computing centres. Additionally, there are several recent works on EPNs considering the design of optimal energy distribution architectures [93] and of optimal flows that maximize particular utility functions [94, 95].

2.3.2.1.1 Energy Network EPNs consider task service times such that both the consumption of energy and the processing or transmission of jobs or packets happens over some continuous time. A further paradigm, also introduced by Gelenbe [63, 96], has been motivated by energy harvesting wireless devices (i.e. IoT devices and wireless sensor networks) [58], [59] wherein processing or transmission times are very fast (and hence negligible), in comparison to the time it takes to acquire data (as in a sensor) and energy (as through harvesting). This type of model is called the 'Energy Network' (EN). Therefore, IoT devices and wireless sensor networks (WSN)s can be considered as a perfect application area for the EN paradigm.

2.4 Markov Chain: Review

This section presents the Markov chain review, which is one of the important theoretical background of this thesis. We will introduce some basics, properties and classifications related to Markov chain.

A Markov process is a stochastic process where the past of the process has no effect on the future if the current state is known. In other words, the present state contains all the information from past related to the future state. A Markov chain is basically a discrete valued Markov process where the discrete valued stands for finite or countable state space of the Markov chain.

For a discrete-time Markov chain (DTMC), both time and space are discrete which means that the states can only change by taking some discrete values only happening at one of specified discrete time incidents. On the other hand, for a continuous-time Markov chain (CTMC), the change of the states can happen at any time along a continuous interval. It is basically generalization of DTMC models where the transitions can happen at any time.

2.4.1 Basics

Definition 2.4.1. Assume X_n, $n = 0, 1, 2, ...$ is a discrete time stochastic process and S is a discrete state space where discrete means either finite or countably infinite space.

The Markov property:

$$P\{X_n = i_n | X_{n-1} = i_{n-1}, ..., X_0 = i_0\} = P\{X_n = i_n | X_{n-1} = i_{n-1}\}, \tag{2.23}$$

where $i_0, ..., i_n \in S$. Thus, the Markov property says the future depends on the past only trough the present, i.e., the memory of the past is lost in time by the process.

Definition 2.4.2. Any discrete process $X_n, n \geq 0$ that satisfies the Markov property is called *DTMC*.

Definition 2.4.3. *One-step transition probability* of a Markov chain from state i to state j:

$$p_{ij}(n) \triangleq P\{X_{n+1} = j | X_n = i\}, \tag{2.24}$$

where if there is no dependency on n, the process is called *time homogeneous* or *homogeneous*. In the rest of the section, we assume all the DTMCs are homogeneous and the notation $p_{ij}(n)$ reduces to p_{ij}.

Corollary 2.1. *Any discrete process satisfying Markov property also satisfies the followings:*

$$P\{X_{n+m} = i_{n+m}, ..., X_n = i_n | X_{n-1} = i_{n-1}, ..., X_0 = i_0\} = \tag{2.25}$$

$$P\{X_{n+m} = i_{n+m}, ..., X_n = i_n | X_{n-1} = i_{n-1}\}, \tag{2.26}$$

where $n, m \geq 1$, $i_k \in S$ and $k \in \{0, ..., n+m\}$. Also,

$$P\{X_n = i_n, ..., X_0 = i_0\} = \tag{2.27}$$

$$P\{X_n = i_n | X_{n-1} = i_{n-1}, ..., X_0 = i_0\}\ P\{X_{n-1} = i_{n-1}, ..., X_0 = i_0\} = \tag{2.28}$$

$$p_{i_{n-1}i_n}\ P\{X_{n-1} = i_{n-1}, ..., X_0 = i_0\} = \tag{2.29}$$

$$p_{i_{n-1}i_n}\ p_{i_{n-2}\ i_{n-1}}\ P\{X_{n-2} = i_{n-2}, ..., X_0 = i_0\} = \tag{2.30}$$

$$\alpha_{i_0}\ p_{i_0 i_1}\ ...\ p_{i_{n-1}i_n}, \tag{2.31}$$

where $\alpha_{i_0} = P\{X_0 = i_0\}$. Thus, the joint probability can be computed by the multiplication of one-step transition probabilities.

Definition 2.4.4. The transition matrix P for a Markov chain:

$$P = \begin{bmatrix} p_{11} & p_{12} & \cdots & p_{1N} \\ p_{21} & p_{22} & \cdots & p_{2N} \\ \vdots & \vdots & \ddots & \vdots \\ p_{N1} & p_{N2} & \cdots & p_{NN} \end{bmatrix}$$

where state space $S = \{1, 2, ..., N\}$. If the state space S is countably infinite, then P is defined as infinite matrix with elements p_{ij}s. Also, the matrix P satisfies $\sum_{j=1}^{N} p_{ij} = 1$ and $0 \leq p_{ij} \leq 1$, $1 \leq i, j \leq N$.

2.4.2 Higher Order Transition Probabilities

Definition 2.4.5. *n-steps transition probability* of a Markov chain from state i to state j in n steps:

$$p_{ij}^{(n)} \triangleq P\{X_{n+k} = j | X_k = i\} = P\{X_n = j | X_0 = i\} \tag{2.32}$$

where the last equality is due to the fact that the process X_n has time homogeneity property.

Lemma 2.2. *$p_{ij}^{(n)} = P_{ij}^n$ for all $n \geq 0$ and $i, j \in S$ where P_{ij}^n is the i, j^{th} element of the matrix P^n.*

Proof. The proof will be done by induction. Note that equality is satisfied when $n = 0$ and $n = 1$. For $n = 2$ we may write the following:

$$\begin{aligned} p_{ij}^{(2)} &= P\{X_2 = j | X_0 = i\} && (2.33) \\ &= \sum_{k \in S} P\{X_2 = j | X_1 = k, X_0 = i\} P\{X_1 = k | X_0 = i\} && (2.34) \\ &= \sum_{k \in S} p_{ik}\ p_{kj} && (2.35) \end{aligned}$$

where $\sum_{k \in S} p_{ik}\ p_{kj} \leq \sum_{k \in S} p_{ik} = 1$ so that it converges. Thus, $p_{ij}^{(2)} = P_{ij}^2$.

We assume $p_{ij}^{(n)} = P_{ij}^{n}$ and will check $p_{ij}^{(n+1)} = P_{ij}^{n+1}$ so that:

$$\begin{aligned} p_{ij}^{(n+1)} &= P\{X_{n+1} = j | X_0 = i\} && (2.36)\\ &= \sum_{k \in S} P\{X_{n+1} = j, X_n = k | X_0 = i\} && (2.37)\\ &= \sum_{k \in S} P\{X_{n+1} = j | X_n = k, X_0 = i\} P\{X_n = k | X_0 = i\} && (2.38)\\ &= \sum_{k \in S} P\{X_{n+1} = j | X_n = k\} P\{X_n = k | X_0 = i\} && (2.39)\\ &= \sum_{k \in S} p_{ik}^{(n)} p_{kj} && (2.40)\\ &= \sum_{k \in S} P_{ik}^{n} P_{kj} && (2.41)\\ &= P_{ij}^{n+1} && (2.42) \end{aligned}$$

□

Corollary 2.3. *For all $i, j \in S$ and $m, n \geq 0$,*

$$p_{ij}^{(n+m)} = \sum_{k \in S} p_{ik}^{(m)} p_{kj}^{(n)} \tag{2.43}$$

which is called Chapman-Kolmogorov equations.

Corollary 2.4. *The probability that the Markov chain will be in state $i \in S$ at time n:*

$$P\{X_n = i\} = \sum_{k \in S} P\{X_n = i | X_0 = k\} P\{X_0 = k\} = \sum_{k \in S} \pi_k^{(0)} \; p_{ki}^{(n)}, \tag{2.44}$$

where $\pi_k^0 = P\{X_0 = k\}$. In matrix notation we may write:

$$\pi^n = \pi^0 P^n. \tag{2.45}$$

2.4.3 Classification of States

2.4.3.1 Reducibility

Definition 2.4.6. The state $j \in S$ is *accessible* from state $i \in S$, if there exist a probability $p_{ij}^{(n)} > 0$. We write $i \to j$ to show j is accessible from i.

Definition 2.4.7. If states $i, j \in S$ *communicate* with each other, we write $i \leftrightarrow j$. The relation $\leftrightarrow$ is reflexive ($i \leftrightarrow i$), symmetric ($i \leftrightarrow j$ implies $j \leftrightarrow i$), and transitive ($i \leftrightarrow k$ and $k \leftrightarrow j$ imply $i \leftrightarrow j$).

Definition 2.4.8. If $i \leftrightarrow j$ for all $i, j \in S$, then the Markov chain is called *irreducible*.

Definition 2.4.9. A subset of the state space $C \subset S$ is called *closed* if $p_{ij} = 0$ for all $i \in C$ and $j \notin C$.

2.4.3.2 Periodicity

Definition 2.4.10. The period of a state $i \in S$:

$$p(i) = \gcd\{n : p_{ii}^{(n)} > 0\}, \tag{2.46}$$

where 'gcd' stands for greater common divisor. If $\{n : p_{ii}^{(n)} > 0\}$ returns an empty set then we take $p(i) = 1$. If $p(i) = 1$, then state i is called *aperiodic*, otherwise it is periodic with period $p(i) > 1$.

2.4.3.3 Recurrence and Transience

Definition 2.4.11. The state $i \in S$ is *recurrent* if

$$P_i\{\tau_i < \infty\} = 1, \tag{2.47}$$

where $P_i\{a\} = P\{a|X_0 = i\}$ and $\tau_i \triangleq min\{n \geq 1 : X_n = i\}$. Otherwise it is called *transient*.

Theorem 2.5. *A state i is transient if and only if the expected number of returns is finite, which occurs if and only if $\sum_{n=0}^{\infty} p_{ii}^{(n)} < \infty$. Further, if i is recurrent, then with a probability of one, X_n returns to i infinitely often, whereas if i is transient, there is a last time a visit occurs.*

Proof. Number of times the chain returns to state $i \in S$:

$$R_i = \sum_{n=0}^{\infty} l_{\{X_n = i\}}. \tag{2.48}$$

The expected value of R:

$$E[R_i] = \sum_{n=0}^{\infty} P_i\{X_n = i\} = \sum_{n=0}^{\infty} P\{X_n = i|X_0 = i\} = \sum_{n=0}^{\infty} p_{ii}^{(n)}. \tag{2.49}$$

Assume that the state i is transient and let $\Theta = P_i\{\tau_i < \infty\} < 1$ so that:

$$P_i\{R = 1\} = 1 - \Theta, P_i\{R = 2\} = \Theta(1 - \Theta), \cdots P_i\{R = k\} = \Theta^{k-1}(1 - \Theta), \tag{2.50}$$

and

$$E[R_i] = \sum_{k=0}^{\infty} k\Theta^{k-1}(1-\Theta) = \frac{1}{1-\Theta} < \infty \tag{2.51}$$

Thus, the state i is transient if $\sum_{n=0}^{\infty} p_{ii}^{(n)} < \infty$ and the state i is recurrent if $\sum_{n=0}^{\infty} p_{ii}^{(n)} = \infty$. □

Corollary 2.6. *The state i is recurrent if and only if state j is recurrent when $i \leftrightarrow j$.*

Corollary 2.7. *All states are recurrent in an irreducible Markov chain with finite state space.*

2.4.4 Stationary Distributions

Definition 2.4.12. A vector $\pi > 0$ is called an *invariant measure* if:

$$\pi^T P = \pi^T, \tag{2.52}$$

so that we may write the following:

$$\pi_i = \sum_j \pi_j p_{ji}, \quad \text{for all} \quad i \in S. \tag{2.53}$$

which means that the probability of being state i is basically equal to the summation of the probability of being state j times p_{ji}, the flow rate from state j to i.

Also, if π satisfies the following condition $\sum_j \pi_j = 1$, then it is said to be *steady-state (stationary or equilibrium) probability distribution.*

Theorem 2.8. *A finite, aperiodic and irreducible Markov chain has an unique stationary distribution π such that:*

$$\pi^T P = \pi^T, \quad \pi_i > 0. \tag{2.54}$$

Also, we may write the following for any probability vector v:

$$\lim_{n\to\infty} v^T P^n = \pi^T. \tag{2.55}$$

2.4.5 Reversibility

Definition 2.4.13. A stochastic process X is called *reversible* if $(X(t_1), \cdots, X(t_n))$ has the same distribution with $(X(\tau - t_1), \cdots, X(\tau - t_n))$.

Corollary 2.9. *A reversible process is stationary, since* $(X(t_1), \cdots, X(t_n)) \sim (X(\tau - t_1), \cdots, X(\tau - t_n)) \sim (X(-t_1), \cdots, X(-t_n)) \sim (X(\tau + t_1), \cdots, X(\tau + t_n))$.

Theorem 2.10. *A stationary Markov process is reversible if and only if the following detailed balance equations are satisfied:*

$$\pi_i p_{ij} = \pi_j p_{ji} \quad \textit{for all } i, j \in S. \tag{2.56}$$

Theorem 2.11. *If* X *is a stationary Markov process, then the reserved chain is also an stationary Markov process with the same equilibrium distributions and the transitions rates are:*

$$p_{ij}^{'} = \frac{\pi_j}{\pi_i} p_{ji}, \ i, j \in S. \tag{2.57}$$

This is intuitive and means that the probability flux from state i *to* j *in the reversed process equals to the probability flux from state* j *to* i *in the original process.*

Also, since the process is reversible $p_{ij}^{'} = p_{ij}$ *and* $\pi_i = \sum_{j \in S} \pi_j p_{ij}$.

2.5 Conclusion

In the first part of this chapter, the basic queueing theory is presented together with some related background information. In the next part, queuing networks are examined along with the basics and properties of Jackson's network and G-networks. Furthermore, the basics of the EPN paradigm is presented together with some related previous studies. In addition to the EPN paradigm, the EN paradigm is also introduced. The EN is basically the fundamental basis of the system model for this thesis and it is motivated by the energy harvesting devices. In the final part, the Markov chain review is presented since it plays a key role to examine performance analysis of the system model. The Markov chain representation in this work is basically used for showing state transitions to understand and visualize the system behaviour.

Chapter 3

Packet Transmission via Perfect Transmitter

3.1 Introduction

This chapter is based on references [66, 69, 70]. In this chapter we investigate a sensor node in which the packet transmission occurs via perfect transmitter. First, we studied a model where single EP is consumed to successfully transmit one DP. We obtained a closed-form solution for the stationary distributions and made further analysis on quantities of interest such as excessive packet losses and stability of the system. Next, we assumed a model in which a DP can be successfully transmitted by consuming $K > 1$ EPs. The motivation is based on noise or interference; the transmitter may need to make use of a higher transmission power level or it may wish to reduce it to save energy. A closed-form solution for the stationary distributions of the model was obtained and further analysis was carried out.

3.2 Transmission with Single Energy Packet

3.2.1 Mathematical Model

It was assumed that an energy harvesting wireless sensor node (EHWSN) receives data, at a rate of λ DPs per second, and energy, at a rate of Λ EPs per second, in a random manner. Figure (3.1) depicts the arrival of DPs and EPs that occur according to two distinct independent Poisson processes. The abstraction of "packet" offers a discrete

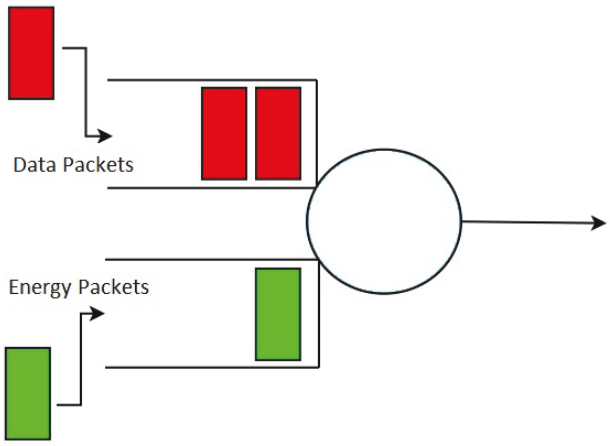

FIGURE 3.1: DP and EP arrivals at the sensor node as two distinct independent Poisson processes.

representation of the amount of energy and data that are gathering from the environment. An EHWSN stores energy in a battery or a capacitor and data in a buffer.

It was assumed that energy leaks at a rate of μ due to the self-discharging nature of the batteries or capacitors, when there is no data to transmit in the buffer. Similarly, data leaks at a rate of γ when there is no energy in the storage.

In addition, it has been assumed that the energy gathering rate Λ and the data gathering at rate λ are very small. However, once enough sensed bits have been gathered and there is at least one energy packet in the system, the time it takes to create packets and transmit the packets via wireless is extremely fast compared to these rates (i.e. the transmission time of one packet may be a few picoseconds provided energy is available). Thus we will assume that transmission is instantaneous (i.e. it takes zero time on the time scales of sensing and data gathering, and of energy harvesting).

Heinzelman has previously proposed an energy consumption model for sensors. He stated that the amount of energy required to transmit 1 bit is $50nJ$ [97]. In this model, it is assumed that 1 EP has the amount of energy required to transmit 1 DP. Thus, 1 EP should have '50nJ x (number of bits in a DP)' amount of energy. Moreover, 1 DP size can typically be considered as tens of kbits. For instance, a wireless protocol Zigbee's data rates are 20 kbits (868MHz) and 40 kbits (915MHz). Alternatively, there are several modules that harvest different amounts of energy per second such as 4.6mW (585-EH300), 30mW (585-EH300A), 275mW (582-P2110B), 400mW (932-MIKROE-651). For example, if we have a 30mW energy harvesting module, then typical values of Λ can be calculated as 60 and 15 EPs/sec for 10 and 40 kbits data packet size, respectively.

Alternatively, energy can be stored in a capacitor or battery. However, this form of storage discharges its energy due to standby where transmission does not occur. This

self-discharge is an energy leakage process in energy storages where the internal chemical reactions reduce the stored charge of batteries or capacitors. Energy storage leakage typically varies between 0.1% - 30%, depending on the chemicals used for the energy storage [98].

We model the state of the sensor node using the pair $(D(t), E(t))$ where $D(t)$ is the number of DPs stored at the node and $E(t)$ is the number of stored EPs, both at time $t \geq 0$. Because of the very small processing and transmission times at the node, whenever energy is available and there are DPs waiting they will be instantaneously transmitted until the energy packets are depleted. Thus, any state $D(t) > 0,\ E(t) > 0$ will instantaneously (in zero time) transit to either the state $(0, E(t) - D(t))$ if $E(t) \geq D(t)$, or to the state $(D(t) - E(t), 0)$ if $D(t) \geq E(t)$.

Let us write $p(d, e, t) = Prob[D(t) = d, E(t) = e]$. From the above remark, we only consider $p(d, e, t)$ for the state space S of pairs of integers $(d, e) \in S$ such that:

$$S = \{\ (0,0),\ (d,0),\ (0,e)\ : D \geq d > 0,\ E \geq e > 0\ \}. \tag{3.1}$$

First, note that if both the data buffer and the energy storage capacity are finite, then the system can be modelled as a finite CTMC whose set of states are given in equation (3.1) with $0 \leq d \leq D$, $0 \leq e \leq E$. It is noted that the process $[D(t), E(t),\ t \geq 0]$ is irreducible and aperiodic such that the stationary probabilities $p(d, e) = \lim_{t\to\infty} Pr[D(t) = d, E(t) = e]$ exist uniquely and are computed from the following balance equations:

$$p(0,0)[\lambda + \Lambda] = (\Lambda + \gamma)\ p(1,0) + (\lambda + \mu)\ p(0,1), \tag{3.2}$$

$$p(d,0)[\lambda + \Lambda + \gamma] = (\Lambda + \gamma)\ p(d+1,0) + \lambda\ p(d-1,0), \tag{3.3}$$

$$p(D,0)[\Lambda + \gamma] = \lambda\ p(D-1,0), \tag{3.4}$$

$$p(0,e)[\lambda + \Lambda + \mu] = \Lambda\ p(0,e-1) + (\lambda + \mu)p(0,e+1), \tag{3.5}$$

$$p(0,E)[\lambda + \mu] = \Lambda\ p(0,E-1). \tag{3.6}$$

Note that these equations have a solution of the form:

$$p(d,0) \quad = \quad \alpha^n C_1,\ \alpha = \frac{\lambda}{\Lambda + \gamma},\ 1 \leq d \leq D, \tag{3.7}$$

$$p(0,e) \quad = \quad \theta^m C_2,\ \theta = \frac{\Lambda}{\lambda + \mu},\ 1 \leq e \leq E, \tag{3.8}$$

where C_1 and C_2 are arbitrary constants. The following is obtained on considering equation (3.2):

$$p(0,0)(\lambda+\Lambda) = (\Lambda+\gamma)(\frac{\lambda}{\Lambda+\gamma})C_1 + (\lambda+\mu)(\frac{\Lambda}{\lambda+\mu})C_2, \tag{3.9}$$

$$0 = (p(0,0)-C_1)\lambda + (p(0,0)-C_2)\Lambda. \tag{3.10}$$

Thus, $C_1 = C_2 = p(0,0)$ satisfies the equation.

Using the fact that the probabilities sum to one we have:

$$1 = p(0,0) + \sum_{d=1}^{D} p(d,0) + \sum_{e=1}^{E} p(0,e), \tag{3.11}$$

$$= p(0,0)[1 + \sum_{d=1}^{D} \alpha^d + \sum_{e=1}^{E} \theta^e], \tag{3.12}$$

$$= p(0,0)[1 + (\frac{\alpha(\alpha^D-1)}{\alpha-1}) + (\frac{\theta(\theta^E-1)}{\theta-1}). \tag{3.13}$$

Hence:

$$p(0,0) = \frac{1-\alpha-\theta+\alpha\theta}{\alpha^{D+1}(\theta-1)+\theta^{E+1}(\alpha-1)+1-\alpha\theta}, \tag{3.14}$$

$$p(d,0) = \alpha^d \frac{1-\alpha-\theta+\alpha\theta}{\alpha^{D+1}(\theta-1)+\theta^{E+1}(\alpha-1)+1-\alpha\theta},\ 0 \le d \le D, \tag{3.15}$$

$$p(0,e) = \theta^e \frac{1-\alpha-\theta+\alpha\theta}{\alpha^{D+1}(\theta-1)+\theta^{E+1}(\alpha-1)+1-\alpha\theta},\ 0 \le e \le E. \tag{3.16}$$

Thus, we are able to express closed-form solutions for the stationary probability distributions. In addition, we can express the marginal probabilities for the queue length of DPs and EPs as:

$$p_d(d) = \sum_{e=0}^{\infty} p(d,e) = p(d,0),\ d > 0, \tag{3.17}$$

$$p_d(0) = \sum_{e=0}^{\infty} p(0,e) = \sum_{e=0}^{\infty} \theta^e p(0,0) = \frac{1-\theta^{E+1}}{1-\theta} p(0,0), \tag{3.18}$$

and similarly,

$$p_e(e) = \sum_{d=0}^{\infty} p(d,e) = p(0,e),\ e > 0, \tag{3.19}$$

$$p_e(0) = \sum_{d=0}^{\infty} p(d,0) = \sum_{d=0}^{\infty} \alpha^d p(0,0) = \frac{1-\alpha^{D+1}}{1-\alpha} p(0,0). \tag{3.20}$$

Hence:

$$p_d(d) = \alpha^d \frac{1-\alpha-\theta+\alpha\theta}{\alpha^{D+1}(\theta-1)+\theta^{E+1}(\alpha-1)+1-\alpha\theta},\ 0 < d \leq D, \tag{3.21}$$

$$p_e(e) = \theta^e \frac{1-\alpha-\theta+\alpha\theta}{\alpha^{D+1}(\theta-1)+\theta^{E+1}(\alpha-1)+1-\alpha\theta},\ 0 < e \leq E. \tag{3.22}$$

3.2.2 Energy and Data Packet Losses

There is bound to be some level of energy or data packet loss when either the energy storage capacity or the data packet buffer is finite. These rates of loss in energy (L_e) and data packets (L_d) per second can be computed as:

$$\begin{aligned} L_e &= \Lambda \sum_{d=0}^{\infty} p(d,E) && (3.23)\\ &= \Lambda p(0,E) && (3.24)\\ &= \Lambda\theta^E \frac{1-\alpha-\theta+\alpha\theta}{\alpha^{D+1}(\theta-1)+\theta^{E+1}(\alpha-1)+1-\alpha\theta}. && (3.25)\\ L_d &= \lambda \sum_{e=0}^{\infty} p(D,e) && (3.26)\\ &= \lambda p(D,0) && (3.27)\\ &= \lambda\alpha^D \frac{1-\alpha-\theta+\alpha\theta}{\alpha^{D+1}(\theta-1)+\theta^{E+1}(\alpha-1)+1-\alpha\theta}. && (3.28) \end{aligned}$$

For the assumption of very large buffer sizes, i.e. both D and E tend to infinity, the following cases can be considered:

Case 1 *If $\alpha > 1$ and hence $\theta < 1$ or equivalently $\Lambda < \lambda$, such that the energy is not sufficient for the data and $L_e \to 0$ and $L_d \to \lambda - (\Lambda + \gamma)$, as would be expected.*

Case 2 *If $\alpha = 1$ and hence $\theta < 1$ or equivalently $\Lambda < \lambda + \mu$, the expressions for L_e and L_d are in indeterminate forms. However, following some algebra we obtain $L_e \to 0$ and $L_d \to 0$.*

Case 3 *If $\alpha < 1$ and $\theta < 1$ or equivalently $\Lambda < \lambda + \mu$ and $\lambda < \Lambda + \gamma$, in this case there is no leakage for both buffers, and $L_e \to 0$ and $L_d \to 0$.*

Case 4 *If $\alpha < 1$ and $\theta > 1$ or equivalently $\Lambda > \lambda + \mu$, so that the energy is more plentiful than is needed, and $L_e \to \Lambda - (\lambda + \mu)$ and $L_d \to 0$, as would be expected.*

Case 5 *If $\alpha < 1$ and $\theta = 1$ or equivalently $\lambda < \Lambda + \gamma$, the expressions for L_e and L_d are in indeterminate form. However, following some algebra we obtain $L_e \to 0$ and $L_d \to 0$.*

3.2.3 Optimum Energy Efficiency of the Transmission

The sensor we considered receives Λ EPs/sec (in power units, e.g. milliwatts) from energy harvesting. However it can not use all this energy due to the finite capacity energy loss and energy leakage of the system. Similarly, it can not transmit all the DPs gathered from the environment due to finite capacity data loss and data leakage. Thus, its energy consumption per effectively transmitted packet is:

$$\sigma = \frac{\Lambda}{\lambda - g(\Lambda)}. \tag{3.29}$$

where

$$g(\Lambda) = \gamma \sum_{d=1}^{D} p(d,0) + L_d = \gamma \frac{\alpha^{D+1} - \alpha}{\alpha - 1} p(0,0) + \lambda \alpha^D p(0,0). \tag{3.30}$$

Thus, it is of interest to investigate what the best operating point may be for this system, in terms of consumed energy. Therefore, we take the derivative of various terms in the expression with respect to Λ and see that:

$$\sigma' = \frac{\lambda - g(\Lambda) + \Lambda g'(\Lambda)}{(\lambda - g(\Lambda))^2}, \tag{3.31}$$

so that the extremum for σ is reached for the value of Λ which gives:

$$\lambda - g(\Lambda) + \Lambda g'(\Lambda) = 0. \tag{3.32}$$

In addition, we have

$$\sigma'' = \frac{[\Lambda g''(\Lambda)][(\lambda - g(\Lambda))^2] + [2(\lambda - g(\Lambda))][\lambda - g(\Lambda) + \Lambda g'(\Lambda)]}{(\lambda - g(\Lambda))^4}, \tag{3.33}$$

so that the value for Λ which satisfies equation (3.32) gives the following:

$$\sigma'' = \frac{\Lambda g''(\Lambda)}{(\lambda - g(\Lambda))^2}. \tag{3.34}$$

Following the use of algebra we obtain the value of Λ that satisfies equation (3.32), this is a point of inflection on the efficiency function σ, since $\sigma'' = 0$.

Figure 3.2 indicates the energy consumption per effectively transmitted packet, σ, for different energy and data arrival rates, assuming $\mu = 0.1\Lambda, \gamma = 0.1\lambda, D = E = 100$. It was observed that in order to keep the energy efficiency high, i.e. to have σ as low as possible, the power Λ that is supplied from harvesting should remain *below* the nominal need to satisfy all the flow λ of DPs that are being sensed.

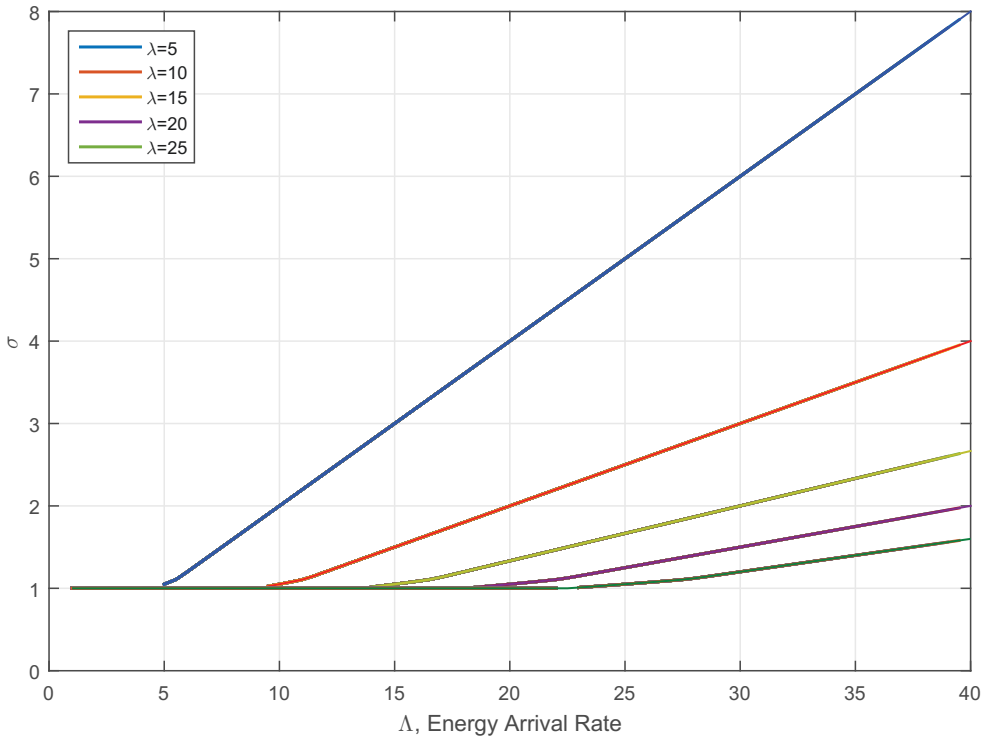

FIGURE 3.2: The energy consumption per effectively transmitted packet, σ, for different energy and data arrival rates.

3.2.4 Stability of the System

System stability is only of interest for data and energy buffers with unlimited storage capacity. In this case, the system will be stable when the backlog of stored energy and the backlog of data packets remain finite with probability one when $t \to \infty$ for $D \to \infty$ and $E \to \infty$. Otherwise, the system is said to be unstable.

For some finite G and H with $0 \leq G < D$ and $0 \leq H < E$, the probabilities that the respective backlogs of data and energy packets do not exceed G and H, in steady-state are:

$$P_d(G) = lim_{t\to\infty} Prob[0 \leq D(t) \leq G \leq D], \tag{3.35}$$

$$P_e(H) = lim_{t\to\infty} Prob[0 \leq E(t) \leq H \leq E]. \tag{3.36}$$

Moreover, using our obtained results gives:

$$\begin{aligned} P_d(G) &= p_d(0) + \sum_{d=1}^{G} p_d(d), && (3.37)\\ &= \frac{1-\theta^{E+1}}{1-\theta} p(0,0) + \sum_{d=1}^{G} (\alpha^d p(0,0)), && (3.38)\\ &= p(0,0)(\frac{1-\theta^{E+1}}{1-\theta} + \frac{\alpha-\alpha^{G+1}}{1-\alpha}), && (3.39)\\ &= \frac{\alpha^{G+1}(\theta-1)+\theta^{E+1}(\alpha-1)+1-\alpha\theta}{\alpha^{D+1}(\theta-1)+\theta^{E+1}(\alpha-1)+1-\alpha\theta}, && (3.40) \end{aligned}$$

and

$$\begin{aligned} P_e(H) &= p_e(0) + \sum_{e=1}^{H} p_e(e), && (3.41)\\ &= \frac{1-\alpha^{D+1}}{1-\alpha} p(0,0) + \sum_{e=1}^{H} (\theta^e p(0,0)), && (3.42)\\ &= p(0,0)(\frac{1-\alpha^{D+1}}{1-\alpha} + \frac{\theta-\theta^{H+1}}{1-\theta}), && (3.43)\\ &= \frac{\alpha^{D+1}(\theta-1)+\theta^{H+1}(\alpha-1)+1-\alpha\theta}{\alpha^{D+1}(\theta-1)+\theta^{E+1}(\alpha-1)+1-\alpha\theta}. && (3.44) \end{aligned}$$

This leads to the following:

Case 1 *If $\alpha > 1$ and hence $\theta < 1$ as $E \to \infty$ and $D \to \infty$, $P_d(G) \to 0$ for all finite G and $P_e(H) \to 1$ for all finite H, the system is stable with respect to EPs and unstable with respect to DPs.*

Case 2 *If $\alpha = 1$ and hence $\theta < 1$ as $E \to \infty$ and $D \to \infty$, one can easily see that the expression for p(0,0) is an indeterminate form, so that we apply L'Hospital's rule and obtain :*

$$\lim_{\alpha\to 1} p(0,0) = \lim_{\alpha\to 1} \frac{\theta-1}{(D+1)(\theta-1)\alpha^D + \theta^{E+1} - \theta} = \frac{\theta-1}{(D+1)(\theta-1)+\theta^{E+1}-\theta},$$

and

$$\lim_{(D,E)\to\infty} [\lim_{\alpha\to 1} p(0,0)] = \lim_{(D,E)\to\infty} [\frac{\theta-1}{(D+1)(\theta-1)+\theta^{E+1}-\theta}] \to 0.$$

Hence:

$$\lim_{\substack{(D,E)\to\infty \\ \alpha\to 1}} [P_d(G)] = \lim_{\substack{(D,E)\to\infty \\ \alpha\to 1}} [p(0,0)] \lim_{\substack{(D,E)\to\infty \\ \alpha\to 1}} [\sum_{m=0}^{E} \theta^m + \sum_{n=1}^{G} \alpha^n] \to 0.$$

in this case a similar analysis can be made for the $P_e(H)$, which leads to $P_d(G) \to 0$ for all finite G and $P_e(H) \to 0$ for all finite H. Therefore, the system is unstable with respect to both DPs and EPs.

Case 3 *If $\alpha < 1$ and $\theta < 1$ as $E \to \infty$ and $D \to \infty$, $P_d(G) \to \frac{\alpha^{G+1}(\theta-1)+1-\alpha\theta}{1-\alpha\theta}$ and that limit is obviously in the interval (0,1), since $-1 < \alpha^{G+1}(\theta-1) < 0$ for all finite G and similarly $P_e(H) \to \frac{\theta^{H+1}(\alpha-1)+1-\alpha\theta}{1-\alpha\theta}$ and similarly that limit is in the interval (0,1), for all finite H. Therefore, the system is unstable with respect to both DPs and EPs.*

Case 4 *If $\alpha < 1$ and hence $\theta = 1$ as $E \to \infty$ and $D \to \infty$, it is easily seen that the expression for p(0,0) is an indeterminate form, such that the analysis can be made by applying the exact same procedure used in Case 2. Therefore, since $P_d(G) \to 0$ for all finite G and $P_e(H) \to 0$ for all finite H, the system is unstable with respect to both DPs and EPs.*

Case 5 *If $\alpha < 1$ and $\theta > 1$ as $E \to \infty$ and $D \to \infty$, $P_d(G) \to 1$ for all finite G and $P_e(H) \to 0$ for all finite H; the system is stable with respect to DPs and unstable with respect to EPs.*

3.2.5 Unlimited Capacity Data and Energy Buffers with Transmission Errors

If a reduction of the average probability of transmission error over the wireless sensor network is considered or a certain transmission error detected, then retransmission of the same DP may be required. Two separate error probabilities (p and π) are considered to model the effect of retransmissions in a system. The retransmission probability p occurs when there are plenty of EPs in storage and one DP arrives at the node. In this case, the data transmission occurs immediately but retransmission may be needed due to unsuccessful transmission and a further EP will be consumed with probability p. This process may be repeated independently of the previous outcome with the same probabilities of success $1 - p$ and failure p. Additionally, the retransmission probability π occurs when there is at least one DP in the buffer to be transmitted. In this case, the DP may not be transmitted successfully and remains in the queue so that another EP will be needed with probability π. Again, the process will repeat itself independently of the previous event when another EP arrives at some later time.

Let λ be the data arrival rate to the node, Λ the energy harvesting rate, μ the standby loss rate and γ the time-out loss rate of the system. Thus, the state space of interest is

still

$$S = \{(0,0),(d,0),(0,e) :\ d,e \geq 1\ \}, \tag{3.45}$$

but the possible state transitions differ from those of the previous section. The following state transition rates can be obtained:

- λ : for $(d,0) \to (d+1,0),\ d \geq 0$, when a DP arrives,
- Λ : for $(0,e) \to (0,e+1),\ e \geq 0$, when an EP arrives,
- μ : for $(0,e) \to (0,e-1),\ e \geq 1$, when an EP leaves through leakage.
- γ : for $(d,0) \to (d-1,0),\ d \geq 1$, when a DP is lost by leakage.
- $\Lambda\pi$: for $(d,0) \to (d,0),\ d \geq 1$, when an EP arrives at an empty energy buffer, and if the DP waiting in the queue can not be transmitted successfully, so that DP retransmission is needed by consuming another EP with the probability π. However, retransmission can not occur due to lack of energy and the state of the system is retained.
- $\Lambda(1-\pi)$: for $(d,0) \to (d-1,0),\ d \geq 1$, when an EP arrives to an empty energy buffer, and if a DP waiting in the queue can be transmitted successfully, data packet retransmission is not necessary with the probability $1-\pi$.
- λp : for $(0,1) \to (1,0)$, when a DP arrives at an empty data buffer and there is only one EP in the storage to be consumed, DP transmission may be unsuccessful. In this case, EP is already consumed and DP will be stored in the buffer with the probability p.
- $\lambda(1-p)$: for $(0,e) \to (0,e-1),\ e > 0$,
- $\lambda p^{k-1}(1-p)$: for $(0,e) \to (0,e-k),\ e \geq k > 1$, when there are several EPs in storage and only one DP arrives at the node. Consecutive retransmissions may be needed in the case of repetitive unsuccessful attempts. In this transition, DP can be transmitted before the all EPs are depleted.
- λp^e : for $(0,e) \to (1,0),\ i.e.\ k = e$, the arriving DP reduces the number of EPs by 1 and then there may be another DP transmission request and so on, but when all the EPs are depleted, the e^{th} and final transmission request cannot be satisfied and the system moves into state $(1,0)$ having depleted all its EPs and having one final DP waiting to be transmitted. Also, notice that for any $e > 0$ the sum of these probabilities is one:

$$\sum_{k=0}^{e-1} p^k(1-p) + p^e = 1. \tag{3.46}$$

Thus, the equilibrium equations for the system in steady-state are the followings:

$$p(0,0)[\lambda+\Lambda] = \lambda\sum_{l=1}^{\infty}p^{l-1}(1-p)p(0,l)+(\Lambda(1-\pi)+\gamma)p(1,0)+\mu p(0,1), \tag{3.47}$$

$$p(1,0)[\lambda+\Lambda(1-\pi)+\gamma] = \lambda\sum_{l=0}^{\infty}p^{l}p(0,l)+(\Lambda(1-\pi)+\gamma)p(2,0), \tag{3.48}$$

$$p(d,0)[\lambda+\Lambda(1-\pi)+\gamma] = \lambda p(d-1,0)+(\Lambda(1-\pi)+\gamma)p(d+1,0), \tag{3.49}$$

$$p(0,e)[\lambda+\Lambda+\mu] = \lambda\sum_{l=1}^{\infty}p^{l-1}(1-p)p(0,e+l)+\Lambda p(0,e-1)+\mu p(0,e+1). \tag{3.50}$$

Theorem 3.1. *If* $(\Lambda-\mu)(1-p)<\lambda<\Lambda(1-\pi)+\gamma$*, the stationary distribution exists and is given by:*

$$p(0,e) = p(0,0)Q^{e},\ e\geq 1, \tag{3.51a}$$

$$p(d,0) = p(1,0)q^{d-1},\ d\geq 1, \tag{3.51b}$$

where

$$q = \frac{\lambda}{\Lambda(1-\pi)+\gamma}, \tag{3.52}$$

$$Q = \frac{\lambda+\mu+\Lambda p-\sqrt{(\lambda+\mu+\Lambda p)^2-4\mu\Lambda p}}{2\mu p}, \tag{3.53}$$

and

$$p(0,0) = \frac{(1-q)(1-Q)(1-pQ)}{q(1-Q)+(1-q)(1-pQ)} \tag{3.54}$$

$$= \Big(\frac{2\mu\lambda}{(\Lambda(1-\pi)-\lambda)(\mu-\lambda-\Lambda p+\sqrt{(\lambda+\Lambda p+\mu)^2-4\mu\Lambda p})} \tag{3.55}$$

$$+ \frac{2\mu p}{2\mu p-(\lambda+\Lambda p+\mu)+\sqrt{(\lambda+\mu+\Lambda p)^2-4\mu\Lambda p}}\Big)^{-1}, \tag{3.56}$$

$$p(1,0) = \frac{q}{(1-pQ)}p(0,0) \tag{3.57}$$

$$= \frac{2\mu\lambda}{(\Lambda(1-\pi)+\gamma)[\mu-\lambda-\Lambda p+\sqrt{(\lambda+\Lambda p+\mu)^2-4\mu\Lambda p}]}. \tag{3.58}$$

Proof. To proceed with the proof, we substitute equation (3.51a) in (3.50), which gives the following after some algebra:

$$Q^e[\lambda+\Lambda+\mu] = \lambda(1-p)Q^{e+1}\frac{1}{1-pQ} + \Lambda Q^{e-1} + \mu Q^{e+1}, \tag{3.59}$$

$$0 = (Q-1)[Q^2(\mu p) + Q(-\Lambda p - \lambda - \mu) + \Lambda]. \tag{3.60}$$

Thus, the Q are determined as:

$$Q_{1,2} = \frac{\lambda+\mu+\Lambda p \pm \sqrt{(\lambda+\mu+\Lambda p)^2 - 4\mu\Lambda p}}{2\mu p}. \tag{3.61}$$

Note that Q has to be smaller than 1, while:

$$\frac{\lambda+\mu+\Lambda p + \sqrt{(\lambda+\mu+\Lambda p)^2 - 4\mu\Lambda p}}{2\mu p} \geq \frac{\lambda+\mu+\Lambda p}{2\mu p} > \frac{1}{2}(\frac{1}{p} + \frac{\Lambda}{\mu}) > 1, \tag{3.62}$$

since $p < 1$ and $\mu < \Lambda$.

Therefore, the only viable root is

$$Q = \frac{\lambda+\mu+\Lambda p - \sqrt{(\lambda+\mu+\Lambda p)^2 - 4\mu\Lambda p}}{2\mu p}, \tag{3.63}$$

and we may consider the following:

$$\frac{\lambda+\mu+\Lambda p - \sqrt{(\lambda+\mu+\Lambda p)^2 - 4\mu\Lambda p}}{2\mu p} < 1, \tag{3.64}$$

$$(\lambda+\mu+\Lambda p - 2\mu p)^2 < (\lambda+\mu+\Lambda p)^2 - 4\mu\Lambda p, \tag{3.65}$$

$$\Lambda + \mu p < (\lambda+\mu+\Lambda p), \tag{3.66}$$

$$(\Lambda-\mu)(1-p) < \lambda. \tag{3.67}$$

Note that the equation (3.49) has a solution of the form:

$$p(d,0) = (\frac{\lambda}{\Lambda(1-\pi)+\gamma})^{d-1}\ p(1,0). \tag{3.68}$$

Since $q < 1$, then $\lambda < \Lambda(1-\pi)+\gamma$.

The ratio between $p(1,0)$ and $p(0,0)$ can also be calculated, when substituting equation (3.50) in (3.47):

$$p(0,0)[\lambda+\Lambda] = \lambda(1-p)\frac{Qp(0,0)}{1-pQ} + (\Lambda(1-\pi)+\gamma)p(1,0) + \mu Q p(0,0), \tag{3.69}$$

$$(\lambda+\Lambda) = \lambda(1-p)\frac{Q}{1-pQ} + (\Lambda(1-\pi)+\gamma)\frac{p(1,0)}{p(0,0)} + \mu Q. \tag{3.70}$$

Thus,

$$\frac{p(1,0)}{p(0,0)} = \frac{Q^2(\mu p) - Q(\Lambda p + \lambda + \mu) + \Lambda + \lambda}{(\Lambda(1-\pi)+\gamma)(1-pQ)} \tag{3.71}$$

$$= \frac{\lambda}{(\Lambda(1-\pi)+\gamma)(1-pQ)} \tag{3.72}$$

$$= \frac{2\mu\lambda}{(\Lambda(1-\pi)+\gamma)[\mu - \lambda - \Lambda p + \sqrt{(\lambda+\Lambda p+\mu)^2 - 4\mu\Lambda p}]}. \tag{3.73}$$

Moreover, using the fact that the probabilities must sum to one, gives followings:

$$1 = p(0,0) + p(1,0) + \sum_{d=2}^{\infty} p(d,0) + \sum_{e=1}^{\infty} p(0,e), \tag{3.74}$$

$$1 = p(0,0)[1 + \xi + \xi\frac{q}{1-q} + \frac{Q}{1-Q}], \tag{3.75}$$

$$1 = p(0,0)[\xi\frac{1}{1-q} + \frac{1}{1-Q}], \tag{3.76}$$

where $\xi = \frac{p(1,0)}{p(0,0)} = \frac{q}{1-pQ}$.

Thus, $p(0,0)$ is calculated as:

$$p(0,0) = \frac{(1-q)(1-Q)}{\xi(1-Q)+(1-q)} \tag{3.77}$$

$$= \frac{(1-q)(1-Q)(1-pQ)}{q(1-Q)+(1-q)(1-pQ)} \tag{3.78}$$

$$= \frac{1}{\frac{q}{1-q}\frac{1}{1-pQ} + \frac{1}{1-Q}} \tag{3.79}$$

$$= [\frac{\frac{2\mu\lambda}{(\Lambda(1-\pi)-\lambda)}}{[\mu - \lambda - \Lambda p + \sqrt{(\lambda+\Lambda p+\mu)^2 - 4\mu\Lambda p}]} \tag{3.80}$$

$$+ \frac{2\mu p}{2\mu p - (\lambda + \Lambda p + \mu) + \sqrt{(\lambda+\mu+\Lambda p)^2 - 4\mu\Lambda p}}]^{-1}. \tag{3.81}$$

□

Remark 1 Based on the above results, notice that:

- The *probability that the data queue is empty* can be obtained as:

$$\begin{aligned} P[d=0] &= p(0,0)+\sum_{e=1}^{\infty} p(0,e) && (3.82)\\ &= p(0,0)(1+\sum_{e=1}^{\infty} Q^e) && (3.83)\\ &= p(0,0)(\frac{1}{1-Q}) && (3.84)\\ &= \frac{1}{1+\frac{q}{1-q}\frac{1-Q}{1-pQ}} && (3.85)\\ &= \frac{1}{1+\frac{\lambda}{\Lambda(1-\pi)-\lambda}\frac{2\mu p-(\lambda+\Lambda+\mu)+\sqrt{(\lambda+\mu+\Lambda p)^2-4\mu\Lambda p}}{2\mu-(\lambda+\Lambda+\mu)+\sqrt{(\lambda+\mu+\Lambda p)^2-4\mu\Lambda p}}}. && (3.86) \end{aligned}$$

- The *probability that the data queue is non-empty* is:

$$\begin{aligned} P[d>0] &= \sum_{d=1}^{\infty} p(d,0) && (3.87)\\ &= p(1,0)\sum_{d=0}^{\infty} q^d && (3.88)\\ &= \frac{q}{(1-pQ)}\frac{1}{1-q}p(0,0) && (3.89)\\ &= \frac{1}{1+\frac{1-q}{q}\frac{1-pQ}{1-Q}} && (3.90)\\ &= \frac{1}{1+\frac{\Lambda(1-\pi)-\lambda}{\lambda}\frac{2\mu-(\lambda+\Lambda+\mu)+\sqrt{(\lambda+\mu+\Lambda p)^2-4\mu\Lambda p}}{2\mu p-(\lambda+\Lambda+\mu)+\sqrt{(\lambda+\mu+\Lambda p)^2-4\mu\Lambda p}}}. && (3.91) \end{aligned}$$

- As a sanity check, the *probability that the data queue is either full or empty* is:

$$P[d\geq 0] = \frac{1}{1+\frac{q}{1-q}\frac{1-Q}{1-pQ}} + \frac{1}{1+\frac{1-q}{q}\frac{1-pQ}{1-Q}} = 1. \quad (3.92)$$

Similarly,

- The *probability that the energy queue is empty* can be obtained as:

$$\begin{aligned} P[e=0] &= p(0,0) + P[d>0], && (3.93)\\ &= p(0,0) + \sum_{d=1}^{\infty} p(d,0), && (3.94)\\ &= p(0,0)(1+\gamma\sum_{d=1}^{\infty} q^{d-1}), && (3.95)\\ &= p(0,0)(1+\frac{q}{(1-q)(1-pQ)}), && (3.96)\\ &= \frac{q(1-Q)+(1-q)(1-pQ)(1-Q)}{q(1-Q)+(1-q)(1-pQ)}. && (3.97)\\ &= \frac{1}{A_1+A_2}+\frac{1}{A_3}, && (3.98)\\ & && (3.99) \end{aligned}$$

where

$$\begin{aligned} A_1 &= \frac{2\mu\lambda}{(\Lambda(1-\pi)-\lambda)[2\mu-(\lambda+\Lambda+\mu)+\sqrt{(\lambda+\mu+\Lambda p)^2-4\mu\Lambda p}]}\\ A_2 &= \frac{2\mu p}{2\mu p-(\lambda+\Lambda+\mu)+\sqrt{(\lambda+\mu+\Lambda p)^2-4\mu\Lambda p}}\\ A_3 &= 1+\frac{\Lambda(1-\pi)-\lambda}{\lambda}\frac{2\mu-(\lambda+\Lambda+\mu)+\sqrt{(\lambda+\mu+\Lambda p)^2-4\mu\Lambda p}}{2\mu p-(\lambda+\Lambda+\mu)+\sqrt{(\lambda+\mu+\Lambda p)^2-4\mu\Lambda p}}. \end{aligned}$$

- The *probability that the energy queue is non-empty* is:

$$\begin{aligned} P[e>0] &= P[d=0]-p(0,0), && (3.100)\\ &= \sum_{e=1}^{\infty} p(0,e), && (3.101)\\ &= p(0,0)\sum_{e=1}^{\infty} Q^e, && (3.102)\\ &= p(0,0)\frac{Q}{1-Q}, && (3.103)\\ &= \frac{Q(1-q)(1-pQ)}{q(1-Q)+(1-q)(1-pQ)}. && (3.104)\\ &= \frac{\frac{\lambda+\mu+\Lambda p-\sqrt{(\lambda+\mu+\Lambda p)^2-4\mu\Lambda p}}{2\mu p-(\lambda+\mu+\Lambda p)+\sqrt{(\lambda+\mu+\Lambda p)^2-4\mu\Lambda p}}}{A_1+A_2}. && (3.105) \end{aligned}$$

- As a sanity check, the *probability that the energy buffer is either full or empty* is:

$$P[e\geq 0] = \frac{q(1-Q)+(1-q)(1-pQ)(1-Q)+Q(1-q)(1-pQ)}{q(1-Q)+(1-q)(1-pQ)} = 1. \qquad (3.106)$$

Remark 2 The total power used by a node for transmission is simply the power entering the node from harvesting, minus that lost via leakage:

$$X = [\Lambda - \mu \sum_{e=1}^{\infty} p(0,e)] = [\Lambda - \frac{\mu Q(1-q)(1-pQ)}{1-Q(p+q-pq)}]. \tag{3.107}$$

Remark 3 If leakage rates μ and γ are assumed to be negligible, then $\lambda < \Lambda$ and $\pi < p$.

3.2.6 Analysis of the Transmission Error with Negligible Leakage Rates

Understandably, a given EHWSN will not radiate power at all if it is not transmitting. Thus for any sensor node i among a set of N nodes, its transmission power when transmitting a DP is given by:

$$X_i = [(\lambda_i - \mu_i) \sum_{e=1}^{\infty} p_i(0,e) + (\Lambda_i - \gamma_i) \sum_{d=1}^{\infty} p_i(d,0)], \tag{3.108}$$

where the subscript i relates to the parameters of the i-th node.

Furthermore, if the probability of correctly receiving (or decoding) the packet sent by a given node i that transmits at power level X_i is denoted by:

$$C_i = f(\frac{X_i}{\sum_{\substack{j=1 \\ j \neq i}}^{N} \phi_i + B_i}), \tag{3.109}$$

where f is some increasing function of its argument which is the signal to interference plus noise B_i. Assume that all nodes are identical, then equation (3.109) can be replaced by:

$$C = f(\frac{(\lambda - \mu) \sum_{e=1}^{\infty} p(0,e) + (\Lambda - \gamma) \sum_{d=1}^{\infty} p(d,0)]}{(N-1)[\Lambda - \mu \sum_{e=1}^{\infty} p(0,e)] + B}), \tag{3.110}$$

and if the leakage rates μ and γ are negligible, we obtain:

$$C = f(\frac{\frac{\lambda}{\Lambda} \sum_{e=1}^{\infty} p(0,e) + \sum_{d=1}^{\infty} p(d,0)]}{(N-1) + \frac{B}{\Lambda}}), \tag{3.111}$$

$$= f(\frac{\frac{\lambda}{\Lambda} p(0,0) \frac{Q}{1-Q} + p(1,0) \frac{1}{1-q}]}{(N-1) + \frac{B}{\Lambda}}) \tag{3.112}$$

In order to make further analysis, there is a need to re-calculate stationary distributions when the leakages μ and γ are neglected:

$$\lim_{(\mu,\gamma)\to 0} Q = \lim_{(\mu,\gamma)\to 0} \frac{\lambda+\mu+\Lambda p-\sqrt{(\lambda+\mu+\Lambda p)^2-4\mu\Lambda p}}{2\mu p} \tag{3.113}$$

$$= \lim_{(\mu,\gamma)\to 0} \frac{\frac{\partial}{\partial u}[\lambda+\mu+\Lambda p-\sqrt{(\lambda+\mu+\Lambda p)^2-4\mu\Lambda p}]}{\frac{\partial}{\partial u}(2\mu p)} \tag{3.114}$$

$$= \lim_{(\mu,\gamma)\to 0} \frac{1-\frac{(\mu+\lambda-\Lambda p)}{\sqrt{(\lambda+\mu+\Lambda p)^2-4\mu\Lambda p}}}{2p} = \frac{1-\frac{\lambda-\Lambda p}{\lambda+\Lambda p}}{2p} = \frac{\Lambda}{\lambda+\Lambda p}. \tag{3.115}$$

$$\lim_{(\mu,\gamma)\to 0} q = \lim_{(\mu,\gamma)\to 0} \frac{\lambda}{\Lambda(1-\pi)+\gamma} = \frac{\lambda}{\Lambda(1-\pi)}. \tag{3.116}$$

$$\tag{3.117}$$

and

$$\lim_{(\mu,\gamma)\to 0} p(0,0) = \lim_{(\mu,\gamma)\to 0} \frac{1-Q}{1+\frac{q}{1-q}\frac{1-Q}{1-pQ}} = \frac{1-\frac{\Lambda}{\lambda+\Lambda p}}{1+\frac{\frac{\lambda}{\Lambda(1-\pi)}}{1-\frac{\lambda}{\Lambda(1-\pi)}}\frac{1-\frac{\Lambda}{\lambda+\Lambda p}}{1-\frac{\Lambda p}{\lambda+\Lambda p}}}, \tag{3.118}$$

$$= \frac{[\lambda-\Lambda(1-p)][\Lambda(1-\pi)-\lambda]}{\Lambda(p-\pi)(\lambda+\Lambda p)}. \tag{3.119}$$

$$\lim_{(\mu,\gamma)\to 0} \frac{p(1,0)}{p(0,0)} = \lim_{(\mu,\gamma)\to 0} \frac{q}{(1-pQ)} = \frac{\frac{\lambda}{\Lambda(1-\pi)}}{1-\frac{\Lambda p}{\lambda+\Lambda p}} = \frac{\lambda+\Lambda p}{\Lambda(1-\pi)}. \tag{3.120}$$

Thus, equation (3.112) becomes:

$$C = f(\frac{p^2\Lambda+p(2\lambda-\Lambda)-\lambda\pi}{\Lambda(p-\pi)(\frac{\lambda}{\Lambda}+p)((N-1)+\frac{B}{\Lambda})}). \tag{3.121}$$

However, the error probabilities π and p are linked to C in the following context. Knowing that $p > \pi$ from Remark 3 we may assume that $p = \pi + \epsilon$ where $\epsilon > 0$, and error probabilities can be linked as $p = 1 - C$, $\pi = 1 - C - \epsilon$.
Thus, equation (3.121) becomes:

$$C = f(\frac{C^2-C(\varsigma+1)+\varsigma(\epsilon+1)}{\epsilon\kappa(\varsigma+1-C)}). \tag{3.122}$$

where $\varsigma = \frac{\lambda}{\Lambda}$ and $\kappa = (N-1)+\frac{B}{\Lambda}$.

On the other hand, $Q < 1$ and $q < 1$ must be satisfied in order to prevent the summations diverging to infinity.

- If $Q < 1$, then $\Lambda < \lambda + \Lambda p$, so that $C < \varsigma$.
- If $q < 1$, then $\lambda < \Lambda - \Lambda\pi$, so that $\varsigma < C + \epsilon$.

Therefore, the system can only operate, when the condition $0 < C < \varsigma < C + \epsilon < 1$ is satisfied.

It is easily observed that C is equal to a function of C such that $C = f(g(C)) = h(C)$. In this case, finding a closed-form expression for the value C is elusive; however, the existence and uniqueness of the solution can be considered.

Lemma 3.2. *$g(\cdot)$ is a decreasing function on $(0, \varsigma)$, if $(1 + \epsilon) < \frac{1}{\varsigma}$.*

Proof. If $g'(C) < 0$, then $g(\cdot)$ is a decreasing function on $(0, \varsigma)$.

$$g'(C) = \frac{1}{\epsilon\kappa}[\frac{(2C - (\varsigma + 1))(\varsigma + 1 - C)}{(\varsigma + 1 - C)^2} + \frac{(C^2 - C(\varsigma + 1) + \varsigma(1 + \epsilon))}{(\varsigma + 1 - C)^2}] \quad (3.123)$$

$$= \frac{1}{\epsilon\kappa}(\frac{\varsigma(1 + \epsilon)}{(\varsigma + 1 - C)^2} - 1). \quad (3.124)$$

If $g'(C) < 0$, then $\varsigma(1 + \epsilon) < (\varsigma + 1 - C)^2$. We can easily write the following relation $1 < (\varsigma + 1 - C)^2 < (\varsigma + 1)^2$, since $0 < C < \varsigma$. Thus, if the condition $(1 + \epsilon) < \frac{1}{\varsigma}$ holds, then $g(\cdot)$ is a decreasing function. □

Lemma 3.3. *If $g(\cdot)$ is a decreasing function, similarly $h(\cdot)$ is also a decreasing function.*

Proof. $\forall\{C', C''\} \in (0, \varsigma)$, if $C' < C''$ then $g(C') > g(C'')$ and $h(C') = f(g(C')) > f(g(C'')) = h(C'')$, since $f(\cdot)$ is an increasing function. Thus, $h(\cdot)$ is also a decreasing function on $(0, \varsigma)$. □

Theorem 3.4. *If $(1 + \epsilon) < \frac{1}{\varsigma}$ and $\varsigma > h(\varsigma)$, then there exists a unique C^* such that $C^* = h(C^*)$ where $\forall C^* \in (0, \varsigma)$.*

Proof. The proof can be carried out by using geometric interpretation. In Figure 3.3, we can observe that any continuous decreasing function passing through the points $(0, h(0))$ and $(\varsigma, h(\varsigma))$ must cross the line $y = x$ at a unique point provided the condition $\varsigma > h(\varsigma)$ is satisfied. Thus, $\exists C^* \in (0, \varsigma)$ such that $C^* = h(C^*)$ while $(1+\epsilon) < \frac{1}{\varsigma}$ and $\varsigma > h(\varsigma)$. □

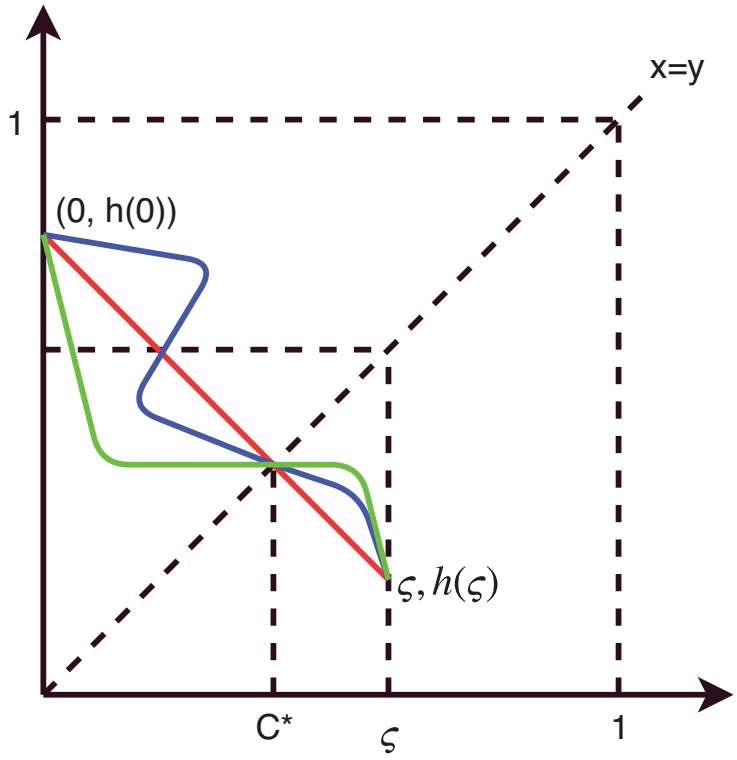

FIGURE 3.3: Arbitrary decreasing functions intersect with the line $x = y$ at only one point, where $C^* = h(C^*)$.

3.2.6.1 A Numerical Example

If an unmodulated binary phase shift keying (BPSK) transmission scheme is used, then each packet consists of n independent binary symbols which are transmitted with noise and interference. In this case, the probability of correctly decoding each binary symbol from node i is [99]:

$$1 - Q\left(\sqrt{\frac{X_i}{\sum_{\substack{j=1 \\ j\neq i}}^{N} \phi_i + B_i}}\right), \tag{3.125}$$

and the function f can be simplified to:

$$f(x) = [1 - Q(\sqrt{x})]^n, \tag{3.126}$$

$$f(g(C)) = [1 - Q(\sqrt{g(C)})]^n. \tag{3.127}$$

Figure 3.4 shows the relation between the probability of transmitted data correctly received and the number of EHWSN in the network for different ς values. The larger networks with more EHWSNs obviously lead to smaller correctly received probabilities, while the larger ς values result in fewer transmission errors.

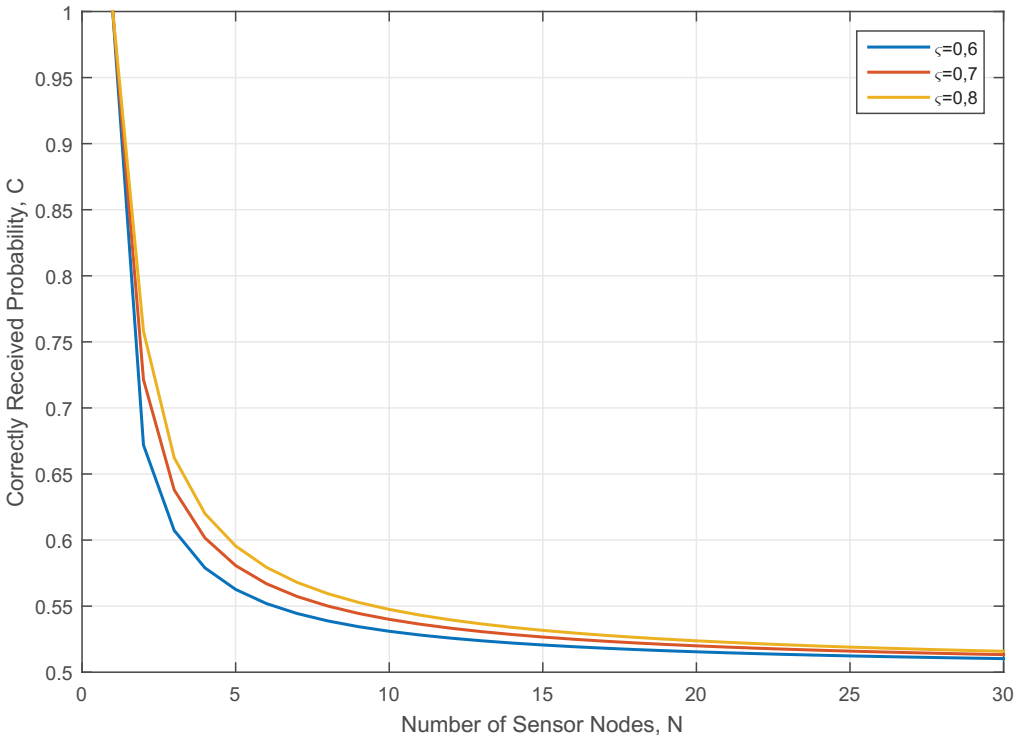

FIGURE 3.4: Relation between correctly received probability, C, and the number of the sensor nodes in the network, N.

3.3 Transmission with K Energy Packets

Again consider an EHWSN in which DPs can be transmitted via a perfect transmitter. However, in this section we assume a model where a successful transmission can occur only by consuming $K > 1$ EPs instead of a single EP. Similarly, we consider that the arrival of DPs and EPs occur according to two distinct independent Poisson processes with rates λ and Λ, respectively. However, we do not consider energy and data leakages from the buffers. In addition, as in the previous section we assume whenever enough energy is available and there are DPs waiting they will be instantaneously transmitted until the EPs or DPs are depleted.

3.3.1 Mathematical Model

Let us write $p(d,e,t) = Prob[D(t) = d, E(t) = e]$. We need only to consider $p(d,e,t)$ for the state space S of pairs of integers $(d,e) \in S$ such that:

$$S = \{(0,0),(d,0),(0,e),(l,k) : \tag{3.128}$$

$$1 \leq d \leq D, 1 \leq e \leq E, 1 \leq l < D, 1 \leq k < K\}, \tag{3.129}$$

where D (E) is the maximum amount of DP (EP), which can be stored in the data (energy) buffer.

Figure 3.5 illustrates the state transition of the CTMC with a defined state space. The following balance equations can be written according to the state diagram in Figure 3.5:

$$p(0,0)[\lambda + \Lambda] = \Lambda\ p(1,K-1) + \lambda\ p(0,K), \tag{3.130}$$

$$p(d,0)[\lambda + \Lambda] = \Lambda\ p(d+1,K-1) + \lambda\ p(d-1,0), \tag{3.131}$$

$$p(D,0)[\Lambda] = \lambda\ p(D-1,0), \tag{3.132}$$

$$p(0,e)[\lambda + \Lambda] = \Lambda p(0,e-1) + \lambda p(0,e+K)1[E \geq e+K], \tag{3.133}$$

$$p(0,E)[\lambda] = \Lambda\ p(0,E-1), \tag{3.134}$$

$$p(l,k)[\lambda + \Lambda] = \Lambda p(l,k-1) + \lambda p(l-1,k), \tag{3.135}$$

$$p(D,k)[\Lambda] = \Lambda p(D,k-1) + \lambda p(D-1,k), \tag{3.136}$$

where equation 3.135 is valid for $0 < l < D,\ 0 < k < K$ and equation 3.136 is valid for $0 < k < K$.

Finding a closed-form expression for the stationary probability distributions is elusive considering above equilibrium equations. However, we can use the cylindrical symmetry of the state diagram of CTMC to define a *one-to-one* and *onto* function. This function combines the data and energy indices into a single index such that:

$$p(d,e) = \tilde{p}(dK - e + E). \tag{3.137}$$

Following the state transformation, it is observed that there is a decreasing order among the states starting from $(DK + E)$ to (0). Thus, the state transitions can be modelled as a one-dimensional Markov chain as in Figure 3.6.

For the one-dimensional CTMC model, state transitions can basically be separated into 3 different regions according to similar transitions behaviours of the states. Therefore,

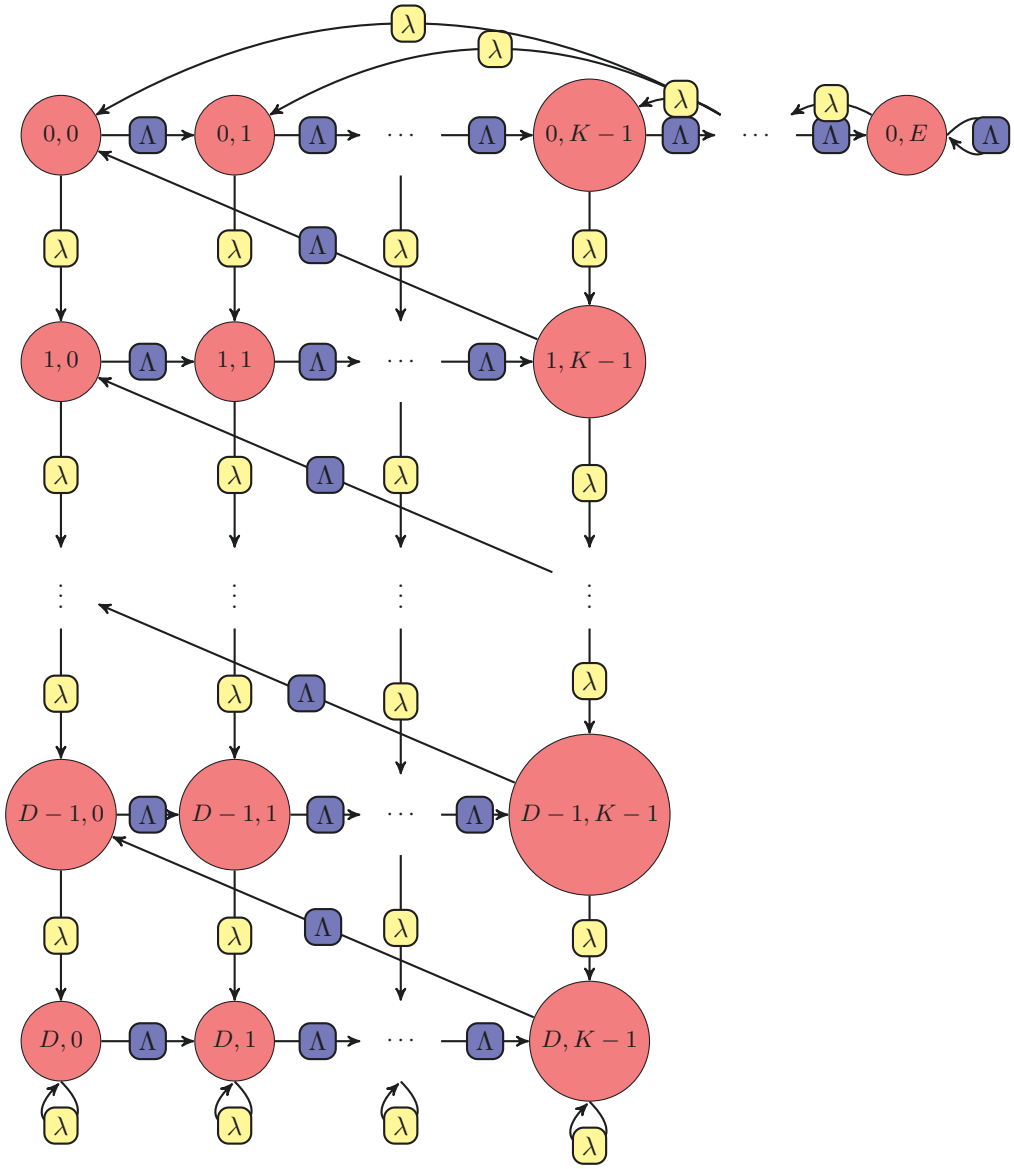

FIGURE 3.5: State transition for the model where a successful DP transmission can occur by consuming K EPs.

complication of the analysis can be reduced and the following balance equations can be written for each region where $\xi \triangleq DK + E - K$:

- *Region1,* $\xi < N \leq \xi + K$*:*

$$\tilde{p}(\xi + K)\Lambda = \lambda \tilde{p}(\xi), \tag{3.138}$$

$$\tilde{p}(N)\Lambda = \lambda \tilde{p}(N - K) + \Lambda \tilde{p}(N + 1). \tag{3.139}$$

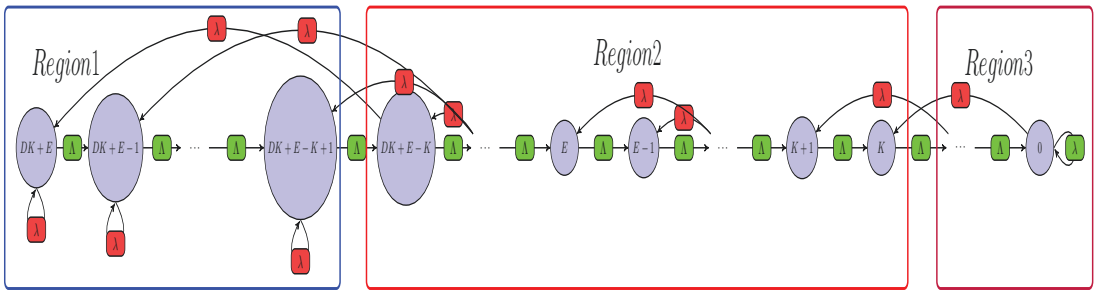

FIGURE 3.6: After the state transition we have one-dimensional CTMC state diagram that simplifies the analysis

- *Region2,* $K \leq N \leq \xi$*:*

$$\tilde{p}(N)[\Lambda + \lambda] = \lambda \tilde{p}(N - K) + \Lambda \tilde{p}(N + 1). \tag{3.140}$$

- *Region3,* $0 < N < K$ *:*

$$\tilde{p}(N)[\Lambda + \lambda] = \Lambda \tilde{p}(N + 1), \tag{3.141}$$

$$\tilde{p}(0)\lambda = \Lambda \tilde{p}(1). \tag{3.142}$$

Equation (3.140) is a recurrence relation of order of $(K + 1)$ and it leads to obtain the stationary probabilities in Region 2. Thus, the characteristic equation is:

$$\Theta^{K+1} - (1 + \frac{\lambda}{\Lambda})\Theta^K + \frac{\lambda}{\Lambda} = 0. \tag{3.143}$$

Equation (3.143) has $K + 1$ roots, namely $\{\vartheta_1, \vartheta_2, ..., \vartheta_{K+1}\}$ so that the closed-form expression for the distribution is given by:

$$\tilde{p}(N) = c\Theta^N = c(\sum_{j=1}^{K+1} a_j \vartheta_j)^N \tag{3.144}$$

where c is an arbitrary constant and the set of $a_j's$ should be such that Θ must be real valued in the interval $(0, 1)$.

Applying Descartes' rule of signs [100], it can be concluded that equation (3.143) has either two or zero positive real roots, one negative real root, and either $K - 3$ or $K - 1$ complex valued roots. Here, equation (3.143) is rewritten as

$$\Theta^K \left(\lambda + \Lambda(1 - \Theta)\right) - \lambda = 0. \tag{3.145}$$

Since 1 is a root of this equation, (3.143) has exactly 2 positive real roots.

When we consider the state $(K-1)$, by equation (3.141) we can write:

$$\tilde{p}(K-1) = \frac{\Lambda}{\Lambda+\lambda} c\Theta^K. \tag{3.146}$$

By using (3.146) in further calculations, the stationary probabilities in Region 3 can be expressed as:

$$\tilde{p}(K-i) = (\frac{\Lambda}{\Lambda+\lambda})^i c\Theta^K,\ 0 < i < K \tag{3.147}$$

or

$$\tilde{p}(N) = (\frac{\Lambda}{\Lambda+\lambda})^{K-N} c\Theta^K,\ 0 < N < K \tag{3.148}$$

and

$$\tilde{p}(0) = \frac{\Lambda}{\lambda}(\frac{\Lambda}{\lambda+\Lambda})^{K-1} c\Theta^K. \tag{3.149}$$

Moreover, when considering the state $(\xi+1)$, using equation (3.140) we can write:

$$\tilde{p}(\xi+1) = c\Theta^{\xi}(1 + \frac{\lambda}{\Lambda}(1-\Theta^{-K})). \tag{3.150}$$

By using (3.150) in further calculations, the stationary probabilities in Region 1 can be expressed as:

$$\tilde{p}(\xi+m) = c\Theta^{\xi}\left(1 + \frac{\lambda}{\Lambda}(1-\Theta^{-K}\sum_{i=0}^{m-1}\Theta^i)\right), \tag{3.151}$$

where $0 < m < K$ and

$$\tilde{p}(\xi+K) = \frac{\lambda}{\Lambda} c\Theta^{\xi}. \tag{3.152}$$

Using the fact that the sum of the probabilities is 1:

$$\sum_{N=0}^{DK+E} \tilde{p}(N) = \sum_{N=0}^{K-1} \tilde{p}(N) + \sum_{N=K}^{\xi} c\Theta^N + \sum_{N=\xi+1}^{DK+E} \tilde{p}(N) = 1, \tag{3.153}$$

where

$$\sum_{N=0}^{K-1}\tilde{p}(N) = \tilde{p}(0)+\sum_{N=1}^{K-1}\tilde{p}(N), \tag{3.154}$$

$$= \frac{\Lambda}{\lambda}(\frac{\Lambda}{\lambda+\Lambda})^{K-1}c\Theta^K + c\Theta^K\sum_{N=1}^{K-1}\frac{\Lambda}{\Lambda+\lambda}^{K-N}, \tag{3.155}$$

$$= \frac{\Lambda}{\lambda}(\frac{\Lambda}{\lambda+\Lambda})^{K-1}c\Theta^K + c\Theta^K\frac{\Lambda}{\lambda}(1-(\frac{\Lambda}{\lambda+\Lambda})^{K-1}), \tag{3.156}$$

$$= c\Theta^K\frac{\Lambda}{\lambda} \tag{3.157}$$

Following some further algebra the summation (3.153) reduces to:

$$c\Theta^K\frac{\Lambda}{\lambda}+\frac{c(\Theta^K-\Theta^{\xi+1})}{1-\Theta}+\sum_{m=1}^{K}\tilde{p}(\xi+m)=1. \tag{3.158}$$

where

$$\sum_{m=1}^{K}\tilde{p}(\xi+m) = c\sum_{m=1}^{K-1}\left(\Theta^\xi+\Theta^\xi\frac{\lambda}{\Lambda}-\Theta^{\xi-K}\sum_{i=0}^{m-1}\Theta^i\right)+c\Theta^\xi\frac{\lambda}{\Lambda}. \tag{3.159}$$

Further simplification can be carried out for equation (3.159) giving:

$$c\Theta^\xi(K(1+\frac{\lambda}{\Lambda})-1)+c\Theta^{\xi-K}\left(\frac{\Theta^K-K(\Theta-1)-1}{(\Theta-1)^2}\right). \tag{3.160}$$

Thus:

$$\sum_{N=0}^{DK+E}\tilde{p}(N) = c\Theta^K\frac{\Lambda}{\lambda}+\frac{c(\Theta^K-\Theta^{\xi+1})}{1-\Theta} \tag{3.161}$$

$$+ c\Theta^\xi[K(1+\frac{\lambda}{\Lambda})-1-\frac{\Theta^{-K}(1+K(\Theta-1))-1}{(\Theta-1)^2}] \tag{3.162}$$

$$= 1. \tag{3.163}$$

Moreover, an infinite data buffer, i.e., $D\to\infty$ can be assumed such that the summation reduces to:

$$\sum_{N=0}^{\infty}\tilde{p}(N) = c\Theta^K\left(\frac{\Lambda}{\lambda}+\frac{1}{1-\Theta}\right)=1. \tag{3.164}$$

Following further analysis, 3.164 becomes:

$$\Theta^{K+1}-\left(1+\frac{\lambda}{\Lambda}\right)\Theta^K+\frac{\lambda}{c\Lambda}-\frac{\lambda\Theta}{c\Lambda}=0. \tag{3.165}$$

Substituting equation (3.143) into equation (3.165) gives:

$$c = 1 - \Theta. \tag{3.166}$$

Thus, the solution is :

$$\tilde{p}(N) = \begin{cases} (1-\Theta)\Theta^N, & K \leq N < \infty \\ (1-\Theta)\Theta^K(\frac{\Lambda}{\Lambda+\lambda})^{K-N}, & 0 < N < K \\ (1-\Theta)\Theta^K\frac{\Lambda}{\lambda}(\frac{\Lambda}{\lambda+\Lambda})^{K-1}, & N = 0 \end{cases}$$

where Θ is the summation of linearly combined roots of equation (3.143).

Note that equation (3.143) cannot be solved in radicals for $K \geq 4$ by the Abel & Ruffini theorem [101]. This means that there does not exist an explicit expression for the roots of such equations as a function of the coefficients by means of algebraic operations and roots of natural degrees. Thus, it is better to adjust the system model in order that one DP can be transmitted by 4 or less EPs. Nevertheless, solutions can be considered numerically for high K values.

3.3.2 Modelling the Interference and the Noise

The arrival rate of EPs Λ is itself in units of power, i.e. the flow of EPs per second maps into power entering the EHWSN via harvesting. Assuming that a single EP contains a unit of energy and that the power level that has been set to transmit one data packet is K.

Alternatively, *on average* the total radiated power ϕ from a node is simply the power entering the node from harvesting, minus that which is lost through energy loss due to the finite capacity of the energy buffer, assuming a "perfect" transmitter that does not waste any power in electronics. Of course this is unreasonable, however the lost effect may be "hidden" in the value Λ, i.e. this rate is merely the amount of power that reaches the transmitter after the energy is harvested and then used (in part) to operate the sensor's electronic circuits. This gives:

$$\phi = \Lambda - L_e, \tag{3.167}$$

where

$$L_e = \Lambda \sum_{n=0}^{\infty} p(n, E) = \Lambda p(0, E) = \Lambda \tilde{p}(0). \tag{3.168}$$

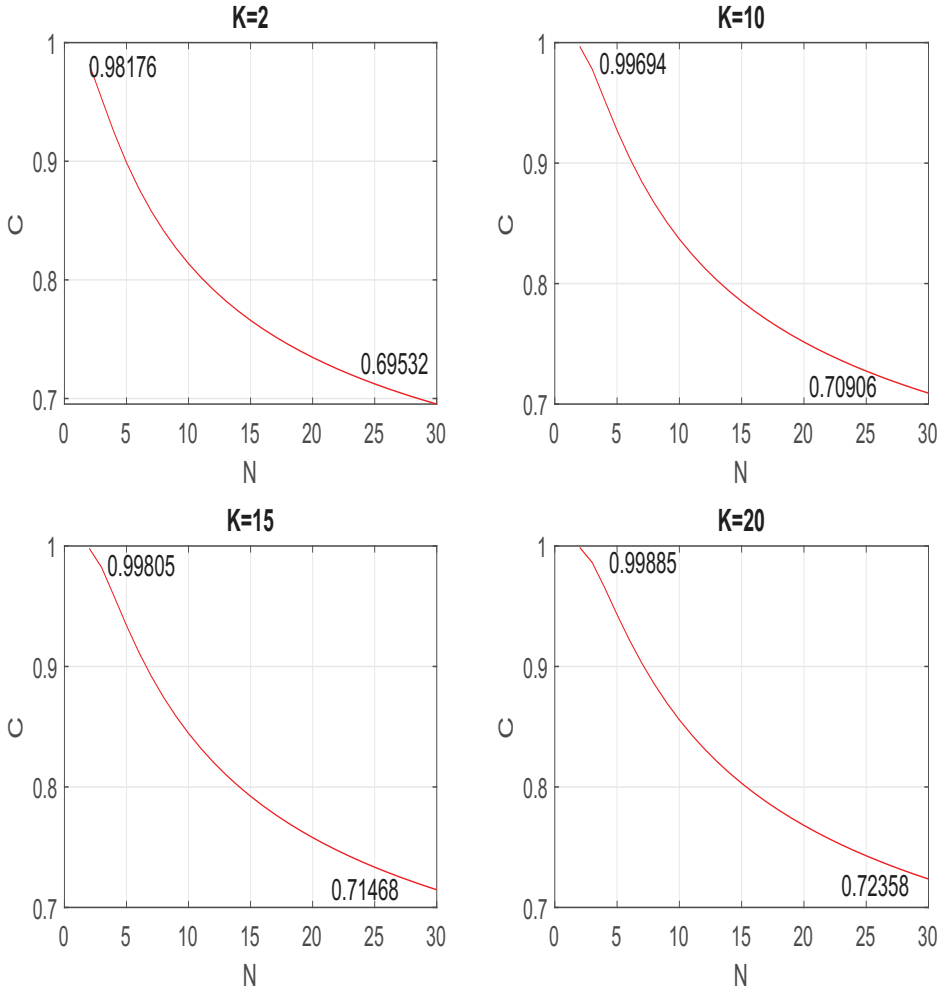

FIGURE 3.7: The relation between the probability of correct detection of a bit C and the number of simultaneously transmitting wireless sensors N, for different transmission power levels K.

Now consider a particular EHWSN, say the i-th, operating in proximity with a total of N wireless sensors all transmitting at the same power level K. In the communication channel due to noise of power level B at the receiver, plus the interference at level I from the other sensors, assuming that the transmission of a $+1$ is as likely as that of the transmission of a -1, the probability C of correct detection of a bit by the receiver can be written as:

$$C = \frac{1}{2}\{Prob[\alpha K > \alpha I + B] + Prob[-\alpha K + \alpha I + B \leq 0]\},$$

where $0 \leq \alpha \leq 1$ is the fraction of transmitter power received with respect to the amount transmitted, and $I = \sigma\phi(N-1)$ where $0 \leq \sigma \leq 1$ represents the "side-band interference" effect. If multiple transmitters use some closely related frequency, they will avoid using exactly the same frequencies, but their side-bands will interfere with each other so that

we may expect σ to be much less than one. With BPSK transmissions where both the interference and the noise are assumed to be Gaussian of zero mean [99] the probability of correctly receiving a binary symbol is then:

$$C = 1 - Q(\sqrt{\frac{\alpha K}{\alpha\sigma\phi(N-1)+B}}), \tag{3.169}$$

where $Q(x) = \frac{1}{2}[1 - \text{erf}(\frac{x}{\sqrt{2}})]$.

The value of K has an interesting effect on the error rates. A large K can cause ϕ to grow, and hence it creates more interference. However, it also provides higher power to overcome interference as well as noise. This interesting effect is illustrated in the next section.

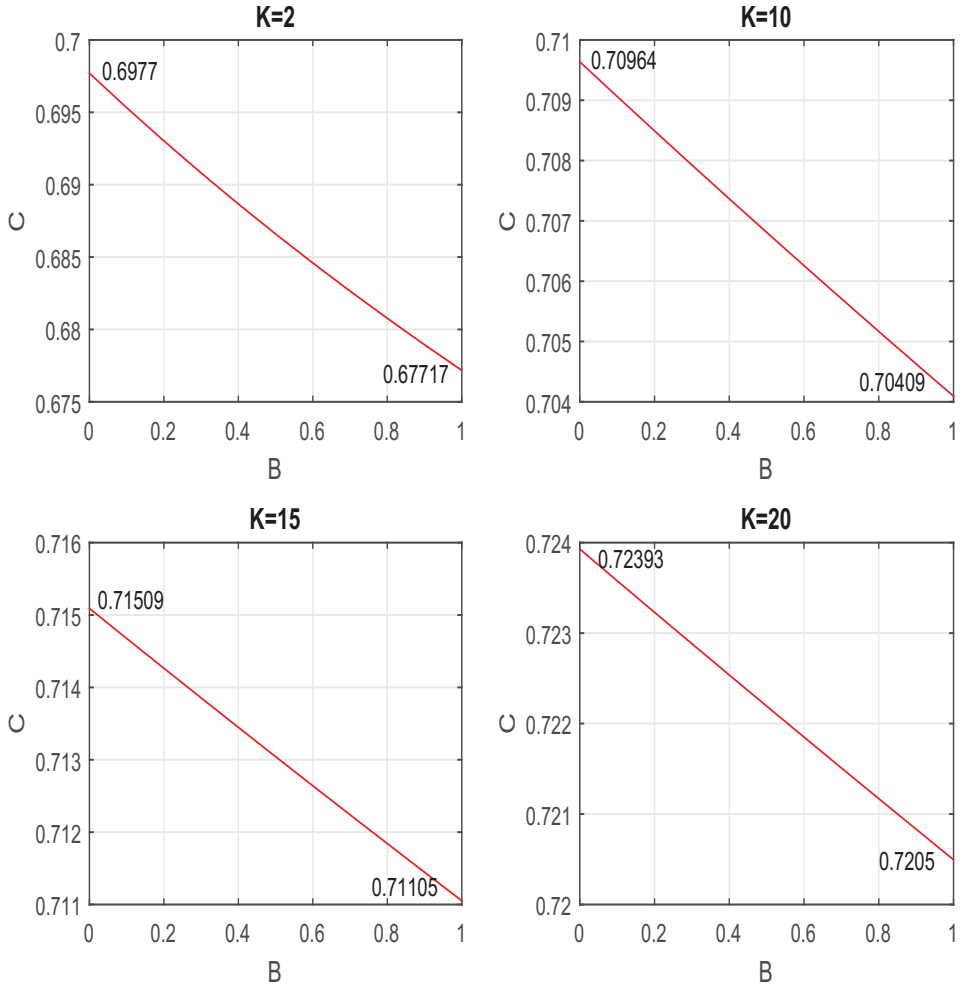

FIGURE 3.8: The relation between C and the noise power B for different values of transmission power K with $N = 30$ mutually interfering transmitters.

3.3.3 Numerical Examples

Figure 3.7 shows the effect of the number of EHWSN N on the correctly received probability C for several values of K. Understandably, an increase in the total number of sensors N will increase the interference in the communication system, so that C will decrease. Moreover, when the required energy to transmit one packet is increased, i.e. K is increased, it is observed that C is slightly higher for the same number of transmitters N.

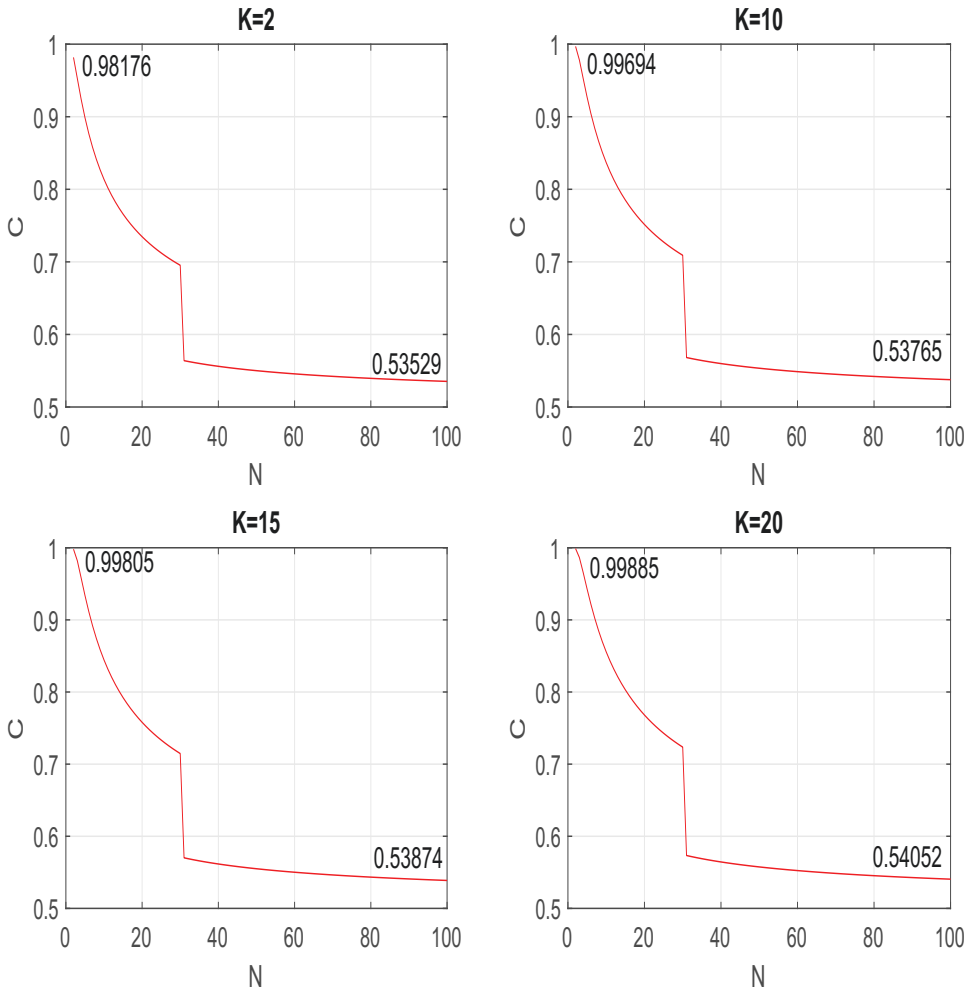

FIGURE 3.9: C versus the number of interfering transmitters as a function of N when we assume a much greater interference effect, represented by $\sigma = 1$, when N exceeds the number of multiplexed frequency bands assumed to be 30. Different transmission power levels K have little effect on the results.

Figure 3.8 illustrates the effect of different noise power levels on C where we set N=30. C is observed to decrease nearly linearly as B increases, and that the effect of transmission power level K is quite limited.

Figure 3.9 reveals an effect not discussed previously. In real systems the total number of frequency bands that are being multiplexed will be limited; here that number is set to 30. Thus when $N = 30$ is exceeded the level of interference is assumed to grow dramatically, i.e. there is a large increase on σ, taking an extreme *worst case* that all the other stations interfere with the one that is being analysed such that $\sigma = 1$.

3.4 Impacts of Modelling Assumptions on the Results

In this chapter, packet arrivals are assumed to be independent Poisson processes, which is a reasonable method to model digital systems studied in this chapter. The justification lies in the fact that the behaviour of large a number of independent arrivals can be firmly approximated by the Poisson distribution. This can be understood by considering three defining properties of the Poisson process: a) one arrival occurs at a time, b) the probability that an arrival occurs at a time is independent of when the other arrivals occurred, and c) the probability that an arrival occurs at a given time does not depend on the time. However, one might think that the arrivals of DPs and EPs at a sensor node may vary with time (for example, energy arrivals from a photovoltaic source will be different for the daytime and the night time). In this case, the packet arrivals can be modelled more faithfully with non-homogeneous Poisson process in which the average rate of arrivals is allowed to vary with time. Although arrival rates changing with time increase the complexity of analysis, several works [102–104] have studied to estimate the long-run average arrival rate. Therefore, the similar steady-state analysis to calculate the stationary probability distributions can be made by using the estimated values of long-average arrival rates.

The other modelling assumption for packet arrivals is that DP and EP arrivals are independent of each other. Although this approach is suitable for many sensor operations, there are some cases where a strong dependency between both packet arrivals exists (e.g. harvesting energy from vibrations to sense vibrations [56]). However, a system can be evaluated in the same way by considering the EP arrival rate is a certain fraction of the DP arrival rate (or vice versa), and the fraction value can be predicted to provide effective operations for a sensor.

Negligible service time is another reasonable assumption since the packet transmission occurs quite fast compared to the time needed to constitute EPs and DPs. This assumption provides simpler random walk and Markov chain models that could be used to analyse sensor states. However, in reality, a certain amount of time (even if it is too small) must be spent for the service. In this case, taking into account of a very small service time will affect the state transition diagrams, and it results in multi-dimensional

Markov chain models. Although it increases the complexity of finding the state distributions, some basic state transformation (as used in Chapter 3) can be applied and solutions for the further analysis can be provided.

In this chapter, the models with both limited and unlimited buffer capacities are examined. Despite the fact that consideration of the unlimited capacity buffers simplifies the computational complexity, they do not have a crucial impact on the results. On the other hand, it must be emphasized that there are some analyses appertaining solely either to the systems with unlimited buffers (e.g. stability) or to the systems with limited buffers (e.g. excessive packets).

It is also assumed that the transmission errors occur with some certain probabilities, which cause retransmissions of the same packets. This retransmission process might repeat itself with the same error and success probabilities, independent of the previous outcome. However, one might expect to observe another transmission error if the previous attempt was not successful. The underlying reason here is the fact that there is an extremely small time interval between the two consecutive transmissions. In this case, a sensor node needs to consume more energy (or EPs) in order to achieve the same correctly received probability of the packet transmission. Hence, the results related to packet transmission errors presented in this chapter are expected to be better than the ones obtaining from the simulation results or the real-time experiments.

3.5 Conclusion

This chapter analyses EHWSN that gather both data and energy from the environment, so that they can operate autonomously. A stochastic model of the harvested energy and the data arrival has been considered in terms of Poisson flows of DPs and EPs. In addition, the effect of energy loss through standby operation, and battery or capacitor leakage, which is represented by an exponentially distributed decay rate is considered. Moreover, time-out data loss, which occurs when a DP has waited too long in the queue due to lack of energy is also considered. As the DP transmission time compared to the DP processing time in the node and sensing time from the ambient environment is very small, it is assumed to occur very fast, i.e. the packet transmission happens instantaneously. Furthermore, a transmission scheme by which DPs can be transmitted via perfect transmitter that does not waste any energy for the node electronics and use all the energy for successful packet transmission is assumed.

In the first part of the chapter, a model where successful transmission can be obtained by consuming a single EP is investigated. First, we obtained a closed-form formula of the

stationary probability distributions through the equilibrium equations. Next, we studied the DP and EP losses due to finite capacity of the data and energy buffers. In addition, the optimum energy efficiency of the transmission to understand the appropriate operating point that would use the minimum amount of energy consumed per transmitted packet was discussed. Moreover, the system stability that can only be a concern when buffer sizes are very large was investigated. A further model that includes energy and data losses, but assumes that the DP buffer, and energy storage capacity, are unlimited was also considered. This is a useful idealisation when the capacities are very large. However, this latter model introduced the interesting question of stability. The model also incorporated transmission error probabilities due to noise and interference. This analysis allowed us to consider the error probabilities when N wireless sensors operate in proximity to each other.

In the second part of the chapter, the system was analysed using a random walk model that represents the random arrivals of DPs, as well as the random arrivals of harvested energy in the form of discrete EPs. Using precise assumptions about the processes that are involved, we obtained the stationary distribution of buffer lengths with limited data and energy buffers, and both DPs and EPs can be lost when their respective buffers are full. This analysis allowed computation of the average transmitted power from a sensor, and to study the behaviour of one sensor in the presence of a collection of interfering sensors as well as of noise at the receiver. In particular, the probability that a receiver in the presence of several identical wireless sensor transmitters receives a finite set of bits correctly was computed. Numerical examples were used to illustrate the contradictory effect of the transmitter power: high power levels can improve the probability of correct packet reception; however, they can also increase interference and have the opposite effect.

Chapter 4

Packet Transmission via Imperfect Transmitter

4.1 Introduction

The work in this chapter is based on references [64, 67, 68]. In this chapter, an EHWSN in which the packet transmission occurs via imperfect transmitter is investigated. In an imperfect transmitter energy is not only consumed for the packet transmission but also for the node electronics, i.e. packet sensing, processing and storing by the sensor node. First, a model in which both node electronics and packet transmission require a single EP, so that successful transmission only occurs by consuming 2 EPs was studied. For this model, a closed-form solution was obtained for the steady-state probability distributions. Other quantities of interest including excessive packet rates and system stability were also investigated. Second, a generalised model in which node electronics and packet transmission require $K_e > 1$ and $K_t > 1$ EPs was considered. Consequently, for a successful transmission an EHWSN needs to consume $K_e + K_t = K$ EPs in total. This model leads a two-dimensional CTMC and several linear algebra techniques have been used to reduce the solution complexity to obtain stationary probability distributions.

4.2 Energy Consumption Model with Single Energy Packet

In this section, an EHWSN where data and energy is received randomly from the ambient environment is modelled. The arrivals of both DPs and EPs at the node are assumed to be independent Poisson process with rates λ and Λ, respectively. In addition, there is standby loss in the system due to self discharge nature of energy storages. This can also be modelled as an independent Poisson process with rate μ.

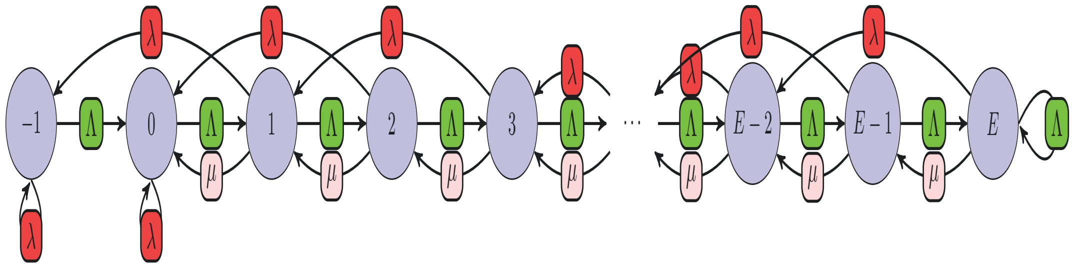

FIGURE 4.1: Random walk representation of the state transitions where the energy consumption for both the node electronics and the packet transmission.

In a typical sensor node, the harvested energy is basically consumed for packet sensing, storing, processing and transmission. In this work, we assume that $K_e = 1$ EP is required for the node electronics (sensing, storing, processing) and $K_t = 1$ EP is required for the packet transmission.

4.2.1 Mathematical Model

Consider a system at a time $t \geq 0$ contains $D(t)$ DPs in the buffer and $E(t)$ EPs in the storage, such that it can model the state of sensor node by the pair of $(D(t), E(t))$. Whenever $E(t) \geq 1$, the node can sense a DP, and one EP is immediately consumed by the node electronics. Moreover, the node can instantaneously transmit the DP by consuming one more EP if there is still available energy in the storage.

On examining the system model carefully, it can be concluded that the system does not allow growing numbers of DPs in the data buffer. In fact, when one DP arrives at the node whose state is $(D(t) = 0, E(t) = 1)$, the state will change as $(D(t) = 1, E(t) = 0)$ and this is the only state where data buffer is not empty. This interesting situation leads to excessive DPs in the system, which will be considered later.

Let us write $p(d, e, t) = Prob[D(t) = d,\ E(t) = e]$. Considering only $p(d, e, t)$ for the state space such that $(e - d) \in S$, where $E \geq (e - d) \geq -1$ and E is the maximum amount of EPs that can be stored in the node.

Consequently, the system can be modelled as a finite CTMC whose states and transition diagram is shown in Figure 4.1. Moreover, the process is irreducible and aperiodic, which means the stationary probabilities $p(e - d) = \lim_{t\to\infty} Prob[D(t) = d,\ E(t) = e]$ exist uniquely and can be computed from the following balance equations:

$$
\begin{aligned}
p(-1)[\Lambda] &= \lambda\, p(1) && (4.1)\\
p(0)[\Lambda] &= \Lambda\, p(-1) + \lambda\, p(2) + \mu\, p(1) && (4.2)\\
p(N)[\Lambda+\lambda+\mu] &= \Lambda\, p(N-1) + \lambda\, p(N+2) + \mu\, p(N+1) && (4.3)\\
p(E-1)[\Lambda+\lambda+\mu] &= \Lambda\, p(E-2) + \mu\, p(E) && (4.4)\\
p(E)[\lambda+\mu] &= \Lambda\, p(E-1). && (4.5)
\end{aligned}
$$

Note that equation (4.3) is valid for $0 < N < E-1$ and has a solution of the form:

$$p(N) = c\ \varphi^N \tag{4.6}$$

where c is an arbitrary constant and φ can be computed from following characteristic equation:

$$\lambda\varphi^3 + \mu\varphi^2 - (\Lambda+\lambda+\mu)\varphi + \Lambda = 0 \tag{4.7}$$

whose roots are $\{\varphi_1 = 1,\ \varphi_{2,3} = \frac{-(\lambda+\mu)\mp\sqrt{(\lambda+\mu)^2+4\Lambda\lambda}}{2\lambda}$. Here the only viable root is φ_3, since the solution must lie in the interval $(0,1)$. In the rest of the section, we consider $\varphi_3 = \varphi$ for the sake of the simplicity.

The followings may also be obtained:

$$
\begin{aligned}
p(-1) &= c\frac{\lambda}{\Lambda}\varphi, && (4.8)\\
p(0) &= c(\frac{\lambda}{\Lambda}\varphi^2 + \frac{\lambda+\mu}{\Lambda}\varphi), && (4.9)\\
p(E-1) &= c[1 + \frac{\lambda+\mu}{\Lambda} - \frac{\mu}{\lambda+\mu}]^{-1}\varphi^{E-2}, && (4.10)\\
p(E) &= c[(\frac{\lambda+\mu}{\Lambda})(\frac{\Lambda+\lambda+\mu}{\Lambda}) - \frac{\mu}{\Lambda}]^{-1}\varphi^{E-2}. && (4.11)
\end{aligned}
$$

Using the fact that summation of the probabilities is one:

$$
\begin{aligned}
\sum_{N=-1}^{E} p(N) &= c(\frac{2\lambda+\mu}{\Lambda}\varphi + \frac{\lambda}{\Lambda}\varphi^2) && (4.12)\\
&+ c\sum_{N=1}^{E-2}\varphi^N + c[\frac{\lambda+\mu}{\Lambda} - \frac{\mu}{\Lambda+\lambda+\mu}]^{-1}\varphi^{E-2} && (4.13)\\
&= 1. && (4.14)
\end{aligned}
$$

Following further calculations, the value of c can be calculated as:

$$c = [\frac{2\lambda+\mu}{\Lambda}\varphi + \frac{\lambda}{\Lambda}\varphi^2 + \frac{\varphi-\varphi^{E-1}}{1-\varphi} + \frac{\Lambda(\Lambda+\lambda+\mu)}{(\lambda+\mu)(\Lambda+\lambda+\mu)-\mu\Lambda}\varphi^{E-2}]^{-1}. \quad (4.15)$$

4.2.2 Excessive Packets due to Finite Buffer Sizes

As the energy storage capacity (maximum E EPs) and data buffer capacity (maximum D DPs) are finite and the data buffer is forced to be empty most of the time, there must be some excessive packets that arrive at the node that cannot be sensed and stored. These excessive packets rates are Γ_d and Γ_e for the DPs and EPs, respectively. They can be computed as:

$$\begin{aligned}
\Gamma_d &= \lambda \sum_{N=0}^{-D} p(N) = \lambda(p(0)+p(-1)) && (4.16)\\
&= c\lambda(\frac{2\lambda+\mu}{\Lambda}\varphi + \frac{\lambda}{\Lambda}\varphi^2), && (4.17)\\
\Gamma_e &= \Lambda p(E) && (4.18)\\
&= c[\frac{1}{\Lambda}[(\frac{\lambda+\mu}{\Lambda})(\frac{\Lambda+\lambda+\mu}{\Lambda}) - \frac{\mu}{\Lambda}]]^{-1}\varphi^{E-2}. && (4.19)
\end{aligned}$$

Figure 4.2 shows the relation between excessive DP rate and data arrival rate at different energy arrival rates assuming $E = 100$ packets and $\mu = 0.1\Lambda$. As can be seen, an increase in the DP arrival rate results in a larger excessive packet rate. Conversely, an increase in the energy arrival has the opposite effect on the excessive packet rate. A reasonable excessive DP rate is observed if λ is below a nominal value according to Λ, even though no more than one DP can be stored in the buffer. This is because DPs can be immediately sensed and transmitted when there are only two or more EPs in the node.

Figure 4.3 shows the relation between excessive EP rate and energy arrival rate for different data arrival rates for $E = 100$ packets and $\mu = 0.1\Lambda$. While an increased EP arrival rate leads to a more excessive EP rate, a larger DP arrival results in a less excessive packet since a larger DP arrival rate triggers EP consumption in the node.

4.2.3 Stability of the System

System stability relates to whether or not a finite number of segregated DPs and EPs remain finite with a certain probability for unlimited data and energy storage capacity when $t \to \infty$. If this condition is satisfied, then the system is said to be stable.

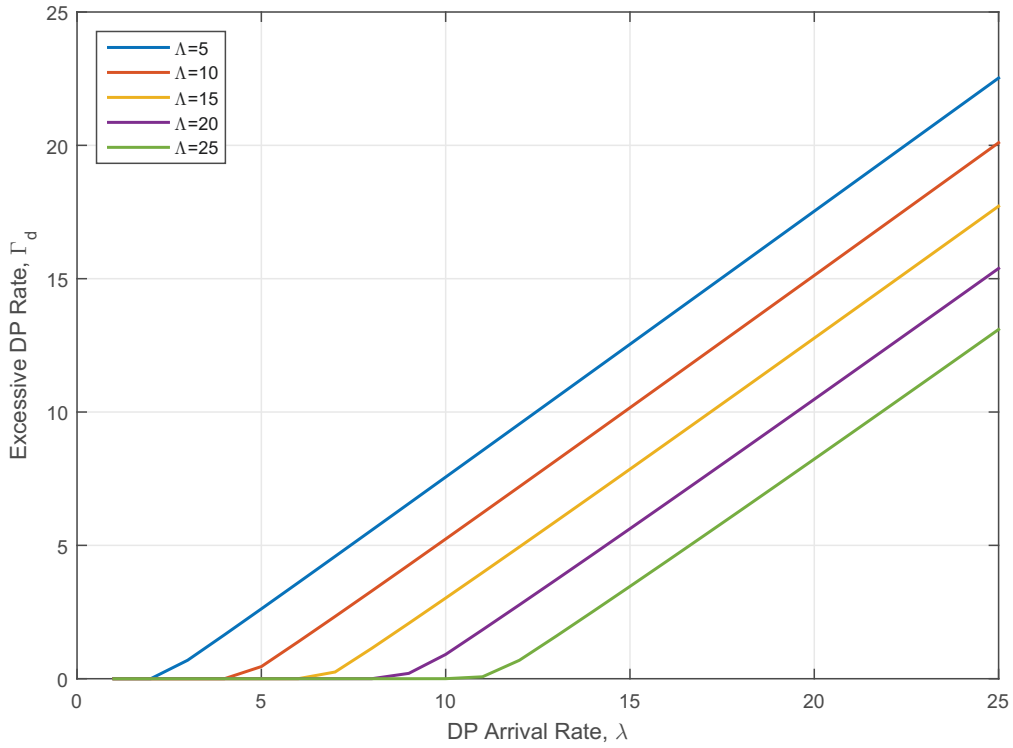

FIGURE 4.2: Excessive DP rate grows with increasing packet arrival rates whereas decreases with increasing energy arrival rates.

In order to make further analysis, a system with unlimited storage is considered. In this case, the following is allowed:

$$p(-1) = c'\frac{\lambda}{\Lambda}\varphi, \tag{4.20}$$

$$p(0) = c'(\frac{\lambda}{\Lambda}\varphi^2 + \frac{\lambda+\mu}{\Lambda}\varphi), \tag{4.21}$$

$$p(N) = c'\varphi^N, \quad N > 0. \tag{4.22}$$

where φ is again solution for equation 4.7 and c' can be computed as:

$$c' = \frac{(\lambda+\mu-2\Lambda)+\sqrt{(\lambda+\mu)^2+4\Lambda\lambda}}{2(2\lambda+\mu)}. \tag{4.23}$$

Moreover, the marginal probabilities can be expressed as:

$$p_d(d) = \sum_{e=0}^{\infty} p(e-d) \tag{4.24}$$

$$p_e(e) = \sum_{d=0}^{\infty} p(e-d) \tag{4.25}$$

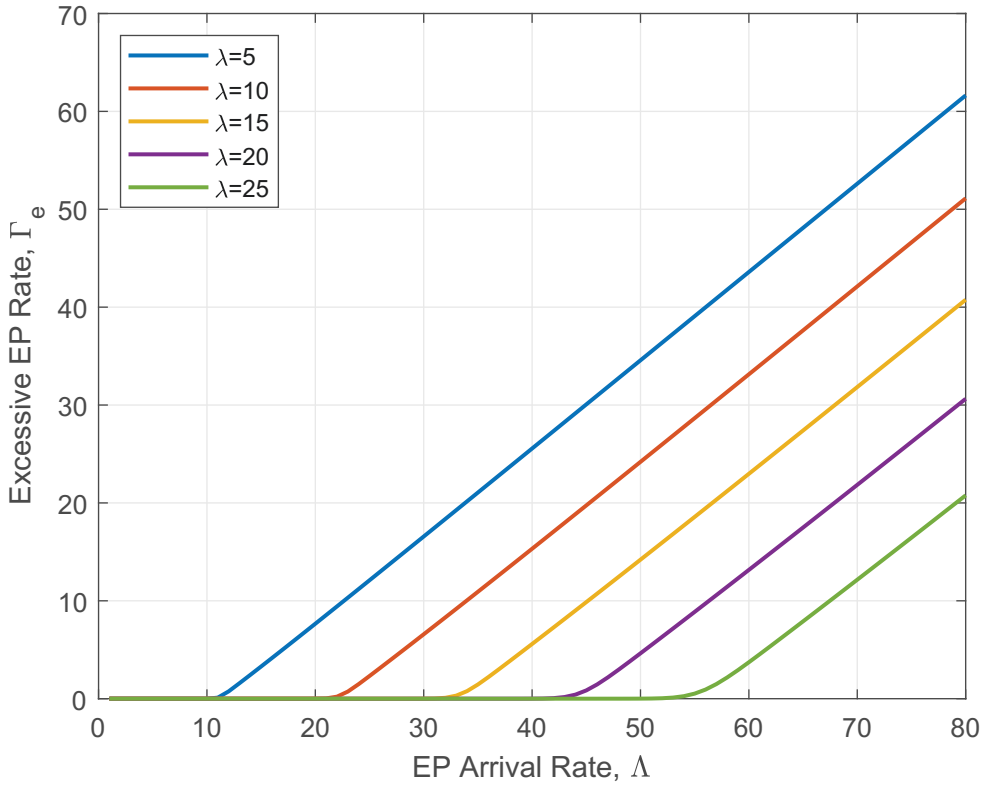

FIGURE 4.3: Excessive EP rate grows with increasing energy arrival rates whereas decreases with increasing data arrival rates.

In steady state, the probabilities that segregate DPs and EPs do not exceed some finite values D' and E':

$$P_d(D') = lim_{t\to\infty} Prob[0 < D(t) \leq D' < \infty], \tag{4.26}$$

$$P_e(E') = lim_{t\to\infty} Prob[0 < E(t) \leq E' < \infty]. \tag{4.27}$$

Thus, the followings can be calculated:

$$P_d(D') = \sum_{d=0}^{D'} \sum_{e=0}^{\infty} p(e-d) \tag{4.28}$$

$$= p_d(1) + p_d(0) \tag{4.29}$$

$$= p(-1) + p(0) + \sum_{N=1}^{\infty} c' \varphi^N \tag{4.30}$$

$$= 1. \tag{4.31}$$

and

$$\begin{aligned} P_e(E') &= \sum_{e=0}^{E'} \sum_{d=0}^{\infty} p(e-d) && (4.32)\\ &= p_e(0) + p_e(e)1[e>0] && (4.33)\\ &= p(-1) + p(0) + \sum_{N=1}^{E'} c'\varphi^N && (4.34)\\ &= 1 - c'\frac{\varphi^{E'+1}}{1-\varphi}. && (4.35) \end{aligned}$$

Thus, it can be concluded that a system with unlimited storage capacity is always stable with respect to DPs and unstable with respect to EPs, as expected.

4.2.4 Analysis of Transmission Error Among a Set of Nodes

The total power entering a sensor node is simply energy harvesting rate Λ, due to the fact that energy rate is in units of power. All harvested power cannot be used by the node, as there are some EP losses. Specifically, standby loss due to the self-discharge nature of the storage and excessive packet loss due to limited storage capacity. Thus, the total power consumed by a node is:

$$\xi_i = \Lambda_i - \Gamma_{e_i} - \mu_i \sum_{N=1}^{E} p_i(N), \tag{4.36}$$

where the subscript i relates to the parameters of the i-th node among a set of M nodes. On transmitting a DP, a node consumes K_e and K_t EPs for the node electronics and the packet transmission, respectively. Assuming $K_e = K_t = 1$, the total radiating power from a sensor on average simplifies to:

$$\phi_i = \frac{\xi_i}{2}. \tag{4.37}$$

Furthermore, the probability of correctly receiving (or decoding) a packet sent by a given node i that transmits at power level K_{t_i} can be denoted by:

$$1 - e_i = f(\frac{\eta_i K_{t_i}}{I_i + B_i}), \tag{4.38}$$

where f is some increasing function of its argument which is the signal to interference I_i plus noise B_i. Moreover, $0 \leq \eta_i \leq 1$ represents the propagation factor of the transmission power that is sensed by the receiver.

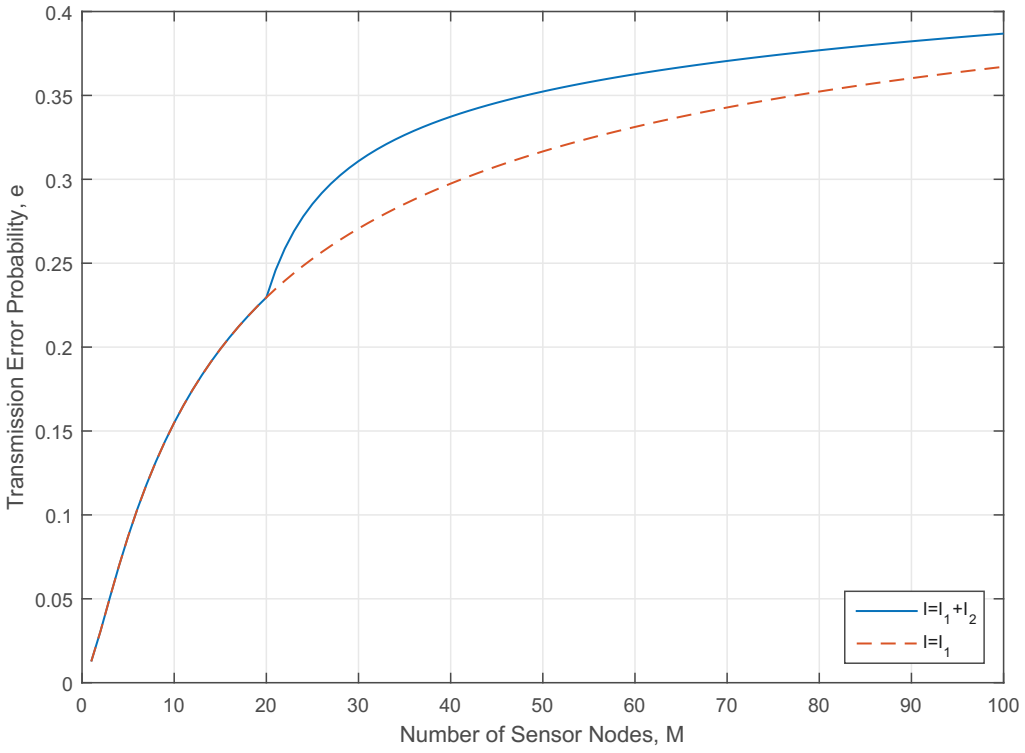

FIGURE 4.4: Transmission error probability vs number of sensor nodes where after a certain number of sensor nodes, α, transmission faces an additional interference, I_2, so that the error probabilities increase.

Some number of 'α' separate frequency channels may be used in the communication medium. If the number of transmitting sensor nodes does not exceed α, distinct frequency channels are being used by each transmitter. In this case, interference can be considered as $I_{1_i} = \sum_{j \neq i} \eta_j \kappa_{0_j} \frac{\xi_j}{2}$, where $0 \leq \kappa_{0_j} \leq 1$ is a factor that represents the effect of side-band frequency channels and its value is expected to be very small. Alternatively, if the number of transmitting sensor nodes exceeds α, some of the transmitters are forced to use a frequency channel already used by others, so that it will cause an additional interference $I_{2_i} = \sum_{j \neq i} \kappa_j \eta_j \frac{\xi_j}{2} \frac{M-\alpha}{M} 1[M > \alpha]$, where κ_i is very close to 1 since interference is direct to the channel. Thus, the total interference is:

$$I_i = I_{1_i} + I_{1_i} = \sum_{j \neq i} \eta_i \frac{\xi_i}{2} (\kappa_{0_i} + (\frac{M-\alpha}{M}) 1[M > \alpha]). \tag{4.39}$$

Assuming that all nodes are identical, we can replace equation (4.38) with:

$$1 - e = f(\frac{\eta K_t}{\eta \frac{\xi}{2} \kappa_0 (M-1) + \eta \frac{\xi}{2} (\frac{M-\alpha}{M}) 1[M > \alpha] + B}). \tag{4.40}$$

Assuming BPSK transmission, we have:

$$1 - e = Q(\sqrt{\frac{\eta K_t}{\eta^{\frac{\xi}{2}}\kappa_0(M-1) + \eta^{\frac{\xi}{2}}(\frac{M-\alpha}{M})1[M > \alpha] + B}}), \tag{4.41}$$

where $Q(x) = \frac{1}{2}[1 - \text{erf}(\frac{x}{\sqrt{2}})]$.

Figure 4.4 shows the effect of number of sensor nodes transmitting in a network on transmission error probability. In this diagram the single bit transmission and system parameters are assumed as $\Lambda = 10, \lambda = 10, \mu = 1, E = 100, B = 0.1, \eta = 0.5, \kappa_0 = 0.05, \alpha = 20$. Consequently, transmission error grows with an increasing number of sensor nodes in the network due to a greater influence of the interference over the transmission. Conversely, following a certain number of sensor nodes, α, the transmission faces an additional interference, I_2, such that the error probabilities increase.

4.3 Generalised Energy Consumption Model

The previous section investigated a model where a DP transmission requires exactly two EPs: one for processing and one for the packet transmission, or $K_e = K_t = 1$. In this section, the approach is generalised by considering arbitrary K_e and K_t values. For each DP, the sensor requires K_e EPs for node electronics including packet sensing, processing, and storing and K_t EPs for the packet transmission. The motivation is that the node electronics and the transmitter may have to vary the power levels they use to deal with the speed of processing or the transmission power to overcome errors. Assuming random processes for sensing and energy harvesting, a two-dimensional random walk model was obtained. Moreover, its complexity was reduced using companion matrices and matrix algebra techniques. The resulting solution allows us to obtain, in steady-state, a closed-form solution for stationary probability distribution for states of the sensor node.

4.3.1 Mathematical Model

It was assumed that a DP can be sensed, processed and stored by a sensor node only when there are at least K_e EPs available in storage. Moreover, these K_e energy packets are effectively expended each time a DP is successfully received by the node. Otherwise, the data will not be received and the sensed data will go unnoticed and be lost. Instead, in order to transmit a DP the node requires an additional number of K_t EPs. Again all K_t EPs will be consumed for one transmission. Thus, the successful sensing and transmission of one DP requires the consumption of $K = K_E + K_t$ EPs.

As in the previous section, both the processing and transmission of a packet were assumed to occur very rapidly, provided enough energy was available to enable instantaneous storage of DP. Moreover, if the amount of energy available is more than K_e but less than K, DP will be both processed and transmitted when the amount of energy available is at least K EPs. Under these assumptions, a two-dimensional continuous time Markov chain was constructed to represent the behaviour of the system.

Let $D(t)$ and $E(t)$ be the number of DPs and EPs in the sensor node at time $t \geq 0$, so that state of the system can be represented by the pair $(D(t), E(t))$ and the state space S is of pairs of integers $(d, e) \in S$ such that:

$$S = \{(0,0), (d,0), (0,e), (l,k) : 0 < d \leq D,\ 0 < e \leq E, \\ 0 < l < D, 0 < k < K,\ K = K_e + K_t\}. \tag{4.42}$$

When considering the general values for $K_e > 1$ and $K_t > 1$, the system is no longer modeled as a one-dimensional CTMC but rather a two-dimensional CTMC as is shown in Figure 4.5. Since the energy consumption for many sensor node applications is mainly dominated by the data transmission subsystem [105], $K_t > K_e$ was assumed for the current system model.

Accordingly, the following global balance equations can be written for the model:

$$\begin{aligned}
p(0,0)[\Lambda] &= \Lambda p(1, K-1) + \lambda p(0, K), && (4.43)\\
p(0,e)[\Lambda] &= \Lambda p(0, e-1) + \lambda p(0, e+K) 1[E \geq e+K],\ 1 \leq e < K_e, && (4.44)\\
p(0,e)[\Lambda+\lambda] &= \Lambda p(0, e-1) + \lambda p(0, e+K) 1[E \geq e+K],\ K_e \leq e < E, && (4.45)\\
p(0,E)[\lambda] &= \Lambda p(0, E-1), && (4.46)\\
p(d,0)[\Lambda] &= \Lambda p(d+1, K-1) + \lambda p(d-1, K_e),\ 1 \leq d < D, && (4.47)\\
p(d,e)[\Lambda] &= \Lambda p(d, e-1) + \lambda p(d-1, e+K_e),\ 1 \leq d < D,\ 1 \leq e < K_e, && (4.48)\\
p(d,e)[\Lambda+\lambda] &= \Lambda p(d, e-1) + \lambda p(d-1, e+K_e),\ 1 \leq d < D,\ K_e \leq e < K_t, && (4.49)\\
p(d,e)[\Lambda+\lambda] &= \Lambda p(d, e-1),\ 1 \leq d < D,\ K_t \leq e < K, && (4.50)\\
p(D,e)[\Lambda] &= \Lambda p(D, e-1) + \lambda p(D-1, e+K_e),\ K_e \leq e < K_t, && (4.51)\\
p(D,e)[\Lambda] &= \Lambda p(D, e-1),\ K_t \leq e < K, && (4.52)\\
p(D,0)[\Lambda] &= \lambda p(D-1, K_e). && (4.53)
\end{aligned}$$

Finding a closed-form solutions for stationary probability distributions and other quantities using these balance equations is elusive. Therefore, different approaches have been explored for this particular system model.

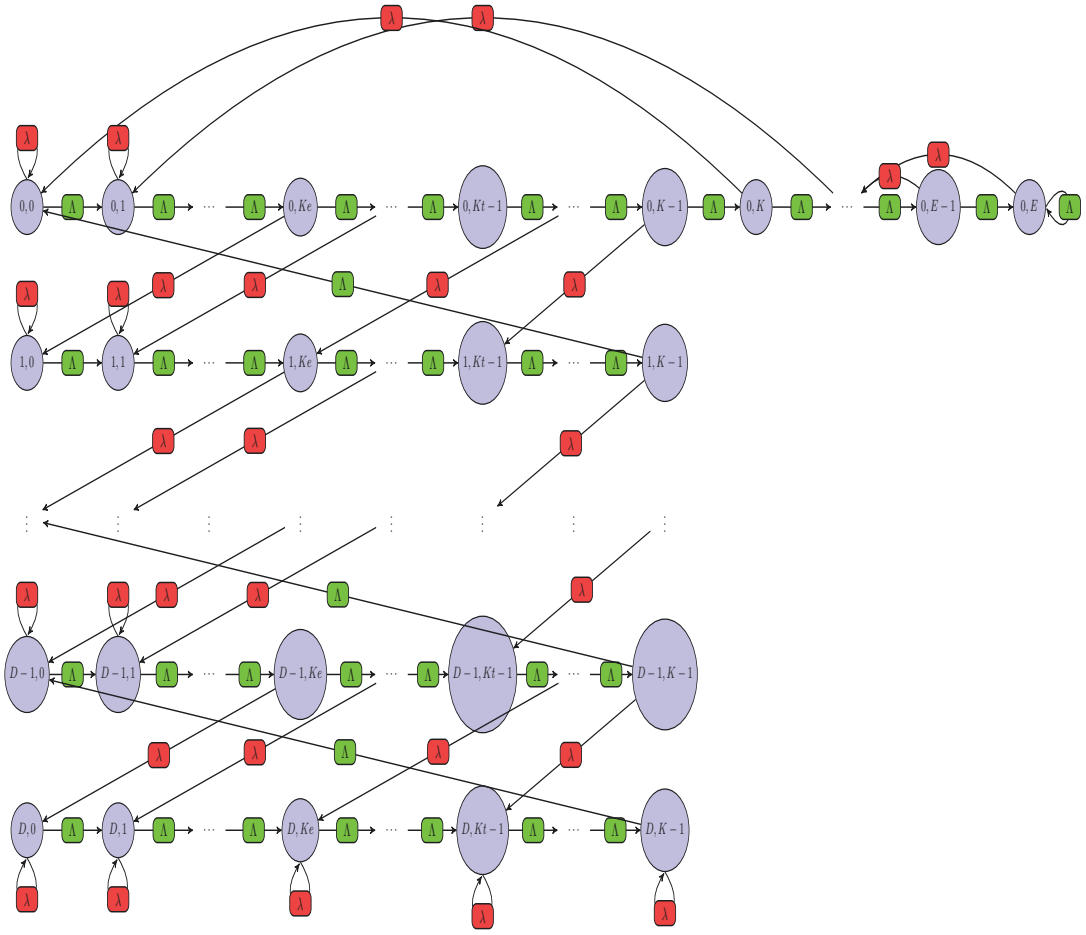

FIGURE 4.5: Two-dimensional CTMC state transition representation for the generalised values of K_e and K_t.

Using a traditional approach, we define a generator matrix Q to find the stationary probabilities. Q is an $n \times n$ matrix of an n state Markov chain. In our system model, it can be easily observed that $n = E + BK + 1$. For matrix Q, the entry in the j^{th} column of the i^{th} row of the matrix $j \neq i$ will be p_{ij}, i.e. the instantaneous transition rate from state x_i to state x_j . In other words, it will be the sum of the parameters labelling arcs that connect nodes i and j in the state transition diagram. The diagonal elements have been selected to ensure that the sum of the elements in every row is zero, i.e. $p_{ii} = -\sum_{j \in S,\ j \neq i} p_{ij}$. When the model is in steady state, in order to maintain the equilibrium, it is assumed that the total probability flux out of a state is equal to the total probability flux into the state. Consequently, for any particular state x_i,

$$\pi_i \sum_{x_j \in S,\ j \neq i} p_{ij} = \sum_{x_j \in S,\ j \neq i} \pi_j p_{ij} \tag{4.54}$$

Since $p_{ii} = -\sum_{j \in S \ j \neq i} p_{ij}$, we have:

$$\sum_{x_j \in S} \pi_j p_{ij} = 0 \tag{4.55}$$

Expressing the stationary probability of each state π_i as a row vector π, the matrix equation can be written as $\pi Q = 0$.

The π_i are unknown and are the values under consideration. As π_i is a probability distribution, the normalisation condition holds: $\sum_{x_i \in S} \pi_i = 1$. Thus, with these $n+1$ equations (global balance equations and normalisation condition) the n unknowns can be solved.

In order to find π_i values, $E+BK+2$ equations are dealt with in the current model. This means that the complexity of the solution increases dramatically with increasing data and energy buffer sizes. Thus, more time and energy is required to deal with the further complexity of the solution. Therefore, a different solution using companion matrices and matrix algebra techniques to decrease the solution complexity is proposed.

4.3.2 Solution with Companion Matrices

In order to simplify the calculations, two state indices of the sensor node can be merged by defining a one-to-one and onto function such that:

$$S_j = p(d, e) : j = dK - e + E, \ j \in \{0, 1, \cdots, DK + E\}. \tag{4.56}$$

Thus, each state (d, e) can be mapped uniquely onto states j. Next, each row of the two-dimensional CTMC can be considered as a vector V_i where $0 \leq i \leq D$. This gives the following:

$$\begin{aligned}
V_0 &= [S_E, S_{E-1}, \cdots, S_1, S_0], && (4.57)\\
V_1 &= [S_{E+K}, S_{E+K-1}, \cdots, S_{E+2}, S_{E+1}], && (4.58)\\
V_2 &= [S_{E+2K}, S_{E+2K-1}, \cdots, S_{E+2+K}, S_{E+1+K}], && (4.59)\\
&\vdots && (4.60)\\
V_D &= [S_{E+DK}, \cdots, S_{E+2+DK-K}, S_{E+1+DK-K}]. && (4.61)
\end{aligned}$$

Following careful examination of the diagram, it was observed that each row, except the first and the last one, has the similar state transition behaviours. Consequently, there may be some recurrence relations that might reduce the total number of equations and ultimately the system complexity.

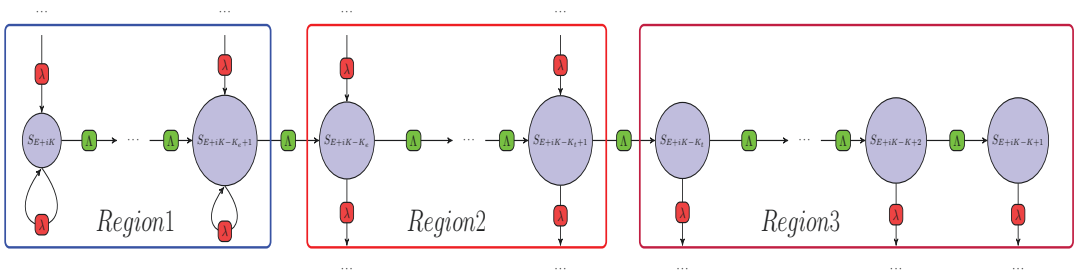

FIGURE 4.6: State diagram representation of the vector V_i

Figure 4.6 shows the state representation of the i^{th} row of the two-dimensional state diagram or vector V_i, $i \in \{1, 2, ..., D-1\}$. Each vector has 3 different transition characteristics among the states. Thus, the vectors can be subdivided into 3 separate regions represented by the following equations:

- *For Region1*, $0 \leq e < K_e$ or $\varsigma - K_e < N \leq \varsigma$ where $\varsigma = iK + E$ and $0 < i < D$:

$$S_{N+1} = S_N - (\frac{\lambda}{\Lambda})\ S_{N-K-K_e}, \tag{4.62}$$

- *For Region2*, $K_e \leq e < K_t$ or $\varsigma - K_t < N \leq \varsigma - K_e$:

$$S_{N+1} = S_N + (\frac{\lambda}{\Lambda})\ (S_N - S_{N-K-K_e}), \tag{4.63}$$

- *For Region3*, $K_t \leq e < K$ or $\varsigma - K < N \leq \varsigma - K_t$:

$$S_{N+1} = (1 + \frac{\lambda}{\Lambda})\ S_N. \tag{4.64}$$

Note that equations (4.62) and (4.63) are linearly recursive sequence of order $K + K_e + 1$. Moreover, there is no known solution in radicals to the general polynomial equations of degree 5 and more according to Abel & Ruffini theorem [101]. Thus, it is not easy to solve these equations, leading to a closed-form solution for stationary probability distributions. However, companion matrices of each equation can be used to express transitions among states. To provide consistency among the companion matrices, each one will be considered as a square matrix with dimension $K + K_e + 1$. On considering the vector V_1, the state transitions of Region 3 can be written using companion matrix. These are represented as follows:

$$\begin{bmatrix} S_{E+2} \\ S_{E+1} \\ \vdots \\ S_{E+2-K-K_e} \end{bmatrix} = \begin{bmatrix} (1+\frac{\lambda}{\Lambda}) & 0 & \dots & 0 & 0 \\ 1 & 0 & \dots & 0 & 0 \\ \vdots & \vdots & \ddots & \vdots & 0 \\ 0 & 0 & \dots & 1 & 0 \end{bmatrix} \begin{bmatrix} S_{E+1} \\ S_E \\ \vdots \\ S_{E+1-K-K_e} \end{bmatrix}$$

or equivalently:

$$\overrightarrow{S_{E+2}} = C_3 \ \overrightarrow{S_{E+1}}.$$

Other state vectors in *Region3* can also be expressed iteratively as follows:

$$\begin{aligned} \overrightarrow{S_{E+3}} &= C_3 \ \overrightarrow{S_{E+2}} = C_3^2 \ \overrightarrow{S_{E+1}}, \\ \overrightarrow{S_{E+4}} &= C_3 \ \overrightarrow{S_{E+3}} = C_3^3 \ \overrightarrow{S_{E+1}}, \\ &\vdots \\ \overrightarrow{S_{E+K_e+1}} &= C_3 \ \overrightarrow{S_{E+K_e}} = C_3^{K_e} \ \overrightarrow{S_{E+1}}. \end{aligned}$$

Similarly, for *Region2*:

$$\begin{aligned} \overrightarrow{S_{E+K_e+2}} &= C_2 \ \overrightarrow{S_{E+K_e+1}} = C_2 \ C_3^{K_e} \ \overrightarrow{S_{E+1}}, \\ \overrightarrow{S_{E+K_e+3}} &= C_2 \ \overrightarrow{S_{E+K_e+2}} = C_2^2 \ C_3^{K_e} \ \overrightarrow{S_{E+1}}, \\ &\vdots \\ \overrightarrow{S_{E+K_t+1}} &= C_2 \ \overrightarrow{S_{E+K_t}} = C_2^{K_t-K_e} \ C_3^{K_e} \ \overrightarrow{S_{E+1}}, \end{aligned}$$

and for *Region1*:

$$\begin{aligned} \overrightarrow{S_{E+K_t+2}} &= C_1 \ \overrightarrow{S_{E+K_t+1}} = C_1 \ C_2^{K_t-K_e} \ C_3^{K_e} \ \overrightarrow{S_{E+1}}, \\ \overrightarrow{S_{E+K_t+3}} &= C_1 \ \overrightarrow{S_{E+K_t+2}} = C_1^2 \ C_2^{K_t-K_e} \ C_3^{K_e} \ \overrightarrow{S_{E+1}}, \\ &\vdots \\ \overrightarrow{S_{E+K}} &= C_1 \ \overrightarrow{S_{E+K-1}} = C_1^{K_e-1} \ C_2^{K_t-K_e} \ C_3^{K_e} \ \overrightarrow{S_{E+1}}, \\ \overrightarrow{S_{E+K+1}} &= C_1 \ \overrightarrow{S_{E+K}} = C_1^{K_e} \ C_2^{K_t-K_e} \ C_3^{K_e} \ \overrightarrow{S_{E+1}}, \end{aligned}$$

where

$$C_1 = \begin{bmatrix} 1 & 0 & \dots & 0 & -\frac{\lambda}{\Lambda} \\ 1 & 0 & \dots & 0 & 0 \\ \vdots & \vdots & \ddots & \vdots & \\ 0 & 0 & \dots & 1 & 0 \end{bmatrix}, C_2 = \begin{bmatrix} (1+\frac{\lambda}{\Lambda}) & 0 & \dots & 0 & -\frac{\lambda}{\Lambda} \\ 1 & 0 & \dots & 0 & 0 \\ \vdots & \vdots & \ddots & \vdots & \vdots \\ 0 & 0 & \dots & 1 & 0 \end{bmatrix}$$

It has been showed that all the state vectors in V_1 can be expressed in terms of $\overrightarrow{S_{E+1}}$ and the companion matrices. In fact, the same procedure can be followed for the other row vectors and any state vector $\overrightarrow{S_N} : S_N \in V_i, 0 < i < D$ can be expressed as:

$$\overrightarrow{S_N} = \begin{cases} {C_3}^{\alpha}\ C^{\lfloor \frac{N-E-1}{K} \rfloor}\ \overrightarrow{S_{E+1}}, & 0 \leq \alpha \leq K_e \\ {C_2}^{\alpha-K_e}\ {C_3}^{K_e}\ C^{\lfloor \frac{N-E-1}{K} \rfloor}\ \overrightarrow{S_{E+1}}, & K_e < \alpha \leq K_t \\ {C_1}^{\alpha-K_t}\ {C_2}^{K_t-K_e}\ {C_3}^{K_e}\ C^{\lfloor \frac{N-E-1}{K} \rfloor}\ \overrightarrow{S_{E+1}}, & K_t < \alpha < K \end{cases} \tag{4.65}$$

where $\lfloor \cdot \rfloor$ is a function that returns the largest integer less than or equal to its argument, C is the multiplication of companion matrices, i.e., $C = C_1^{K_e}\ C_2^{K_t-K_e}\ C_3^{K_e}$, and the parameter $\alpha = (N-E+K-1) \pmod K$. Thus, the state vectors $\overrightarrow{S_N} : S_N \in V_i, 0 < i < D$ can be expressed with respect to the companion matrices and the state vector $\overrightarrow{S_{E+1}}$.

Now consider V_0 so that the following characteristic equations can be written:

- *For* $0 < N \leq K-1$*:*

$$S_{N+1} = (\frac{\lambda}{\Lambda})(1+\frac{\lambda}{\Lambda})^N S_0 \tag{4.66}$$

- *For* $K-1 < N \leq E-K_e$*:*

$$S_{N+1} = (1+\frac{\lambda}{\Lambda})S_N - \frac{\lambda}{\Lambda}S_{N-K} \tag{4.67}$$

- *For* $E-K_e < N \leq E$*:*

$$S_{N+1} = S_N - \frac{\lambda}{\Lambda}S_{N-K} \tag{4.68}$$

such characteristic equations can be written when the condition $E > 2K$ holds.

Thus, $\overrightarrow{S_{K+1}}$ can be expressed by equation (4.67):

$$\begin{bmatrix} S_{K+1} \\ S_K \\ \vdots \\ S_{-K_e+1} \end{bmatrix} = \begin{bmatrix} (1+\frac{\lambda}{\Lambda}) & 0 & \dots & -\frac{\lambda}{\Lambda} & \dots & 0 \\ 1 & 0 & \dots & 0 & \dots & 0 \\ \vdots & \vdots & \ddots & \vdots & \vdots & \vdots \\ 0 & 0 & \dots & 0 & 1 & 0 \end{bmatrix} \begin{bmatrix} S_K \\ S_{K-1} \\ \vdots \\ S_{-K_e} \end{bmatrix}$$

where $-\frac{\lambda}{\Lambda}$ is in the K^{th} column of the matrix B_2 whose size is also $K+K_e+1$ to provide consistency among dimensions of companion matrices.

Thus, the iteration may be kept and the other state vectors can be expressed as:

$$\begin{aligned}
\overrightarrow{S_{K+1}} &= B_2\ \overrightarrow{S_K}, \\
\overrightarrow{S_{K+2}} &= B_2\ \overrightarrow{S_{K+1}} = B_2^2\ \overrightarrow{S_K}, \\
&\vdots \\
\overrightarrow{S_{E-K_e+1}} &= B_2\ \overrightarrow{S_{E-K_e}} = B_2^{E-K-K_e+1}\ \overrightarrow{S_K}.
\end{aligned}$$

and

$$\begin{aligned}
\overrightarrow{S_{E-K_e+2}} &= B_1\ \overrightarrow{S_{E-K_e+1}} = B_1\ B_2^{E-K-K_e+1}\ \overrightarrow{S_{E-K+1}}, \\
\overrightarrow{S_{E-K_e+3}} &= B_1\ \overrightarrow{S_{E-K_e+2}} = B_1^2\ B_2^{E-K-K_e+1}\ \overrightarrow{S_{E-K+1}}, \\
&\vdots \\
\overrightarrow{S_{E+1}} &= B_1\ \overrightarrow{S_E} \qquad\quad = B_1^{K_e}\ B_2^{E-K-K_e+1}\ \overrightarrow{S_{E-K+1}}.
\end{aligned}$$

where

$$B_1 = \begin{bmatrix} 1 & 0 & \dots & -\frac{\lambda}{\Lambda} & \dots & 0 \\ 1 & 0 & \dots & 0 & \dots & 0 \\ \vdots & \vdots & \ddots & \vdots & \vdots & \vdots \\ 0 & 0 & \dots & 0 & 1 & 0 \end{bmatrix}$$

whose size is also $K + K_e + 1$.

$\overrightarrow{S_{K+1}}$ can also be expressed by equation (4.66) as follows:

$$\overrightarrow{S_{K+1}} = \begin{bmatrix} S_{K+1} \\ S_K \\ S_{K-1} \\ \vdots \\ S_0 \\ \vdots \\ S_{2-K_e} \\ S_{1-K_e} \end{bmatrix} = \frac{\lambda}{\Lambda} S_0 \begin{bmatrix} (1+\frac{\lambda}{\Lambda})^K \\ (1+\frac{\lambda}{\Lambda})^{K-1} \\ (1+\frac{\lambda}{\Lambda})^{K-2} \\ \vdots \\ \frac{\Lambda}{\lambda} \\ \vdots \\ 0 \\ 0 \end{bmatrix} = \frac{\lambda}{\Lambda} S_0\, \overrightarrow{\gamma} = \overrightarrow{\gamma_0}$$

Thus, we may write $\overrightarrow{S_N} : S_N \in V_0$:

$$\overrightarrow{S_N} = \begin{cases} \overrightarrow{\gamma_0}, & 0 < N \le K \\ {B_2}^{N-K}\ \overrightarrow{\gamma_0}, & K < N \le E - K_e + 1 \\ {B_1}^{N-E+K_e-1}\ {B_2}^{E-K-K_e+1}\ \overrightarrow{\gamma_0}, & E - K_e + 1 < N \le E + 1 \end{cases} \tag{4.69}$$

$\overrightarrow{S_{E+1}}$ in equation (4.65) may also be replaced and rewritten as:

$$\overrightarrow{S_N} = \begin{cases} {C_3}^{\alpha}\ C^{\lfloor \frac{N-E-1}{K} \rfloor} B', & 0 \leq \alpha \leq K_e \\ {C_2}^{\alpha-K_e}\ {C_3}^{K_e}\ C^{\lfloor \frac{N-E-1}{K} \rfloor} B', & K_e < \alpha \leq K_t \\ {C_1}^{\alpha-K_t}\ {C_2}^{K_t-K_e}\ {C_3}^{K_e}\ C^{\lfloor \frac{N-E-1}{K} \rfloor} B', & K_t < \alpha < K \end{cases} \tag{4.70}$$

where $B' = B_1^{K_e}(B_2)^{E-K-K_e+1}\overrightarrow{\gamma_0}$.

Moreover, for the states of V_D, the followings can be written:

- *For* $\varsigma_1 \leq N < \varsigma_1 + K_e$*:*

$$S_{N+1} = S_N \tag{4.71}$$

- *For* $\varsigma_1 + K_e \leq N < \varsigma_1 + K$*:*

$$S_{N+1} = S_N - \frac{\lambda}{\Lambda} S_{N-K-K_e} \tag{4.72}$$

where $\varsigma_1 = DK + E - K$. Therefore, the following can be written:

$$\overrightarrow{S_{\varsigma_1+K_e}} = \overrightarrow{S_{\varsigma_1+K_e-1}} = \cdots = \overrightarrow{S_{\varsigma_1+1}}$$

and

$$\begin{aligned} \overrightarrow{S_{\varsigma_1+K_e+1}} &= C_1\ \overrightarrow{S_{\varsigma_1+1}}, \\ \overrightarrow{S_{\varsigma_1+K_e+2}} &= C_1^2\ \overrightarrow{S_{\varsigma_1+1}}, \\ &\vdots \\ \overrightarrow{S_{\varsigma_1+K}} &= C_1^{K_t}\ \overrightarrow{S_{\varsigma_1+1}}. \end{aligned}$$

We can express the state vector $\overrightarrow{S_{\varsigma_1+1}}$ from equation (4.70) as,

$$\overrightarrow{S_{\varsigma_1+1}} = C^{D-1}B'.$$

Therefore, $\overrightarrow{S_N} : S_N \in V_D$ can be written as:

$$\overrightarrow{S_N} = \begin{cases} C^{D-1}B', & \varsigma_1 \leq N < \varsigma_1 + K_e \\ {C_1}^{N-(\varsigma_1+K_e)} C^{D-1} B', & \varsigma_1 + K_e \leq N < \varsigma_1 + K \end{cases} \tag{4.73}$$

Thus, the state vector $\overrightarrow{S_N} : \{S_N : 0 \leq N \leq DK + E\}$ can be written as a function of companion matrices C_1, C_2, C_3, B_1, B_2, required EPs, K_t and K_e, the vector $\overrightarrow{\gamma}$, and the state S_0 by combining equations (4.69), (4.70), (4.73). It is also known that the normalisation condition holds $\sum_{i=0}^{BK+E} S_i = 1$, so that the stationary probability distribution of S_0 can be found as well as all the other states in the system.

4.4 Impacts of Modelling Assumptions on the Results

The similar comments that have been made in section 3.4 can also be considered for this chapter. However, one additional assumption is that the number of EPs required for the packet transmission (K_t) is more than the amount required for the node electronics (K_e). Although it is a reasonable assumption for many sensor node applications [105], the invalidation of the assumption (i.e. $K_e \geq K_t$) does not have a significant impact on the results. In this case, there will be a minor change in the state transition diagram, which only affects the intervals (or regions) where the solutions are valid. In addition, the condition related to the energy buffer size and the number of EPs required for a successful transmission ($E > 2K$) has been assumed. It is another reasonable assumption since a few EPs would be enough for the packet processing and transmission while the energy buffers can store plenty of EPs.

4.5 Conclusions

In this chapter, an EHWSN in which packet transmission occurs through an imperfect transmitter was investigated. The energy consumption in a node was divided into two different operations: for the packet transmission by consuming K_t EPs, and for the node electronics by consuming K_e EPs. At least K_e EPs are required in the storage to sense, store and process a DP. Otherwise, DP cannot be received and the information will be lost. Moreover, in order to complete a successful DP transmission the node requires an extra K_t EPs.

First, a data transmission scheme was modelled as a one-dimensional random walk by assuming $K_t = K_e = 1$ and closed-form solutions for stationary probability distributions were expressed. The excessive packet rates and the system stability were then investigated.

The probability of a transmitted bit being correctly received by a receiver node that operates in a set of M identical sensor nodes with the existence of noise and interference

was also considered. Numerical results reveal the effect of number of sensors in the network on interference values and transmission error probability.

Then, a generalized energy consumption model was investigated assuming $K_t > K_e > 1$. A solution method was proposed for this model that uses companion matrices and linear algebra to reduce its computational complexity. Certain regularity properties of the matrix structure were also exploited, resulting in efficient numerical computation of all the metrics of interest. In particular, the steady-state distribution of the backlog of data and energy packets, the system throughput in terms of successfully transmitted packets and the possible loss of energy when the energy storage device is full and energy is harvested have been obtained.

Chapter 5

Product-form Solution Of Cascade Networks with Intermittent Sources

5.1 Introduction

This chapter is based on reference [74]. In this chapter, product-form analysis for N-Hop cascade network powered by intermittent sources is studied.

The power needs of digital devices, their installation in locations where it is difficult to connect to the power grid, and the difficulty of frequently replacing batteries, creates a need to operate digital systems with harvested energy. In such cases, local storage batteries must overcome the intermittent nature of the energy supply and system performance dependence on the intermittent energy supply, possible energy leakage and system workload. Queueing networks with product form solution are standard tools for analysing interconnected systems. They efficiently predict relevant performance metrics including job queue lengths, throughput, system turnaround times and queueing delays. However, existing queueing network models assume unlimited energy availability, while intermittently harvested energy can affect system performance due to insufficient supply of energy.

Networks can be designed to operate with intermittent or harvested sources of energy and with local battery storage at various nodes. These networks can be used as feeders for data packets coming from stand-alone Internet of Things (IoT) devices towards sink nodes that forward data to backbone networks and the Cloud. In such systems, the quality of service (QoS) depends on both the flow of energy into the system and on the flow of network traffic.

This chapter develops a new product form solution for the joint probability distribution of energy availability, and job queue length for an N-node tandem system. Such models can represent production lines in manufacturing systems, supply chains, cascaded repeaters for optical links, or a data link with multiple input data ports that feeds into a switch or server. Our result enables the rigorous computation of all the performance metrics for such systems operating with intermittent energy.

We model energy and traffic flow and represent the number of DPs and discrete EPs at each node. Moreover, the effect of energy loss through EP leakage from batteries or devices, and loss of DPs due to time-outs is included. When EP and DP flows entering the network are independent Poisson processes and certain stability conditions regarding the flow and loss of EPs and DPs are satisfied, it is shown that a multi-hop feed-forward network has a steady-state solution for the probability of the number of EPs and DPs at all nodes. This is the product of their marginal probabilities at each node. This is a new instance of a network with "product form solution" where state transitions involve simultaneous state changes in multiple nodes. This is due to DPs that flow through several nodes consuming EPs before stopping at nodes that have no EPs, or leave the network.

5.2 Single Node Model

The corresponding single node model was investigated in Chapter 3 and Chapter 4, where two independent Poisson processes with rates λ and Λ represented the arrivals of DPs and EPs at a node. One EP is the amount of energy needed to transmit one DP, and a model with both finite and infinite DP buffer and battery size was considered. In these previous chapters and in the current chapter, the rates at which the node senses and collected DPs and the rate at which it harvests energy may be very slow with respect to the mere nano-seconds it takes to transmit a DP. Therefore, it was assumed that the DP forwarding or transmission time is zero.

In addition, the node's battery may leak energy at rate $\mu \geq 0$ such that EPs are lost through leakage at random instants that are separated by identically and exponentially distributed intervals. Moreover, the node may also lose DPs from its data buffer due to time-outs resulting from the loss of each DP's value of information over time. Again, these instants when DPs are lost, are modelled as independent and exponentially distributed intervals with parameter $\gamma \geq 0$. Furthermore, if a DP arrives to a node when its DP buffer is full, the arriving packet will be lost. Similarly, if energy is harvested when its battery is full, then the arriving EP will be lost. Figure (5.1) shows the state transition diagram of Node i.

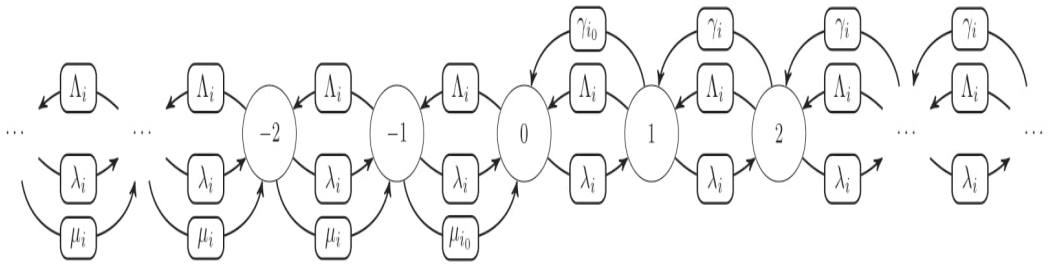

FIGURE 5.1: State transition diagram of some Node i.

5.3 The Cascaded N-Hop Network

The cascaded N-hop model considered in this chapter is shown in Figure 5.2. It was assumed that the data and energy buffers at each node are of unlimited storage capacity, and that one DP (or job) is forwarded using one EP. At node 1, the arrival rate of DPs from outside sources is denoted λ_1, while the remaining nodes are just transit nodes and they do not receive external arrivals of DPs. On the other hand, all nodes i receive EPs at rate Λ_i. EP leakage at node i, and DP loss due to impatience or errors at rate γ_i are also considered.

The leakage rate at node i is μ_i when there is more than one EP at node i, and is μ_i^0 when there is just one EP at node i. With current electronic technology, the DP transmission time will be in the nanoseconds, while the constitution of a full DP through sensing of external events (i.e. the harvesting of a significant amount of energy, the leakage of an EP and the loss of a DP due to impatience or errors) will take much longer. Thus, it can be assumed that the DP forwarding times are negligibly small compared to these other time durations.

The state of node $i \in \{1, \ ... \ , N\}$ at time t can be represented by the pair (x_i^t, y_i^t) where the first variable represents the backlog of DPs at the node, and the second variable is the amount of energy (in EPs) available at the same node. As with the single node model we must have $x_i^t \ . \ y_i^t = 0$ since if there is both an EP and a DP at a node, the transmission occurs until either all DPs or all EPs are depleted at node i. Thus the state of a node may be represented by a single variable $n_i^t = x_i^t - y_i^t$. Therefore, if:

- $n_i^t > 0$ then node i has $n_i^t = x_i^t$ DPs waiting to be forwarded, but it does not have the EPs at that node to start the transmission from that node,
- $n_i^t < 0$, then node i has a reserve of $-y_i^t$ EPs, but does not have any DPs to transmit,

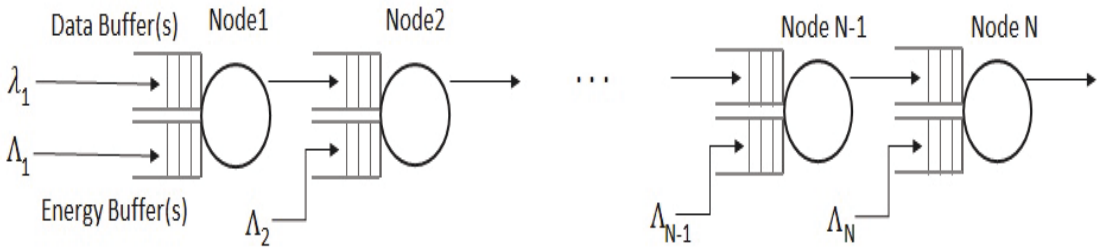

FIGURE 5.2: A cascade network comprised of several nodes that store and forward DPs. Each node operates with EPs that arrive to it intermittently through energy harvesting. The first node in the cascade receives DPs from the outside world, while the last node forwards them out of the network, and intermediate nodes forward DPs to subsequent nodes.

- $n_i^t = 0$, then node i does not have any DP and EP in their respective buffers.

A vector of positive, negative or zero integers then represents the cascaded network: $\bar{n}^t = (n_1^t, \ ... \ , n_N^t)$, $t \geq 0$, and $\bar{n}$ denotes a particular value of the vector, such the probability $p(\bar{n}, t) = Prob[\bar{n}^t = \bar{n}]$ can be studied.

Let $\bar{e_i} \triangleq (0, 0, \cdots, 1, \cdots, 0)$ be a vector whose i^{th} element is 1 and other $N-1$ elements are 0. The equilibrium equations for the steady-state probability distribution $\pi(\bar{n})$ for this system are:

$$\pi(\bar{n})\lambda_1 + \pi(\bar{n}) \sum_{i=1}^{N} [\Lambda_i + \gamma_i 1_{n_i>1} + \gamma_i^o 1_{n_i=1} + \mu_i 1_{n_i<-1} + \mu_i^o 1_{n_i=-1}] \tag{5.1}$$

$$= \sum_{i=1}^{N} \pi(\bar{n} + e_i)[\ \gamma_i 1_{n_i>0} + \gamma_i^o 1_{n_i=0} + \Lambda_i 1_{n_i<0}\ ] \tag{5.2}$$

$$+ \sum_{i=1}^{N} \pi(\bar{n} - e_i)[\ \mu_i 1_{n_i<0} + \mu_i^o 1_{n_i=0}\ ] + \pi(\bar{n} - e_1)\lambda_1 1_{n_1>0} \tag{5.3}$$

$$+ \sum_{i=2}^{N} \lambda_1 \pi(\bar{n} - e_1 - ... - e_{i-1} - e_i) \prod_{j=1}^{i-1} 1_{n_j \leq 0} 1_{n_i>0} \tag{5.4}$$

$$+ \lambda_1 \pi(\bar{n} - e_1 - ... - e_N) \prod_{j=1}^{N} 1_{n_j \leq 0} + \Lambda_N \pi(\bar{n} + e_N) 1_{n_N \geq 0} \tag{5.5}$$

$$+ \sum_{i=1}^{N-1} \Lambda_i \pi(\bar{n} + e_i - \sum_{k=1}^{N-i} e_{i+k}) 1_{n_i \geq 0} \prod_{k=1}^{N-i} 1_{n_{i+k} \leq 0} \tag{5.6}$$

$$+ \sum_{i=1}^{N-1} \sum_{l=1}^{N-i} \Lambda_i \pi(\bar{n} + e_i - \sum_{k=1}^{l-1} e_{i+k} - e_{i+l}) 1_{n_i \geq 0} \prod_{k=1}^{l-1} 1_{n_{i+k} \leq 0} 1_{n_{i+l}>0}. \tag{5.7}$$

In these equations:

- Line (5.1) corresponds to a case where there are no arrivals or departures of DPs and EPs, while the first two terms in line (5.2) correspond to the removal of DPs due to impatience. Moreover, the third term relates to the arrival of a EP to any Node i where no DPs are being stored.

- The first two terms in line (5.3) correspond to the leakage of EPs, while the third term is due to the arrival of a DP to Node 1 (the only node where DPs can arrive) when Node 1 does not contain any EPs.

- The term in line (5.4) corresponds to the arrival of a DP to Node 1 when nodes 1 to $i-1$ contain EPs, while Node i does not contain any EPs. Thus, the DP progresses directly to Node i where it stops to join the DP queue.

- In line (5.5), the first term corresponds to the case where an arriving DP proceeds directly to the exit from Node N because all nodes contain at least one EP. The second term in line (5.5) describes the arrival of an EP to Node N which contains at least one DP which then leaves the network.

- In line (5.6), an EP arrives to Node i containing at least one DP, which then moves all the way to the output of the network because all nodes after node i contain at least one EP.

- Finally line (5.7) describes the arrival of an EP to Node i when it contains at least one DP; the DP is then able to move through nodes $i+1$ to $i+l-1$ which all contain EPs, but it joins the DP queue at Node $i+l$ which has no EPs.

The equilibrium equations may be rewritten in more compact form as:

$$\pi(\bar{n})\ [\lambda_1 + \sum_{i=1}^{N}(\Lambda_i + \gamma_i 1_{n_i>1} + \gamma_i^0 1_{n_i=1} + \mu_i 1_{n_i<-1} + \mu_i^0 1_{n_i=-1})] \tag{5.8}$$

$$= \sum_{i=1}^{N}[\pi(\bar{n}+e_i)(\gamma_i 1_{n_i>0} + \gamma_i^0 1_{n_i=0} + \Lambda_i 1_{n_i<0} 1_{i\neq N} + \Lambda_N 1_{i=N})] \tag{5.9}$$

$$+ \sum_{i=1}^{N}[\pi(\bar{n}-e_i)(\mu_i 1_{n_i<0} + \mu_i^0 1_{n_i=0} + \lambda_1 1_{n_1>0} 1_{i=1})] \tag{5.10}$$

$$+ \sum_{j=1}^{N-1}[\pi(\bar{n} - \sum_{i=1}^{j+1} e_i)\lambda_1 \prod_{i=1}^{j} 1_{n_i\leq 0}(1_{n_{1+j=N}} + 1_{n_{j+1}\geq 1} 1_{n_{1+j\neq N}})] \tag{5.11}$$

$$+ \sum_{j=1}^{N-1}\sum_{i=1}^{j}[\pi(\bar{n} + e_i - \sum_{k=1}^{N-j} e_{i+k})\Lambda_i 1_{n_i\geq 0}(1_{N-j\leq 1}. \tag{5.12}$$

$$+.1_{N-j\geq 2} \prod_{k=1}^{N-j-1} 1_{n_{i+k}\leq 0})(1_{i=j} + 1_{n_{N+i-j}\geq 1} 1_{i\neq j})\ ]$$

5.3.1 The Equilibrium Condition for Energy and Data Flows (EDF)

Imagine if the amount of energy that the system harvests is not sufficient to allow the transmission of the incoming flow of DPs; then the backlog of DPs will become infinite. Similarly, if the flow of DPs is not large enough to use the incoming flow of energy, then the backlog of EPs will grow indefinitely. Naturally, the effect of time-outs for the DPs, and the leakage of the EPs also needs to be included. Let:

$$v_1 = \lambda_1,\ v_{i+1} = \lambda_1 \prod_{l=1}^{i} \frac{\Lambda_i}{\Lambda_i + \gamma_i}, \tag{5.13}$$

where v_i can be interpreted (see Theorem 2) as the arrival rate of DPs to Node i. The Energy and Data Flow (EDF) condition can then be defined as:

$$v_i - \gamma_i = \Lambda_i - \mu_i, \tag{5.14}$$

where (5.14) says that the net inflow of DPs, after removal of those that time-out, should be the same as the total inflow of EPs minus the loss of EPs due to leakage.

Theorem 1 Assume that the EDF condition is satisfied. Then the steady-state probability distribution for the system $\pi(\bar{n}) = \lim_{t\to\infty} p(\bar{n}, t)$ is given by:

$$\pi(\bar{n}) = \prod_{i=1}^{N} \pi_i(n_i),$$

where

$$\pi_i(n_i) = \begin{cases} C_i, & \text{if } n_i = 0, \\ C_i . \frac{v_i}{\Lambda_i+\gamma_i^0} (\frac{v_i}{\Lambda_i+\gamma_i})^{n_i-1}, & \text{if } n_i \geq 1, \\ C_i . \frac{\Lambda_i}{v_i+\mu_i^0} (\frac{\Lambda_i}{v_i+\mu_i})^{-n_i-1}, & \text{if } n_i \leq -1, \end{cases}$$

where $\mu_i^0 = v_i + 2\mu_i$, $\gamma_i^0 = \Lambda_i + 2\gamma_i$, and the normalising constants C_i are:

$$C_i = (1 + \frac{\frac{v_i}{\Lambda_i+\gamma_i^0}}{1 - \frac{v_i}{\Lambda_i+\gamma_i}} + \frac{\frac{\Lambda_i}{v_k+\mu_i^0}}{1 - \frac{\Lambda_i}{v_i+\mu_i}})^{-1}. \tag{5.15}$$

Using the EDF condition we have:

$$C_i = \frac{2\gamma_i.\mu_i}{2\gamma_i.\mu_i + \Lambda_i.\mu_i + v_i.\gamma_i} \tag{5.16}$$

$$= \frac{2\gamma_i.\mu_i}{(\gamma_i + \mu_i)(v_i + \mu_i)} = \frac{2\gamma_i.\mu_i}{(\gamma_i + \mu_i)(\Lambda_i + \gamma_i)}. \tag{5.17}$$

The proof is provided in the Appendix A.

5.3.2 Data Packet Arrival Rates to Nodes

The second result concerns the steady state arrival rate of DPs to each node.

Theorem 2 Denote the steady-state arrival rate of DPs to Node i by α_i, and obviously $\alpha_1 = \lambda_1$. Then $\alpha_i = v_i,\ i = 1,\ \ldots, N$.

Proof Let :

$$\nu_i = \sum_{n_i<0} \pi_i(n_i) = C_i \frac{\Lambda_i}{2\gamma_i} = \frac{\Lambda_i \mu_i}{(\gamma_i + \mu_i)(v_i + \mu_i)}, \tag{5.18}$$

$$\rho_i = \sum_{n_i>0} \pi_i(n_i) = C_i \frac{v_i}{2\mu_i} = \frac{\gamma_i v_i}{(\gamma_i + \mu_i)(\Lambda_i + \gamma_i)}. \tag{5.19}$$

Then for $i > 1$,

$$\begin{aligned}
\alpha_i &= && (5.20)\\
&= \lambda_1 \prod_{j=1}^{i-1} \nu_j + \sum_{j=1}^{i-2} \Lambda_j \rho_j \prod_{k=j+1}^{i-1} \nu_k + \Lambda_{i-1}\rho_{i-1}, && (5.21)\\
&= v_i \prod_{j=1}^{i-1} \frac{\mu_j}{\gamma_j + \mu_j} + \sum_{j=1}^{i-2} \frac{\gamma_j}{\gamma_j + \mu_j} v_j \frac{\Lambda_j}{\Lambda_j + \gamma_j} \prod_{k=j+1}^{i-1} \frac{\Lambda_k}{\Lambda_k + \gamma_k} \frac{\mu_k}{\gamma_k + \mu_k} && (5.22)\\
&+ \frac{\gamma_{i-1}}{\gamma_{i-1} + \mu_{i-1}} v_{i-1} \frac{\Lambda_{i-1}}{\Lambda_{i-1} + \gamma_{i-1}}, && (5.23)\\
&= v_i \prod_{j=1}^{i-1} \frac{\mu_j}{\gamma_j + \mu_j} + v_i \sum_{j=1}^{i-2} \frac{\gamma_j}{\gamma_j + \mu_j} \prod_{k=j+1}^{i-1} \frac{\mu_k}{\gamma_k + \mu_k} + v_i \frac{\gamma_{i-1}}{\gamma_{i-1} + \mu_{i-1}}, && (5.24)
\end{aligned}$$

or denoting $u_i = \frac{\gamma_i}{\gamma_i + \mu_i}$, we have:

$$\frac{\alpha_i}{v_i} = \prod_{j=1}^{i-1}(1 - u_j) + u_{i-1} + \sum_{j=1}^{i-2} u_j \prod_{k=j+1}^{i-1} (1 - u_k). \tag{5.25}$$

However, it can be easily shown by induction on the integer $M \geq 1$ that:

$$\prod_{j=1}^{M}(1 - u_j) = 1 - u_M - \sum_{j=1}^{M-1} u_j \prod_{k=j+1}^{M} (1 - u_k). \tag{5.26}$$

Hence the arrival rate of DPs to Node i is $\alpha_i = v_i$, completing the proof.

5.4 Total Backlog of Data Packets

The total average number of DPs in the cascade network is:

$$< n >= \sum_{i=1}^{N} \sum_{n_i>0} n_i \pi_i(n_i) = \sum_{i=1}^{N} \frac{C_i}{2} \frac{R_i}{(1-R_i)^2} \tag{5.27}$$

$$= \sum_{i=1}^{N} \frac{C_i}{2} \frac{v_i}{\mu_i} [1 + \frac{v_i}{\mu_i}] = \sum_{i=1}^{N} \frac{\gamma_i}{\gamma_i + \mu_i} \frac{v_i}{\mu_i}, \tag{5.28}$$

where $R_i = \frac{v_i}{v_i+\mu_i}$ and the condition $R_i < 1$ must be satisfied.

Figure (5.3) shows the average backlog of DPs for different energy arrival rates, and different numbers of nodes N in the cascade network. In this example, the external data arrival rate is set to $\lambda_1 = 1$ for the purpose of normalisation. Moreover, all the nodes have identical EP arrival rates $\Lambda_i = \Lambda$, and leakage rates $\mu_i = \Lambda_i + \gamma_i - v_i$. Identical DP impatience rates have been chosen for all nodes, and have been set to $\gamma_i = 0.01$ for the curves on the left hand-side, and $\gamma_i = 0.1$ for the curves on the right hand-side. As expected, the average DP backlog decreases significantly since DPs are more rapidly transmitted when the EP arrival rate is increased. Moreover, higher DP leakage rates result in lower overall packet backlog, as more DPs are dropped by the nodes during the transmissions through the network.

Figure (5.4) shows the throughput for different energy arrival rates, and different numbers of nodes N in the cascade network, assuming the same parameter values as in Figure (5.3). As the number of sensor nodes in the cascaded network increases, the throughput reduces significantly due to the conjugated effect of DP loss at each successive node. On the other hand, the increase in EP arrival elevates the throughput, as more data can be served before their time-out creates losses. Moreover, higher time-out data loss rate causes less throughput.

Parameter	**Description**
λ_1	External DP arrival rate at Node 1
v_i	Total DP arrival rate at Node i
Λ_i	EP arrival rate at Node i
μ_i	EP loss rate at Node i
γ_i	DP loss rate at Node i
$< n >$	Total average number of DPs
N	Number of nodes in the cascade network

TABLE 5.1: Parameters used for numerical examples.

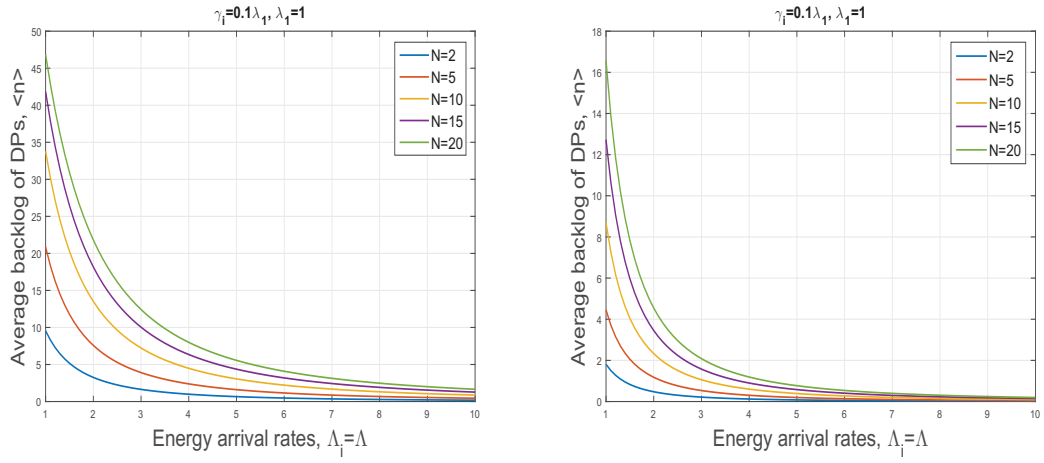

FIGURE 5.3: The total average backlog of DPs at all of the N units or nodes (y-axis), versus the arrival rate of EPs to each node (x-axis) which is set to an identical value at all units, with $\Lambda_i = \Lambda$. The leakage rate of EPs is set to the value of $\mu_i = \Lambda_i + \gamma_i - v_i$. The total number of cascaded units N was also varied. Note that the total EP arrival rate, or power flow into the system is $N\ \Lambda$. In order to normalise the results the arrival rate of DPs to the first node is set to the value $\lambda_1 = 1$. Other parameters are $\gamma_i = 0.01$ (left) and $\gamma_i = 0.1$ (right), respectively. The values of N, Λ and γ_i impact the total DP backlog significantly.

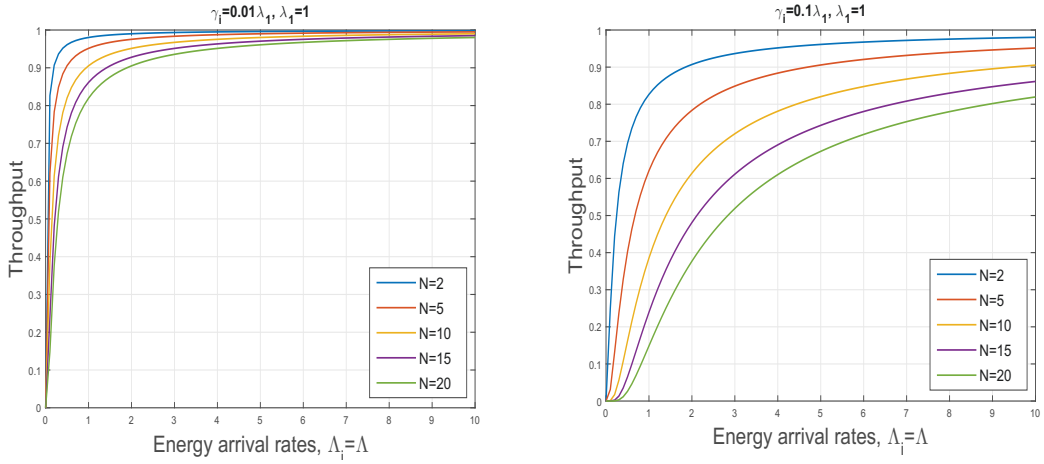

FIGURE 5.4: Throughput versus the EP arrival rate at all units; note that we have set the EP arrival rates to be identical at all nodes with $\Lambda_i = \Lambda$. The number of cascaded nodes or units N is varied. Other parameters are $\lambda_1 = 1$, $\gamma_i = 0.01$ (left) and $\gamma_i = 0.1$ (right), respectively. The values of N, Λ impact the throughput significantly. As the number of nodes increases, it was observed that the amount of energy per node needed to "push" the customers or DPs out of the network so that the throughput tends towards 1, is many times larger than the DP arrival rate. This is particularly true when one notes (again) that the total power consumed by the network is $N\ \Lambda$.

5.5 Impacts of Modelling Assumptions on the Results

The PFS given by this chapter is subject to the EDF condition. The condition states that the consumption rate of EPs must be equal to the consumption rate of DPs. Nonetheless,

it is not a strict condition since the equality can be provided by adjusting the time-out rate (γ) settings. In fact, providing PFS depending on conditions of the models' transition rates is not confounding since some previous works have derived the product-forms by considering certain conditions on the system parameters [15, 17, 106].

5.6 Conclusions

In this chapter, a mathematical model of a cascaded multi-hop network or a service system where each node gathers energy through harvesting has been introduced. DPs (or jobs) arrive to the first node and are forwarded hop-by-hop to the output node. This proceeds provided that there is at least one EP present at each node that is visited. If a DP encounters a node that does not have at least one EP, then the DP must wait for the arrival of enough energy through harvesting at that node. It was also assumed that EPs are lost at each node due to leakage, and that DPs may also be lost at nodes due to time-outs or errors.

It was assumed that DPs arrive to the first node according to a Poisson process and that EPs are harvested at each node according to independent Poisson processes. Moreover, it was assumed that the time it takes to forward a DP from one node to its immediate neighbour when the node has enough energy, is much shorter than the time it takes to constitute an input DP from sensed data, and the time it takes to harvest an EP that is needed to forward a DP.

The main result is a previously unknown PFS (product-form solution) for this system. The use of this analytical solution was illustrated by computing the average backlog of DPs and their waiting at each node, as shown through several numerical results.

Since product-form analytical solutions are very useful computational tools in network and computer system performance analysis, and are economical in terms of computing time as compared to discrete event simulations, it is expected that the results presented in this chapter will be extended in future work to cover more general network topologies. Furthermore, although this work started with using Poisson arrivals, it is expected that (as with other areas of system performance analysis), these results will lead to further work and that they will be generalised to be dependent (rather than independent) inter-arrival times, and to time-varying arrival rates.

Chapter 6

Energy Life-Time of Wireless Nodes under Energy Depletion Attacks

6.1 Introduction

The work in this chapter is based on references [72, 73]. In this chapter, the simple energy depletion attacks are reviewed and a modelling approach is proposed to evaluate the effects of these attacks on life-time of sensor nodes operating with EN paradigm.

In the Internet of Things (IoT), a simple form of attack can deplete the energy available to operate the sensor nodes. Several of these nodes may use batteries, while others may harvest ambient energy, i.e. photovoltaic, or electromagnetic, or vibration-based energy. First a brief survey of the types of attacks that target the nodes' energy provisioning systems is provided. Moreover, this chapter analyses the effect of these attacks on the energy life-time of a wireless node. Models are provided to estimate the effect of attacks, which attempt to deplete a node's energy supply, and for a node that uses energy harvesting. A simple means of attack mitigation based on dropping both attack and "good" traffic was then examined. For nodes that use energy harvesting, the fraction of traffic that must be dropped so as to offer a desired "energy life-time" of the node was computed. It was observed that the required traffic drop-rate is non-linearly dependent on the nominal "good traffic rate" at which the node is expected to operate. Finally, the impact of attacks on the energy life-time of a node that operates with a replaceable battery was analysed.

Energy needed to operate networks is known to be an important issue. This is true for the sustainability of information technology in general. Moreover, with regard to operating stand-alone networks in locations where the electrical grid is not available or

is not reliable and when in a given location it is impossible to provide electrical wired connections to all sensors. For example, in pre-constructed buildings which are later equipped with sensors. Thus there has been a growing concern regarding attacks that directly affect the energy consumption of networks [107–109]. In particular, attacks that may deplete batteries that are required to operate certain network nodes.

These attacks can take three basic forms: they can increase the activity of nodes through useless DPs that the nodes receive and then have to process and respond to. Attackers can also use electromagnetic emissions to create noise that will cause high error rates, and hence force them to take corrective action such as packet retransmissions that increase energy consumption and network delays through multiple data retransmissions [110]. In addition, attacks can change the "sleep-awake" duty cycle of nodes and reduce the proportion of time when the nodes should be asleep to save energy.

6.1.1 Earlier Works

Several types of energy depletion attacks have been discussed in previous work. In *vampire attacks*, a vampire node appears to be benign, but it continuously sends protocol compliant messages to other nodes [111]. Vampire nodes may cause additional traffic (with rate λ_A), which is sent by the node that is under attack. Vampire attacks [112] have been observed to generally take one of two forms: the *carrousel* and the *stretch* attack. In the carrousel attack, a vampire node sends corrupted data leading to routing loops. In the stretch attack, artificially longer routes are chosen despite the fact that shorter routes are available. In general, carrousel attacks result in more energy consumption than stretch attacks [113]. Moreover, the detection of vampire attacks is not easy as one malicious vampire node can affect the whole network. Moreover, a protocol was proposed in reference [113] to detect and mitigate vampire attacks. This protocol provides routing through the network only for legitimate packets, and verifies consistent progress is made by packets towards a destination. Furthermore, reference [114] provides a mitigation method for preventing carrousel attacks by adding extra forwarding logic to check whether there are loops in the source routes. To prevent stretch attacks, the work in references [115, 116] suggests "strict" source routing where the route is exactly specified in the header and there is no need for checking its optimality. An attack packet detection and removal method was previously proposed [117, 118]. This methods employed packet broadcast rates and energy parameters at sensor nodes. Other power-aware routing techniques have been suggested [119, 120].

Sleep deprivation attacks are designed to keep sensor nodes awake as long as possible to increase their energy consumption, and reduce the battery life of a sensor from months

to days. These attacks also include barrage, synchronisation, replay, broadcast, and collision attacks [107, 121, 122]. Typically, a node that receives a request to receive data from another node, can check its routing table to see whether it may receive data from that node; if not, it discards the request and goes to sleep. In sleep deprivation attacks [123], malicious nodes will continuously try to send data to some nodes in order that they do not sleep and consequently waste energy. As a defence, a lightweight scheme was proposed [122]. In this approach, a node is activated only if it receives messages from authenticated and legitimate nodes. Alternatively, attackers can also conduct barrage attacks on awake nodes by bombarding them with legitimate requests, causing significant energy wastage. However, barrage attacks can be easily detected and require more effort from the attacker, while sleep deprivation attacks require only a single message [123, 124].

As nodes have a listen-sleep cycle that can be periodically updated to maintain synchronisation among neighbours, attackers may send *artificial synchronisation packets* to lengthen the nodes' awake time [125]. This can result in 30% or more energy depletion due to shorter sleep times, and a possibly 100% increase in data loss due to the misalignment of synchronisations. A defence strategy to mitigate the effects of such attacks was proposed [125]. This proposal suggested ignoring all synchronisation messages with a relative sleep time longer than a pre-set threshold. Alternatively, in a *replay attack* [126], an adversary repeats a valid transmission in the network. Since the attack uses the replay of messages with small changes, it can fool other nodes by convincing them that repeated messages concern a new message exchange. Note that in wireless networks [121] the received signal can help identify malicious nodes through use of a stronger signal [127].

In *broadcast attacks* [128], malicious nodes broadcast unauthenticated traffic and long messages which must be received by other nodes before being possibly discarded for lack of authentication. These attacks are hard to detect as they have no effect on system throughput. However, nodes that receive them waste energy. In *collision attacks* [129], a hostile node breaks the medium access control protocol and transmits noise packets corrupting neighbourhood transmissions. Thus noise packets collide with legitimate ones. A defence strategy has been proposed [130] based on error correcting codes.

A defence strategy against energy depletion attacks has been investigated [121]. The authors considered *denial of sleep attacks* which dramatically increase the energy consumption of a wireless sensor node. An evaluation and attack detection method was proposed [110] where the quality of service is not necessarily degraded. The method of end-to-end reliability, based on control packet injections and packets replication was also studied [131]. It was shown that the method is vulnerable to energy depletion attacks and it is impossible to keep safe a protocol from such attacks without authentication. A

two-tier secure transmission scheme against energy depletion attacks has been proposed [132]. This scheme uses the hash-chain to generate dynamic session keys, which can provide a mutual authentication key. Moreover, the detection and removal of an energy depletion attack (*vampire attack*), based on the routing protocol of the wireless sensor network has been studied [107, 112, 117, 118]. Furthermore, a hardware-based energy attack (*hardware trojans*) has been investigated [133]. This revealed that significant energy depletion may occur by embedding a hardware trojan trigger to the integrated circuit.

6.2 Results Addressed in this Chapter

In this work we propose a modelling approach to evaluate the effect of attacks on the "energy life-time" of a node, i.e. how long it can operate before its energy is depleted, both for nodes that use energy harvesting, and for nodes that use a conventional battery that will have to be replaced when depleted. The attacks considered are those that force the node to transmit additional traffic, and those which create electromagnetic noise that induces errors and hence packet retransmissions. The following basic aspects have been developed:

1. Nodes send λ_n DPs per unit time under normal operation (i.e. when not being attacked). The traffic of "useless" attack DPs that are transmitted in response to attacks, result in an additional traffic rate λ_A of DPs being sent out from the node. This creates "useless" energy consumption.

2. Electromagnetic attacks create noise that results in DP *transmission errors*, and hence DP re-transmissions with probability $0 \leq r < 1$. Moreover, r will increase with increased attack noise level.

3. In a separate section, we consider a system that has a battery that is regularly replaced, and compare the node's energy life-time with that of the node which uses renewable energy.

For both systems with and without energy harvesting, an initial "normal" DP traffic rate λ_n is transformed into a total traffic rate λ_a under attack. This is given by:

$$\lambda_a = \lambda_n + \lambda_A + r.\lambda_a = \frac{\lambda_n + \lambda_A}{1 - r}. \tag{6.1}$$

Electromagnetic noise causes errors in all of the traffic, including the traffic of rate λ_A that results from the reply packets, which the node sends in response to attack packets. Thus λ_a in equation (6.1) represents the total DP traffic that the node sends when it's

normal traffic would have been λ_n. Furthermore, the attack traffic it receives is λ_A and the noise attack causes retransmissions with probability r.

These two types of attacks are considered when computing the energy life-time of a wireless node based on its energy harvesting rate, both with nominal or "normal" traffic and the resulting traffic rate in the presence of attacks. The reduction of the node's energy life-time due to attacks is computed and illustrated using numerical results.

In this work it is assumed that the node's energy harvesting system has been designed to operate with a nominal value Λ_n of EPs per unit time, which the node is able to harvest in the specific environment being considered. The rate Λ_n then results in an acceptable energy life-time T_n when the system is operating normally without attacks, and is sending DPs at rate λ_n.

Similarly, nodes with a fixed battery size of E_0, that will be measured in units of "energy packets". will have a battery life-time of T_n^b under normal operation when they are meant to provide for a normal DP traffic rate of λ_n.

Based on these parameters, we can compute the value of the node's energy life-time T_a, for nodes that use energy harvesting, and T_a^b if they use a battery, when they operate under the effect of attacks represented by attack traffic rate λ_A and the effect of electromagnetic noise attacks which create transmission errors and require each DP to be retransmitted with probability r.

Thus, both for systems that use energy harvesting, and those that use a fixed battery, we are interested in finding to what extent the energy life-time of the node has been *reduced* by the attacks, and hence in computing the ratio $\frac{T_a}{T_n}$, or $\frac{T_a^b}{T_n^b}$ as a function of the ratio of attack traffic $\frac{\lambda_A}{\lambda_n}$ and of r.

6.3 A System with Renewable Energy and Finite DP and Energy Buffers

In this section, the modelling approach initiated in Chapter 3 is employed. This approach is in relation to a wireless node that exploits renewable energy sources (such as photovoltaic, mechanical vibrations or electromagnetic scavenging) where the node collects data or energy at a relatively slow pace as compared to the time it takes to transmit a DP over a node's wireless channel. Moreover, the node's nominal operating parameters are λ_n and Λ_n, the latter corresponding to the nominal rate in which it harvests EPs in the environment where it is operating. In this section, it has been assumed that the the node has a local energy storage device, possibly a battery or a large capacitor, that can

store up to E EPs. If it is out of energy, it is assumed that it can nevertheless store up to D DPs under the pure effect of the sensing energy. If required, this assumption can be removed by setting $D = 0$.

When under attack, the node transmits λ_a DPs per unit time as indicated in equation (6.1). This is due to the attack packets it receives, which require a response from the node producing an additional packet rate λ_A, and from the retransmission probability r due to errors caused by electromagnetic noise and interference. Note that the noise may be created by nodes that are attacking the system, while the interference may result from the increased volume of wireless traffic as an indirect effect of ongoing attacks.

The state of the node at time t is represented by the pair D_t, E_t where D_t is the backlog of DPs at the node, while E_t is the number of EPs that it stores at that time. Denoting the node's state probability $p(d, e, t) = Prob[D_t, E_t]$, it is known that $p(d, e, t) > 0$ only if $d.e = 0$. This is because if the node has enough energy, it will immediately attempt to transmit DPs until either all DPs in its buffer have been sent out, or its energy has been depleted. The data buffer has a capacity of D packets, and the local battery contains at most E energy packets. Furthermore, DPs will be removed from the data buffer after a time-out of average value $\frac{1}{\gamma}$ with an exponentially distributed departure rate of γ. Similarly, EP leakage occurs at a rate of μ EPs per unit time.

Thus, the probability that the battery is empty can be calculated by using the results obtained in Chapter 3:

$$P_0^a(0) = \sum_{d=0}^{\infty} p(d,0) = \sum_{n=0}^{D} \alpha^n p(0,0) \tag{6.2}$$

$$= \frac{(\alpha^{D+1} - 1)(\theta - 1)}{\alpha^{D+1}(\theta - 1) + \theta^{E+1}(\alpha - 1) + 1 - \alpha\theta}. \tag{6.3}$$

where

$$\alpha = \frac{\lambda_a}{\Lambda_n + \gamma},\ \theta = \frac{\Lambda_n}{\lambda_a + \mu}. \tag{6.4}$$

Note also that the case with D=0, when the node cannot store any sensor data if it has run out of energy, is:

$$P_0^a(0)|_{D=0} = \frac{\theta - 1}{\theta^{E+1} - 1}. \tag{6.5}$$

The expected (average) battery life-time, i.e. the average time it takes the node's battery to empty from the instant at which it contains one EP, can then be obtained from the fact that when the battery empties, on average after $\frac{1}{\Lambda_n}$ time units it will receive an EP

once again, so that:

$$P_0^a = \frac{\frac{1}{\Lambda_n}}{T_a + \frac{1}{\Lambda_n}}, \text{ or} \tag{6.6}$$

$$T_a = \frac{1}{\Lambda_n}[\frac{1}{P_0^a} - 1]. \tag{6.7}$$

If λ_a is replaced with λ_n in all terms, then the average battery life-time when the node is *not* being attacked is obtained, namely:

$$T_n = \frac{1}{\Lambda_n}[\frac{1}{P_0} - 1]. \tag{6.8}$$

If the probabilities P_0^a and P_0 are very small, then:

$$\log \frac{T_a}{T_n} \approx \log P_0 - \log P_0^a. \tag{6.9}$$

Figure 6.1 shows various curves for the battery life-time versus the attack traffic rate λ_A and the retransmission error rate due to electromagnetic attacks r, assuming that the normal operating life-time before the system's energy supply is depleted has been set to $T_n = 6$ months, and $E = D = 100$. In this numerical example, the nominal normal load of the wireless sensor has been set at $\lambda_n = 10$ DPs/hour. Consequently, the energy harvesting rate then needs to be $\Lambda_n = 11.247$ EPs/hour to meet the $T_n = 6$ months average energy life-time of the system when it does *not* suffer from attacks. Figure 6.2 shows a similar set of results for different parameter settings as described in the figure caption.

The effect of E, the energy storage capacity of the system, on its energy life-time is shown in Figure 6.3. The same parameters as used in Figure 6.2 have been retained. Moreover, $r = 0.1$, $D = 100$, and $T_n = 6$ months for $E = 100$. However, the local storage battery capacity E has been varied along the x-axis from 10^2 to 10^3 in order to observe the effect on T_a for four values of attack traffic λ_A and the resulting effect on T_a.

6.3.1 DP Buffer and Battery with Unlimited Capacity

In this section a sensor node with an unlimited battery that stores the energy that is harvested, and a DP buffer of unlimited size has been considered. The model equations for the stationary probabilities for the DP in queue and the amount of energy that is

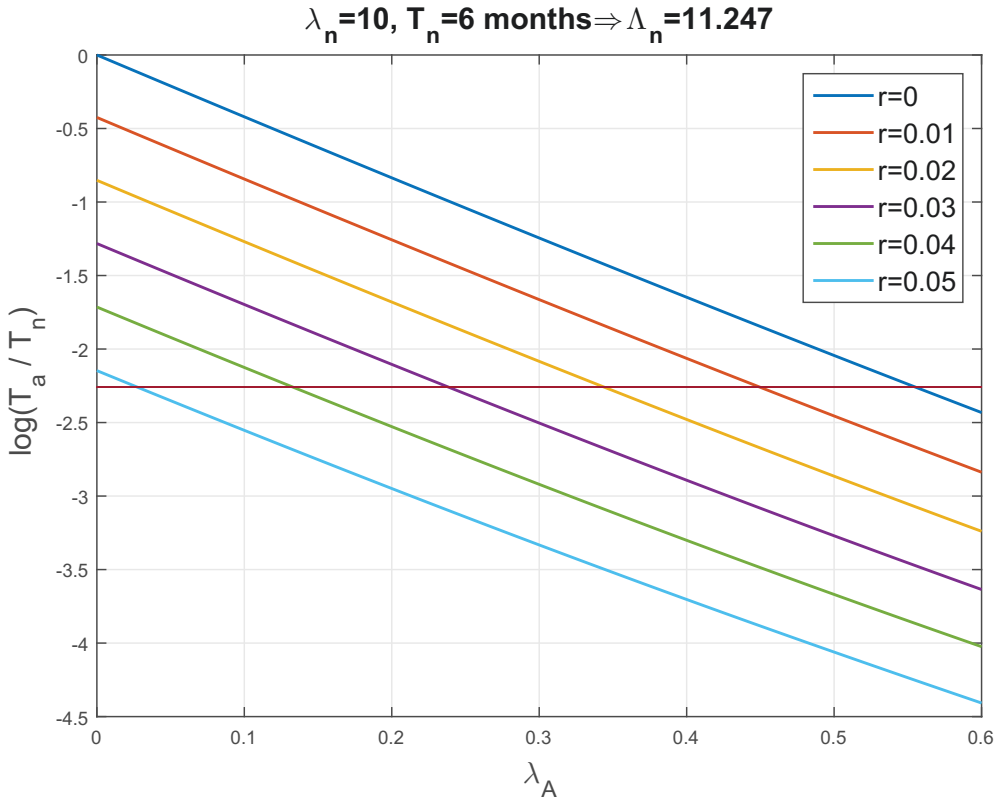

FIGURE 6.1: The curves illustrate the effect of two simultaneous types of attacks, namely the attacks that create added traffic, and those that create retransmissions due to noise that is generated by electromagnetic attacks. We show the variation of the *common logarithm* of the ratio of node energy life-time under attack, to energy life-time without attacks (y-axis), against the arrival rate of attack traffic λ_A with distinct curves for increasing values of the retransmission probability r due to electromagnetic attacks. The parameter settings are $E = D = 100$, $\gamma = 0.01\lambda_a$ and $\mu = 0.01\Lambda_n$. We fix the "normal life-time" of the system until the battery is emptied after $T_n = 6$ months of operation, on average. Thus the EP arrival rate Λ_n representing the required energy harvesting will vary with the normal traffic rate λ_n as shown on each of the graphs. The effect of the attacks is shown by the rapid decrease of the ratio $\log \frac{T_a}{T_n}$ as both λ_A and r increase.

stored then become:

$$p(d,0) = \alpha^d p(0,0),\ \alpha = \frac{\lambda_a}{\Lambda_n + \gamma},\ d > 0, \tag{6.10}$$

$$p(0,e) = \theta^e p(0,0),\ \theta = \frac{\Lambda_n}{\lambda_a + \mu},\ e > 0, \tag{6.11}$$

$$p(0,0) = \frac{(1-\alpha)(1-\theta)}{1-\alpha\theta}. \tag{6.12}$$

The probability that the nodes internal storage battery is empty is then:

$$P_e(0) = \sum_{d=0}^{\infty} p(d,0) = \frac{1}{1-\alpha} p(0,0) = \frac{1-\theta}{1-\alpha\theta}, \tag{6.13}$$

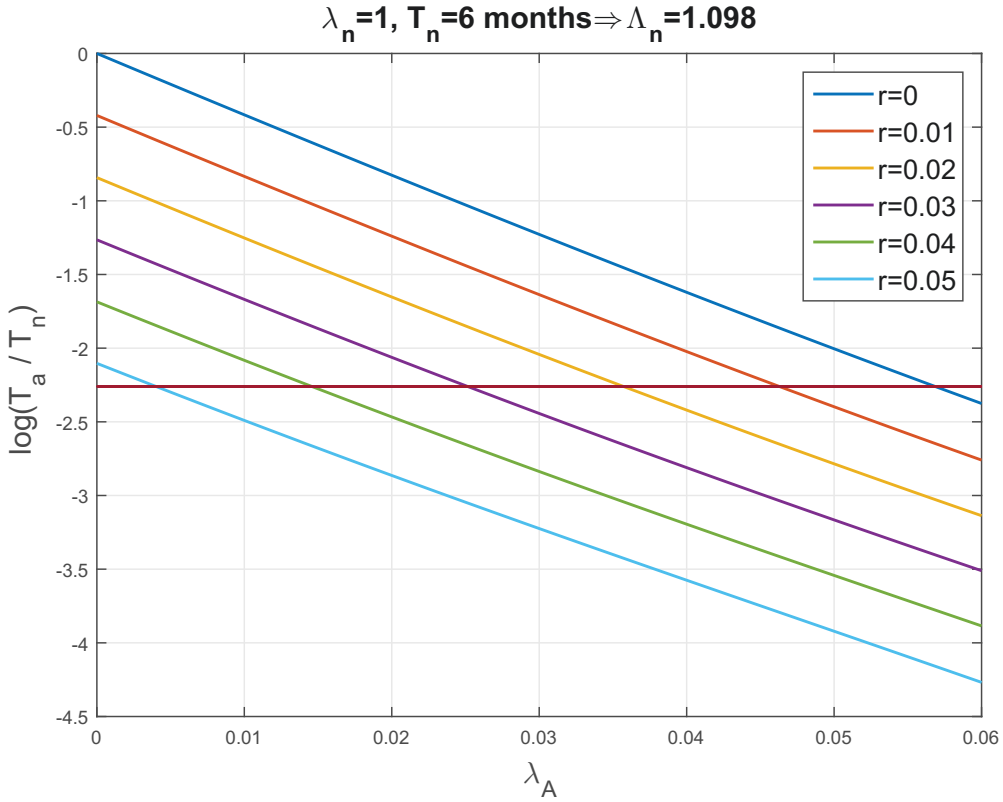

FIGURE 6.2: The curves illustrate the same effects as Figure 1, with the same set of parameters, except that $\lambda_n = 1$ so that Λ_n is chosen so that we again have $T_n = 6$ months, and $\gamma = 0.01\lambda_a$, $\mu = 0.01\Lambda_n$.

and the conditions for system stability conditions are $\lambda_a < \Lambda_n + \gamma$ and $\Lambda_n < \lambda_a + \mu$ such that:

$$\Lambda_n - \mu < \lambda_a < \Lambda_n + \gamma. \tag{6.14}$$

6.4 Mitigation Against Attacks for Energy Harvesting Nodes

One approach to mitigate against attacks would be to impose a forced loss on incoming traffic, so that the total arrival rate of data packets cannot exceed λ_0, which has been selected so that the average energy life-time has a pre-specified value T_0. Note that the total traffic forwarded by the node includes both its "normal" workload and the traffic resulting from attacks. The latter includes all the packet retransmissions due to errors resulting from noise and possible electromagnetic attacks, and the additional traffic that is imposed on the node by other attacks. This approach then requires that a fraction m of the total traffic is forcibly dropped at the node, where m is obtained from the relation:

$$\lambda_0 = (1 - m)\lambda_a, \quad 0 \leq m < 1. \tag{6.15}$$

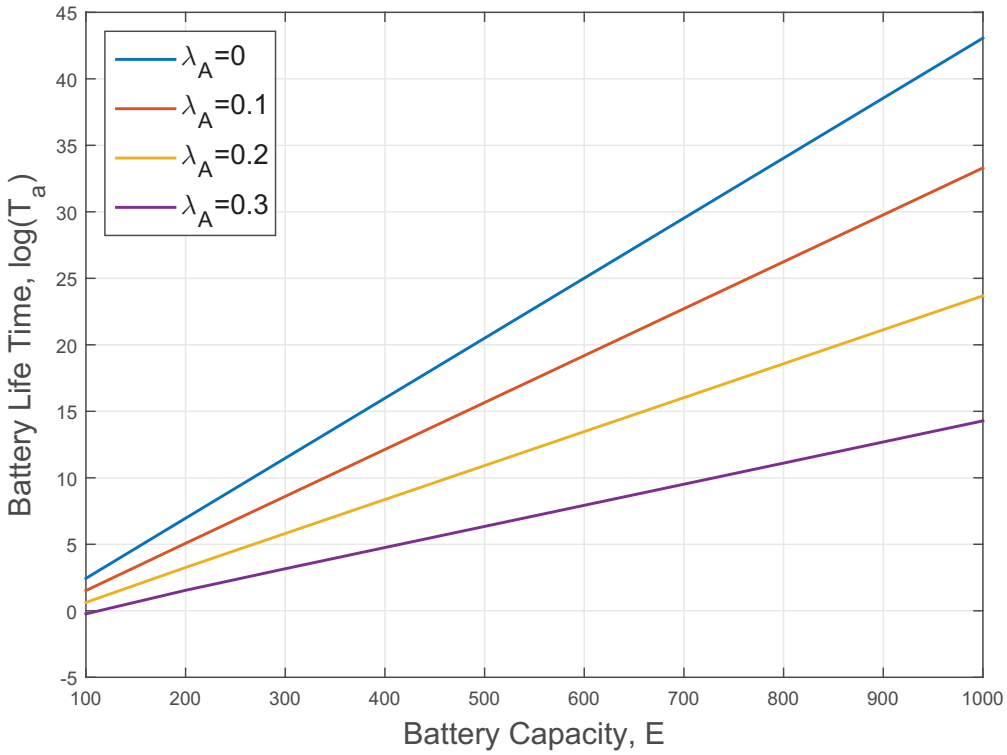

FIGURE 6.3: For a node that uses energy harvesting, its energy life-time is shown on the y-axis versus the local battery capacity E, for for different values of attack traffic and $r = 0.1$. The capacity of the local battery which stores the harvested energy substantially increases the system's energy life-time.

Here m also represents the fraction of good packets that are lost. For a given value of λ_n, and given parameters r and λ_a, $m.\lambda_n$ can be considered as the "cost in the loss rate of good packets" that is paid to achieve a node average life-time of T_0.

The numerical examples in Figure 6.4 show that m varies in a non-linear manner with λ_n. In the examples, $T_0 = 6$ months, $r = 0.1$, $\Lambda_n = 10$, $E = D = 100$ and different values of attack traffic λ_A has been used.

6.5 Energy Life-Time without Energy Harvesting

A conventional alternative to the system described in the previous section is to use a large enough battery, say of size E^o to support the node for a significant amount of time. In that case, suppose an energy life-time of T_a^o can be attained in the presence of attacks. A comparison of this system with the one that uses energy harvesting would be of interest.

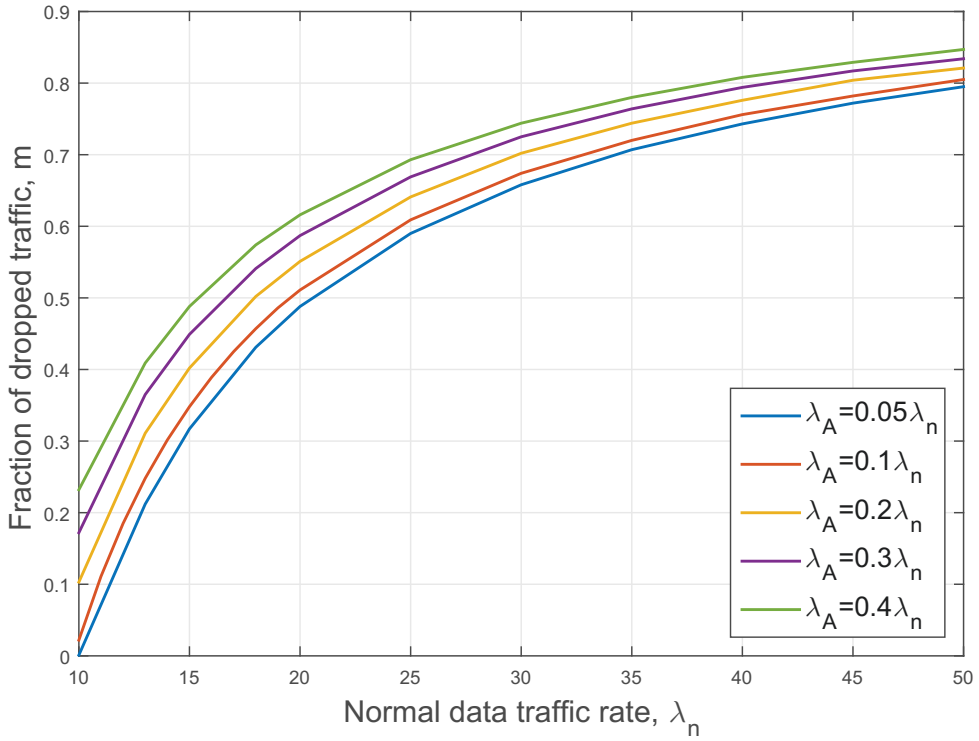

FIGURE 6.4: When we mitigate the attacks in a node with energy harvesting, by dropping a fraction m of DPs, we plot m versus the normal data traffic rate λ_n in DPs per hour. We show numerical results for a fixed required energy life-time of 6 months, and for different fractions of λ_A in proportion to λ_n with $r = 0.1$.

This conventional system would also have a DP buffer of size D and can be represented by a finite capacity single server queue with arrival rate λ_a, while powered in the presence of attacks, with service rate τ, and again with DP time-out rate γ. This will result in a probability that the node is non-empty of:

$$q = \frac{\lambda_a}{\gamma + \tau}[\frac{1 - (\frac{\lambda_a}{\gamma+\tau})^D}{1 - (\frac{\lambda_a}{\gamma+\tau})^{D+1}}], \tag{6.16}$$

and an energy consuming effective transmission rate of DPs given by $R = q\tau$. As observed in the previous analysis we have identified one EP with the energy consumed to transmit one DP. This approach will be retained for the purpose of homogeneity in the comparison between the previous system and this one, so that this system's energy consumption rate is also R.

If this system's average energy life-time is T_a^o and the battery has a leakage rate of μ, then during this time on average $T_a^o\mu$ EPs will have been wasted. We then have:

$$E_a^o = [q\tau + \mu].T_a^o, \tag{6.17}$$

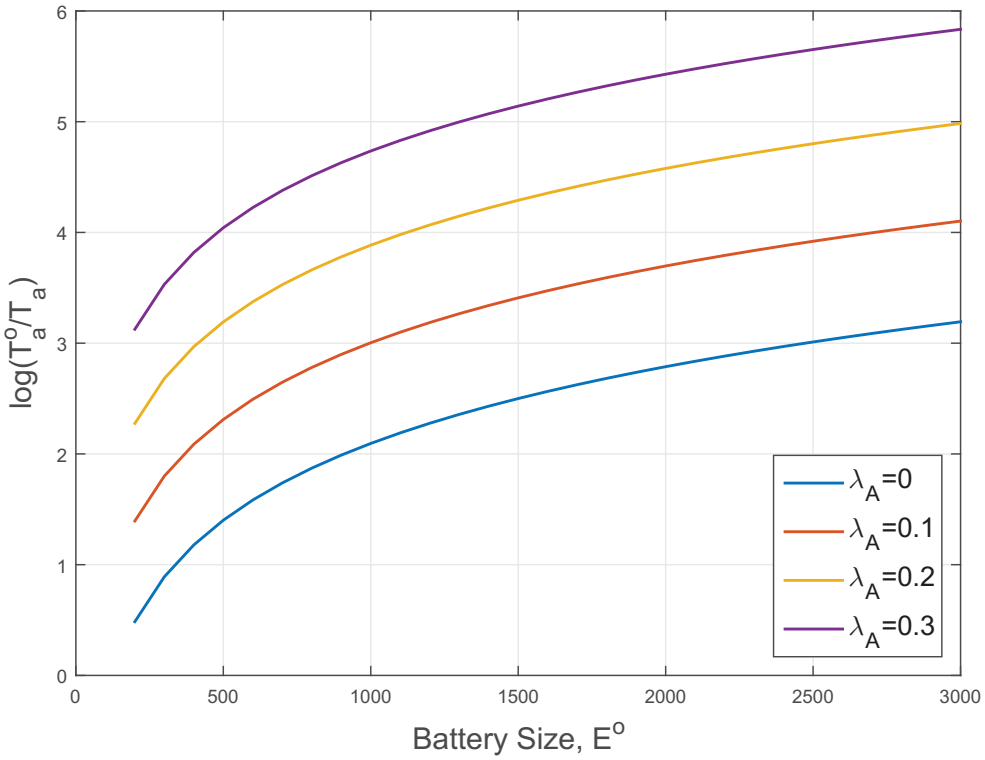

FIGURE 6.5: Comparison of a system without harvesting that uses a battery of size E^o with one that uses energy harvesting. All parameters are as in Figure 1, with $E = D = 100$ for the system with energy harvesting, and we fix $r = 0.1$. The ratio $\log \frac{T_a^o}{T_a}$ is shown in the y-axis, versus the battery capacity of the node without harvesting E^o, for three different values of λ_A. We see that a node that uses a large replaceable battery is potentially more robust. All other parameters are the same as for Figure 2.

or

$$T_a^o = \frac{E_a^o}{\mu + \lambda_a \frac{\tau}{\tau+\gamma} \frac{1-(\frac{\lambda_a}{\gamma+\tau})^D}{1-(\frac{\lambda_a}{\gamma+\tau})^{D+1}}}. \tag{6.18}$$

Note that this system will process and forward packets much faster, in the microseconds per DP or even faster, than the one with energy harvesting which processes DPs at the rate at which energy is being harvested, i.e. Λ_n. Thus in general $\tau >> \gamma$ and $\tau >> \lambda_a$ so that:

$$T_a^o \approx \frac{E_a^o}{\mu + \lambda_a}. \tag{6.19}$$

If it is required that an energy life-time for this system which is similar or identical to that of the system with energy harvesting, a battery capacity E_a^o would be required which can be obtained by setting $T_a^o = T_a$. Thus, a battery capacity as shown below will be needed:

$$E_a^o \approx [\mu + \lambda_a].T_n(\lambda_a, E), \tag{6.20}$$

where the dependence of T_n on both the net traffic rate of the system under attack λ_a and

the energy harvesting's local battery capacity E is explicitly shown. The corresponding numerical results are shown in Figure 6.5 where we illustrate the advantage of a system without energy harvesting by examining the ratio $\log \frac{T_a}{T_a^o}$ as a function of E^o. We see that the advantages of using a larger fixed battery slow down as we increase E^o.

6.6 Impacts of Modelling Assumptions on the Results

In this chapter, two types of energy attack have been studied: a) the one creates additional traffic in the network, and b) the one results in packet retransmissions for the sensor nodes. The life-time analysis has been made by considering the fact that the impacts of these attacks on the sensor nodes are independent of each other. However, one might think that there is a link between these two attacks since the additional traffic can also cause the packet retransmission, and the increasing noise level can elevate the additional traffic rate. In this case, the total data arrival rate at a sensor node with the same attack parameters is expected to be more than what is formulated in this chapter. Thus, the outcomes related to the battery life-time presented in this chapter are anticipated to be longer than the ones acquired from the real-time experiments.

6.7 Conclusions

This chapter has focused on the effect of simple energy-based attacks on sensor network nodes. We consider how long it takes to deplete a battery and hence stop the node's operations when a sensor node is in use. Two situations have been considered: (a) where the node exploits ambient but intermittent energy sources and therefore does not require being connected to the grid, or being fed by a replaceable battery, and (b) when the node's energy needs are offered with a replaceable battery, but without an ambient harvested energy source. The analysis carried out focused on the effect of attacks that are meant to deplete the node's energy, either through creating additional "useless" traffic or via electromagnetic noise that results in packet errors and further packet retransmissions. Analytical results and numerical experiments have been shown to compare and evaluate the resulting effects. In particular, the reduction of "energy life-time" of the node was detailed and illustrated for both cases. The study showed that attacks can be used to very rapidly deplete the energy life-time of a node, and that a system which operates with a source of harvested energy is less robust to attacks. Moreover, the use of a large fixed battery can be advantageous for long energy life-times, although it has the inconvenience of requiring human intervention to replace the batteries.

Regarding the proposed mitigation technique discussed in Section 6.4, it is observed in Figure 6.4) for a system that uses energy harvesting, that for low values of normal traffic $\lambda_n \approx 10$, even with high proportions of attack traffic, relatively low packet loss rates are sufficient to maintain the battery life-time at the required length, which in this example is six months. However, for the higher values of λ_n, the packet drop rates required would be too high to be acceptable and one would have to maintain them at a lower level and accept a shorter battery life-time.

Chapter 7

Optimum Sensor Placement

7.1 Introduction

While WSNs operate autonomously in unattended environments, they have to cope with several resource constraints. These include computation, communication and energy requirements in order to extend the battery life-time of sensor nodes in addition to the life-time of WSNs. A typical WSN tends to consist of hundreds of sensor nodes which can send the gathered information to a base station either directly or over a multi-hop route. Sensor nodes operations rely on small batteries which may or may not be capable of harvesting energy from the ambient environment. When a sensor node runs out of its energy, it stops operating and the network may not continue its proper operations due to several sensor nodes that may have already depleted their energy sources. Therefore, while managing the network's application requirements, energy conversion and management must be prudently taken into account.

Several existing techniques for WSNs try to optimise networks at different communication layers. For instance, multi-hop routing and hierarchical network topologies are well-known ways to optimise the network layer [134]. Moreover, preventing idle listening, and managing power consumption are examples of optimisation methods at the medium access layer [135, 136]. Furthermore, data encryption and authentication, and adaptive node activations help to optimise the networks at the application layer [137]. Furthermore, using opportunistic communications that uses low-cost human wearables rather than conventional fixed communications also helps to optimise networks for emergency situations [138].

Optimum sensor placement has gained much attention for various objectives and models as a means to optimise networks with respect to their primary duties, as careful node

placement can be helpful in meeting the system requirements and achieving the desired network goals. However, in many WSN applications sensor placement is primarily driven to ensure that the network topology covers the region being monitored [139]. In fact, sensor placement affects several network performance parameters apart from coverage. These include throughput, communication delays and energy consumption. Ineffective sensor node placement might cause weak communication links, throughput losses and excessive energy depletion.

Although the importance of optimal sensor node placement is straightforward, it is still a very challenging problem for most network topologies and goals [140, 141]. Several heuristic models and techniques have been developed to reach some near-optimal solutions [142, 143]. One crucial point that should be considered for optimising the WSNs is whether sensor node locations will be static during the whole network operations or dynamically changeable according to varying external factors (e.g. change in traffic pattern or load) and some internal factors (e.g. adding new nodes to the network or losing existing nodes due to battery depletions) [144, 145]. Optimisation models that allow dynamic adjustment of node locations might give better results as the initial node placement can lose its importance. In this situation, the network will require an updated placement scheme. However, it also brings its own difficulties. These include continuous monitoring of the network states and network performance. Moreover, relocation of sensor nodes may cause some interruptions of data traffic which may result in the loss of some information. Furthermore, an updated routing path should be immediately provided for each sensor node that is relocated. Therefore, this study will focus on optimisation methods that consider static node placement, i.e. optimum locations are initially determined and then relocation is not considered.

7.2 Static Node Placement

Optimisation strategies for static node placement focus on quality metrics and are independent of the network's current state or performance. These strategies consider unchanged parameters throughout the network operation. For example, traffic load, energy availability, distance, and communication errors. Nevertheless, strategies for initial positioning of nodes still have a great impact on effective operations of WSNs. In reference [139], the static positioning of sensor nodes is categorised according to deployment methodology, optimisation objectives and the functionality of the nodes in the networks.

7.2.1 Deployment Methodologies

Sensor nodes in an environment can be either deterministically or randomly placed by considering sensors type, network applications, and the environmental factors within which the network operates. The controlled placement of sensor nodes is common particularly when their operation depends on location, or they are very expensive. Expensive sensors are usually used for several indoor applications such as surveillance for obtaining high quality images of targets, maintenance of large buildings and contamination detection in air and water supplies [146–149]. Furthermore, sensor placement is crucial for underwater applications, as sensor nodes use acoustic signals and they have to be placed in a specific range for a successful communication [150].

Alternatively, random sensor node deployment could be a feasible solution for several network applications in rough environments, such as disaster areas or battlefields. Controlled sensor node placement is often not possible during a combat or a fire. However, random placement can be done remotely by helicopters or with some sensor grenades. Although the localisation of nodes is random, node densities can be controlled or planned, and some reasonable approximations and analysis can be made based on this density information [151, 152].

7.2.2 Optimisation Objectives

Every WSN is designed in a way that several goals or objectives are satisfied. Area coverage, network connectivity, network longevity and data fidelity are the most common objectives that WSN designers try to optimise [139]. It is clear using large numbers of sensor nodes can achieve these objectives. However, the real challenge is to design networks using the least number of sensor nodes due to limited resources.

Area coverage of the monitored region is one of the main objectives for WSN applications. Network designers generally try to achieve either area coverage maximisation by using a predetermined number of sensor nodes or full coverage of a specific region by minimising the number of sensor nodes in the network. The assessment of the coverage depends on the modelling the sensing range of sensor nodes and the metrics evaluating the collective coverage of the network. Most studies consider that a sensor node is able to sense a disk region whose centre is the location of the node and the radius is the node's sensing range [153]. However, several other metrics such as irregular polygons are used to evaluate area coverage [154, 155].

In addition, network connectivity is a further network objective as false information can be monitored or there might be nothing to show at all without a proper network communication. Although area coverage has always been a constraint for network designs, network connectivity has not been considered due to the fact that the transmission range of a sensor node is assumed to be much greater than the sensing range. However, it becomes a serious concern when these two ranges are close to each other. Locating relay nodes, which are capable of long distance communication, among other sensor nodes and ensuring a traffic route from a sensor to another one, which is closer to the base station, may help to achieve the connectivity objective. Moreover, different placement strategies can overcome both coverage and connectivity concerns [156, 157].

Network longevity is also a crucial objective for WSNs. Communications among sensor nodes and base stations is one of the main energy consumers in WSNs. Consequently, network life-time is highly dependent on the location of the sensor nodes. For instance, network life-time is shortened when sensor nodes are uniformly distributed as the nodes further away from the base station consume energy faster than those closer to the base station [158]. Therefore, designers will tend to maximise network life-time instead of optimising coverage or connectivity objectives by assuming the availability of sufficient number of sensor nodes that have sensing ranges that prevent a lack of coverage or connectivity problems. In several applications, a set of sensor nodes may operate for the same purposes. Thus, the whole network will keep functioning as long as one node in a set has sufficient energy to operate. Alternatively, each sensor node may be assigned a unique job. In this case the node that consumes its energy first determines the network life-time.

The reliability of gathered information or data fidelity is an additional design objective for WSNs. Placement of several sensor nodes, trying to sense the same information, in a specific region increases the data credibility or accuracy as the fused data consists of multiple independent sensor nodes information. For instance, reference [159] uses information from multiple nodes to maximise the target detection probability. However, increased node density in networks results in problems such as extra cost and elevated interference levels. Moreover, it causes a trade-off between data fidelity and coverage, or connectivity objectives when the number of sensor nodes is limited.

7.2.3 Nodes' Functionality

Sensor node placement depends not only on network design targets, such as prolonging life-time or minimising delays, but also the functionality of the nodes in the network. In addition to being a regular sensor, a node can contribute as a base station, relay

or cluster head. Therefore, designers should consider the nodes functionality before positioning strategies. Functionality of the relay nodes may vary according to network design needs. As mentioned previously, the transmission range of the relay nodes is greater than that of regular nodes, as they may play a gateway role for several nodes in a network. It is generally assumed that relay nodes can directly communicate with the base station of the network. In fact, even if they do not have direct communication with the base station, they can still significantly improve network performance.

Clustering of sensor nodes plays a key role in the sense of scalability for large networks [160]. While a relay node can only forward the received data from a regular node, a cluster head can collect and aggregate all the information from other nodes in a cluster. Moreover, some cluster heads are capable of dealing with management responsibilities of clusters. These include assigning and changing sensor nodes tasks. Cluster heads in the same network may have direct connections to the base station, alternatively they constitute a multi-hop cluster head network to reach to the base station.

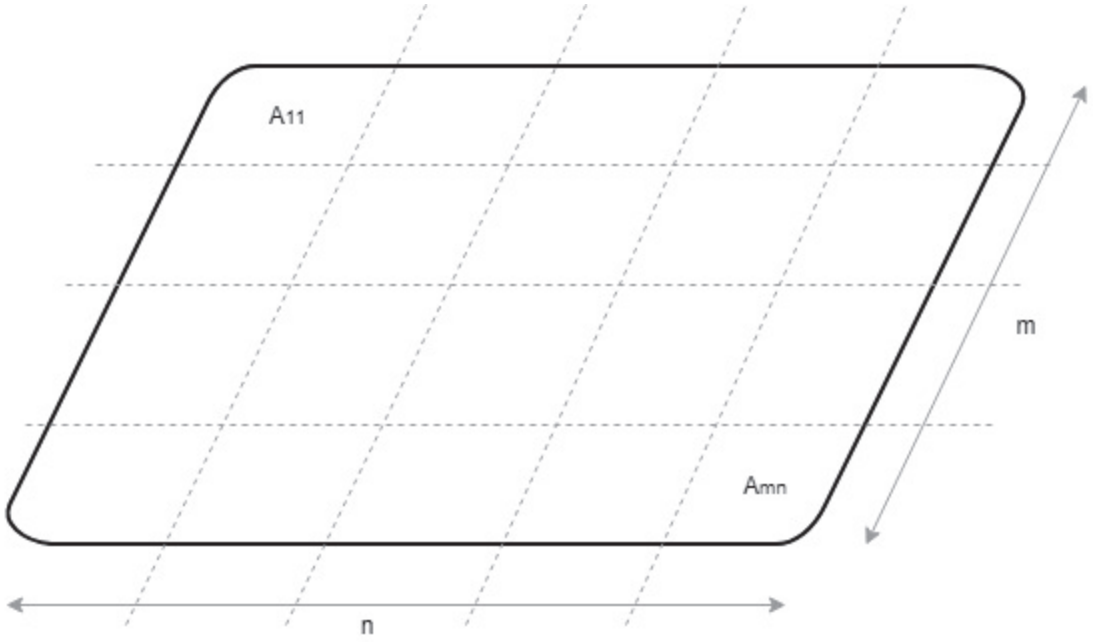

FIGURE 7.1: The area that has to be covered by the sensor nodes.

7.3 System Model

This work proposes a modelling approach to optimise the sensor node placement of WSN when there is a spatial continuous distribution of energy (e.g. photovoltaic) and a continuous spatial density of data traffic. The following statements are assumed:

1. The areas that have to be covered by the sensor nodes consist of $m\ x\ n = M$ unit regions, and each can be represented by $A_{ij}, i \in \{1, \cdots, m\}, j \in \{1, \cdots, n\}$ as shown in Figure (7.1).

2. Each A_{ij} has spatial energy arrivals, which is a Poisson process with rate Λ_{ij}, and spatial data arrivals, another independent Poisson process with rate λ_{ij}.

3. The number of sensor nodes placed in A_{ij} is represented by n_{ij} and the following equation must be satisfied:

$$\sum_{i=1}^{m}\sum_{j=1}^{n} n_{ij} = N, \quad 0 \leq n_{ij} \leq k, \tag{7.1}$$

   where N is the total number of sensor nodes, and k is the maximum number of nodes can be placed into a unit region due to physical constraints i.e, each sensor node occupies a certain area. Furthermore, at least one node has to be placed in each unit region to provide area coverage, so that $N > M$.

4. Each sensor node operating in A_{ij} is capable of capturing the same amount of energy, the full portion of the spatial energy arrival Λ_{ij}. However, sensor nodes divide the traffic load when they are placed into the same unit region, i.e. the traffic load for each sensor node in A_{ij} is $\frac{\lambda_{ij}}{n_{ij}}$.

5. The sensing range of a node is limited to cover the unit region where it is placed. Thus, the node is not occupied with traffic arrivals from neighbouring unit regions.

6. Data can be successfully transmitted by consuming a single EP.

7.4 Single Hop Transmission

Clustering is common in WSNs. Consequently, they are designed such that each node is able to directly communicate with the cluster-head (or the local base station) without requiring multi-hop communication. In other words, the transmission range of a node can cover the distance between the node and the base station to achieve direct communication. In this section, a brief single node analysis which is generally used in the single hop transmission networks is explained together with an explanation of the optimisation problem and the fairness in relation to optimum node placement.

7.4.1 Single Node Analysis

In this section, an identical time-out loss rate γ and energy leakage rate μ have been assumed for all sensor nodes in the network. Alternatively, the energy and data arrivals of sensor nodes depend on their location. Figure (7.2) models a sensor node located in A_{ij}.

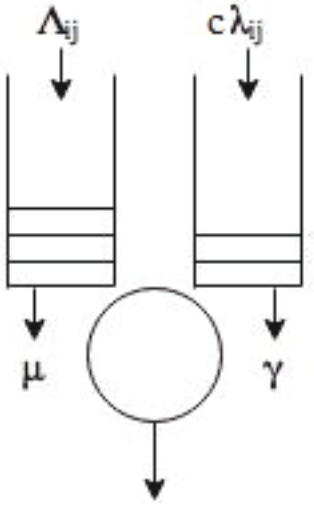

FIGURE 7.2: A single node with spatial energy arrival rate Λ_{ij}, spatial data arrival rate $c\lambda_{ij}$, data time-out loss rate γ, and energy leakage rate μ. If the node operates among total number of n_{ij} sensor nodes, then $c = \frac{1}{n_{ij}}$.

States of a node at time t are represented by $p(d, e, t)$ where the first variable represent the backlog of data and the second one represents the number of EPs. Therefore, stationary state distributions of a node operating among total number of $n_{ij} \leq k$ sensor nodes in A_{ij} can be calculated as:

$$p_{ij}(d,0) = \alpha_{ij}^{d}\, p_{ij}(0,0) = \left(\frac{\frac{\lambda_{ij}}{n_{ij}}}{\Lambda_{ij}+\gamma}\right)^{d} p_{ij}(0,0), \tag{7.2}$$

$$p_{ij}(0,e) = \theta_{ij}^{e}\, p_{ij}(0,0) = \left(\frac{\Lambda_{ij}}{\frac{\lambda_{ij}}{n_{ij}}+\mu}\right)^{e} p_{ij}(0,0), \tag{7.3}$$

$$p_{ij}(0,0) = \frac{(1-\alpha_{ij})(1-\theta_{ij})}{\alpha_{ij}^{D+1}(\theta_{ij}-1)+\theta_{ij}^{E+1}(\alpha_{ij}-1)+1-\alpha_{ij}\theta_{ij}}. \tag{7.4}$$

Furthermore, the average backlogs of DPs waiting in the buffer can be calculated as:

$$\begin{aligned}
\bar{d_{ij}} &= \sum_{d=0}^{D} d\ p_{ij}(d,0), && (7.5)\\
&= \sum_{d=0}^{D} d\ \alpha_{ij}^{d} p_{ij}(0,0), && (7.6)\\
&= \frac{\alpha_{ij}(D\alpha_{ij}^{D+1} - (D+1)\alpha_{ij}^{D} + 1)}{(1-\alpha_{ij})^2}\ p_{ij}(0,0), && (7.7)\\
&= \frac{\alpha_{ij}(1-\theta_{ij})[D\alpha_{ij}^{D+1} - (D+1)\alpha_{ij}^{D} + 1]}{(1-\alpha_{ij})[\alpha_{ij}^{D+1}(\theta_{ij}-1) + \theta_{ij}^{E+1}(\alpha_{ij}-1) + 1 - \alpha_{ij}\theta_{ij}]}. && (7.8)
\end{aligned}$$

7.4.2 The Optimisation and The Fairness Index

Covering the operational area whilst simultaneously minimising the total average backlog of DPs can be considered a design objective for sensor node placement via single hop transmission. The optimisation problem can be defined as follows:

$$\begin{aligned}
\underset{n_{ij}}{\text{minimize}} \quad & g_{ij}(\bar{d_{ij}}) = \sum_{i=1}^{m}\sum_{j=1}^{n} \bar{d_{ij}} \\
\text{subject to} \quad & \sum_{i=1}^{m}\sum_{j=1}^{n} n_{ij} = N, \\
& k \geq n_{ij} \geq 1, \quad \forall i \in \{1,\cdots,m\},\ \forall j \in \{1,\cdots,n\}.
\end{aligned} \tag{7.9}$$

One intuitive strategy to solve the optimisation problem is to place as many sensor nodes as possible in the unit regions with higher energy availability. Apart from the existence of sufficient amounts of energy, traffic load can be shared with other nodes in the same unit, so that the expected backlog of DPs will be low. However, the remaining nodes that operate in the other units may have to deal with heavy traffic loads or a lack of energy. Thus, fairness must be provided among the sensor nodes. For example, having average backlogs of DPs as $d_1 = 1, d_2 = 1, d_3 = 1, d_4 = 1$ is more preferable than having $d_1 = 0, d_2 = 0, d_3 = 0, d_4 = 4$ even if the total backlog of DPs is equal. The reason behind the fairness concern is that long interruptions of updates from a specific region may impact the efficiency of the network functionality and result in incorrect monitoring.

A fairness index can help us understand the effect of unfair sharing among data buffers when their total backlog is the same. Jain's index, the earliest proposed fairness measure, is defined in [161] as:

$$f(x) = \frac{[\sum_{i=1}^{n} x_i]^2}{\sum_{i=1}^{n} x_i^2} \tag{7.10}$$

where $0 \leq f(x) \leq 1$. Jain's index is one of the most widely used fairness measures. The larger value of $f(x)$ represents the fairer strategy for the sensor node placement. Table (7.1) shows the different Jain's index with different average backlog of DPs. In this table, it can be seen that the system becomes fairer when Jain's index is closer to 1.

	Case1	Case2	Case3	Case4	Case5
<d_1>	0	0	0	0	1
<d_2>	0	0	0	1	1
<d_3>	0	1	2	1	1
<d_4>	4	3	2	2	1
f(x)	***0.25***	***0.40***	***0.50***	***0.67***	***1***

TABLE 7.1: Example's of Jain's index, $< d_i >$ represents the average backlog of DPs at node i.

A small modification in the objective function can help to overcome fairness concern. The following could be an example of a modified objective function:

$$g^*_{ij}(\bar{d_{ij}}) = \sum_{i=1}^{m}\sum_{j=1}^{n} \bar{d_{ij}}^2 \tag{7.11}$$

where the summation of $\bar{d_{ij}}^2$s will provide fairer sharing among the sensor nodes.

7.4.3 Numerical Results

As mentioned previously, each unit region must be occupied by at least one sensor node to cover the whole region in which the WSN operates. Thus, the sensor node replacement problem is distributing $N - M$ remaining nodes among $M = m \times n$ unit regions.

Table (7.2) shows a numerical example of optimum node placement using identical sensor nodes whose parameters are $D = 1000, E = 1000, \mu = 0.1, \gamma = 0.1$, and $N = 50, m = 5, n = 5$. Random energy and data arrival rates are assumed for each unit region such that $\Lambda_{ij} \in [1,\ 10]$ and $\lambda_{ij} \in [10,\ 20]$ packets per second. In this numerical example, comparison of three different node placements, optimum placement with and without fairness concern, and equal node placement to each unit region have been considered. While the placement with fairness concern shows the best performance, equal node placement without any optimisation shows the worst.

Energy Arrivals	*Data Arrivals*	*Initial Case*	*Initial Case*	*Optimum Placement without Fairness (k=3)*	*Optimum Placement without Fairness (k=3)*	*Optimum Placement with Fairness (k=3)*	*Optimum Placement with Fairness (k=3)*	*Equal Placement (k=2)*	*Equal Placement (k=2)*
Λ_{ij}	λ_{ij}	n_{ij}=1	d_{ij}	n_{ij}	d_{ij}	n_{ij}	d_{ij}	n_{ij}=2	d_{ij}
2	13	1	99.807	2	99.523	1	99.807	2	99.523
3	16	1	99.76	1	99.76	2	99.367	2	99.367
5	19	1	99.633	2	98.841	1	99.633	2	98.841
6	18	1	99.487	3	18.468	1	99.487	2	97.897
10	16	1	98.288	2	0	2	0	2	0
8	10	1	95.737	2	0	2	0	2	0
10	17	1	98.536	3	0	2	0	2	0
1	19	1	99.939	2	99.869	2	99.869	2	99.869
7	10	1	97.552	2	0	3	0	2	0
10	13	1	96.517	2	0	2	0	2	0
3	12	1	99.652	1	99.652	3	96.556	2	98.831
10	14	1	97.41	3	0	2	0	2	0
10	13	1	96.517	2	0	2	0	2	0
2	20	1	99.883	3	99.54	3	99.54	2	99.734
8	11	1	97.207	2	0	3	0	2	0
2	12	1	99.788	2	99.462	1	99.788	2	99.462
2	19	1	99.876	2	99.716	3	99.504	2	99.716
4	16	1	99.655	1	99.655	2	98.949	2	98.949
4	14	1	99.586	2	98.586	1	99.586	2	98.586
4	13	1	99.539	2	98.292	1	99.539	2	98.292
3	17	1	99.777	1	99.777	1	99.777	2	99.426
4	18	1	99.705	1	99.705	2	99.163	2	99.163
8	18	1	99.182	2	91.001	3	0	2	91.001
10	20	1	98.98	2	21.005	3	0	2	21.005
1	10	1	99.876	3	99.507	2	99.718	2	99.718
		25	***2471.91***	***50***	***1522.49***	***50***	***1490.31***	***50***	***1599.57***

TABLE 7.2: Results of 3 different node placement algorithms. Fairness provides better results for the overall network performance.

7.5 Multi-Hop Transmission

Although the single hop transmission is sufficient for most WSN clusters and small networks, multi-hop transmission is required for larger networks as the transmission range of a sensor node can not cover the distance between the node and the base-station.

The problem definition is slightly different compared to the one considered in the single hop transmission section. In this section:

1. A cascaded network of N sensor nodes is considered and their optimum placement in an area consisting of $M = m \times n$ unit regions.

2. Each unit region can occupy at most one sensor node, i.e., $k = 1$.

3. A sensor node in A_{ij} can forward DPs to only the node in A_{i+1j-1}, A_{i+1j}, or A_{i+1j+1}, as shown in Figure (7.3).

4. The optimisation problem is placing one sensor node into each row $i \in \{1, 2, \cdots, N\}$ as shown in Figure (7.3) such that the final throughput is maximised.

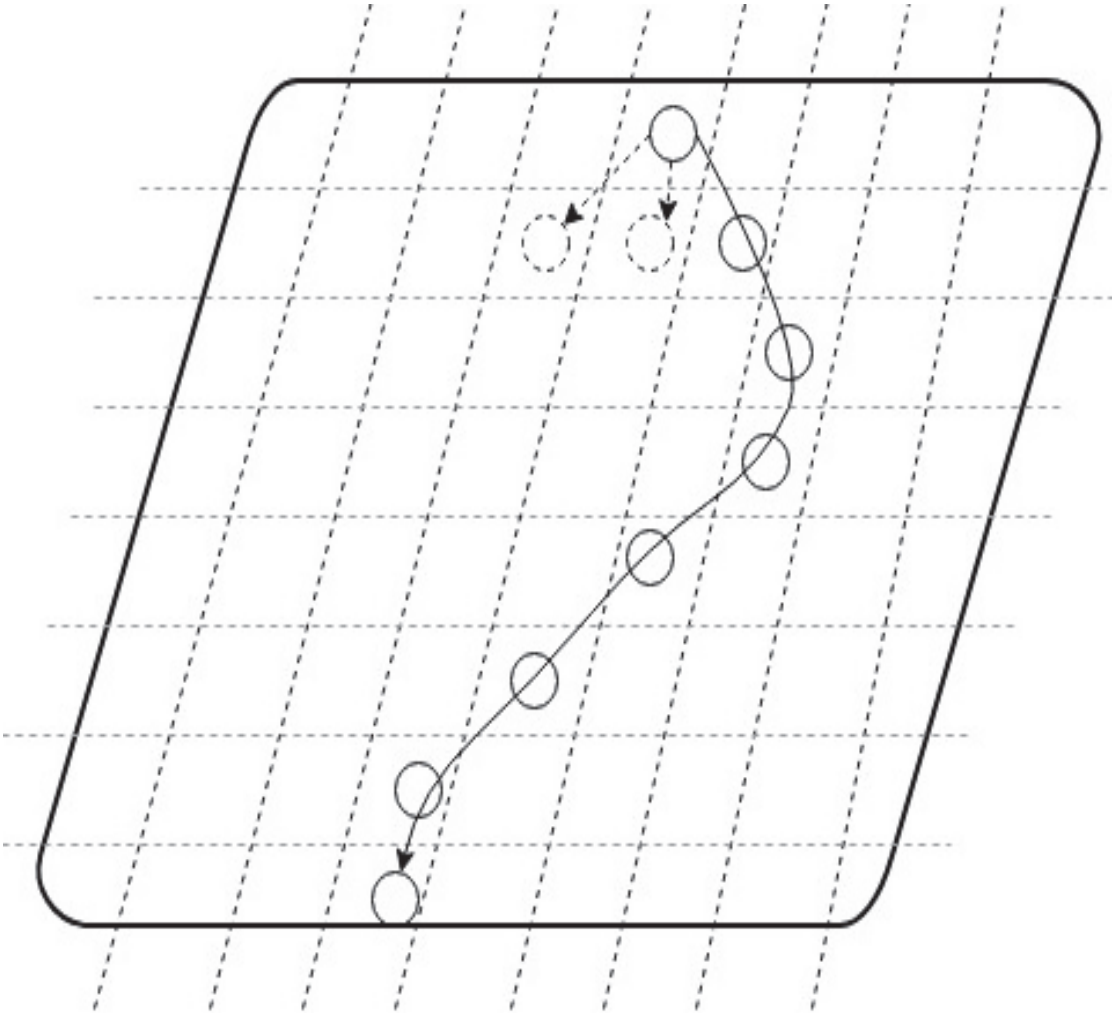

FIGURE 7.3: A node in A_{ij} can only forward its data to specific nodes, which must be located in A_{i+1j-1}, A_{i+1j}, or A_{i+1j+1}.

7.5.1 N-Layers Cascaded Network

In the cascaded N-hop model, it was assumed that the data and energy buffers are unbound. A DP is transmitted using one EP. DP transmission or forwarding times were assumed to be negligibly small compared to the inter-arrival times of DPs and EPs to the system, and to the average time between successive losses of a DP, and to the average time it takes an EP to be lost due to battery leakage. Figure (7.4) shows the cascaded N-hop model.

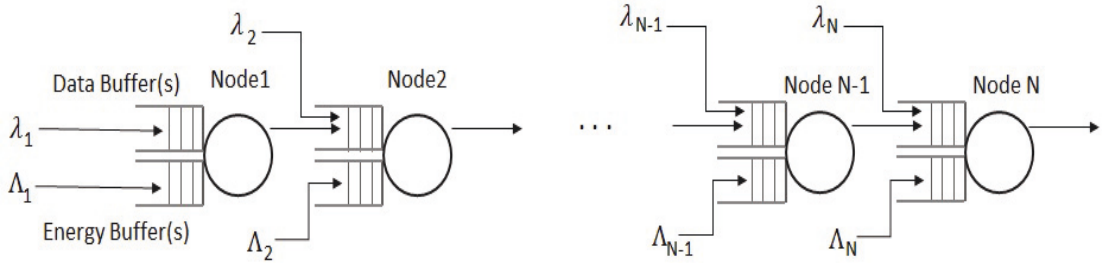

FIGURE 7.4: Cascade network of N nodes that store, process, and forward jobs to their successive node.

States of a node i in steady state are represented by $p(n_i)$ where $n(i) = d_i - e_i$. Thus, the joint distribution of the cascade network can be written as:

Theorem 1 Let:

$$v_1 = \lambda_1, \; v_{i+1} = \lambda_{i+1} + \sum_{j=1}^{i} \lambda_j \prod_{k=j}^{i} \frac{\Lambda_k}{\Lambda_k + \gamma_k}. \tag{7.12}$$

and the conditions

$$v_i + \mu_i = \Lambda_i + \gamma_i, \tag{7.13}$$

$$\mu_i^0 = v_i + 2\mu_i, \tag{7.14}$$

$$\gamma_i^0 = \Lambda_i + 2\gamma_i. \tag{7.15}$$

are satisfied, then the steady state probability distribution:

$$\pi(\bar{n}) = P \prod_{i=1}^{N} \pi_i(n_i), \tag{7.16}$$

where $\bar{n} = (n_1, n_2, \cdots, n_N)$ and

$$\pi_i(n_i) = \begin{cases} 1, & \text{if } n_i = 0 \\ \frac{1}{2}(\frac{v_i}{\Lambda_i + \gamma_i})^{n_i}, & \text{if } n_i \geq 1 \\ \frac{1}{2}(\frac{\Lambda_i}{v_i + \mu_i})^{-n_i}, & \text{if } n_i \leq -1 \end{cases} \tag{7.17}$$

where the normalising constants P is:

$$P = \prod_{k=1}^{N} (1 + \frac{v_k}{2\mu_k} + \frac{\Lambda_k}{2\gamma_k})^{-1}, \tag{7.18}$$

The proof is given in the Appendix B.

The average backlogs of DPs waiting in the network is:

$$< d > = \sum_{i=1}^{N} \sum_{n_i>0} n_i \pi(n_i) \tag{7.19}$$

$$= \sum_{i=1}^{N} \sum_{n_i>0} \frac{P_i}{2} n_i (\frac{v_i}{\Lambda_i + \gamma_i})^{n_i} \tag{7.20}$$

$$= \sum_{i=1}^{N} \frac{P_i}{2} (\frac{v_i}{\mu_i}(1 + \frac{v_i}{\mu_i})) \tag{7.21}$$

$$= \sum_{i=1}^{N} \frac{v_i}{\mu_i} \frac{\gamma_i}{\gamma_i + \mu_i}. \tag{7.22}$$

and the DP throughput of a node i can be calculated as:

$$O_i = \sum_{n_i>0} \pi(n_i)\Lambda_i + \sum_{n_i<0} \pi(n_i) v_i \tag{7.23}$$

$$= \frac{1}{2} P_i [(\frac{\frac{v_i}{\Lambda_i+\gamma_i}}{1 - \frac{v_i}{\Lambda_i+\gamma_i}})\Lambda_i + (\frac{\frac{\Lambda_i}{\Lambda_i+\gamma_i}}{1 - \frac{\Lambda_i}{\Lambda_i+\gamma_i}}) v_i] \tag{7.24}$$

$$= \frac{1}{2} P_i \Lambda_i v_i (\frac{1}{\gamma_i} + \frac{1}{\mu_i}) \tag{7.25}$$

$$= \frac{v_i \Lambda_i}{\Lambda_i + \gamma_i} \tag{7.26}$$

where $P_i = \frac{2\gamma_i \mu_i}{(\gamma_i+\mu_i)(v_i+\mu_i)}$.

7.5.2 Numerical Examples

The optimum placement of $N = m$ sensor nodes that can form as a cascade network, and provide multi-hop communication into a region, consisting of $M = m \times n$ unit regions, for maximising the final throughput of the cascade network have been considered.

Figure (7.5) shows two numerical examples of the optimum sensor placement for final throughput maximisation where the number pairs represent the spatial continuous energy and traffic arrivals at each unit region $(\Lambda_{ij}, \lambda_{ij})$, such that $\Lambda_{ij} \in [1,\ 10]$ and $\lambda_{ij} \in [10,\ 20]$ packets per second. The other parameters of a sensor node operating in A_{ij} are assumed to be $\mu_{ij} = 0.1\Lambda_{ij}$ and $\gamma_{ij} = v_{ij} + \mu_{ij} - \Lambda_{ij}$. The selection of γ_{ij} is to satisfy the energy-data flow condition in equation 7.13.

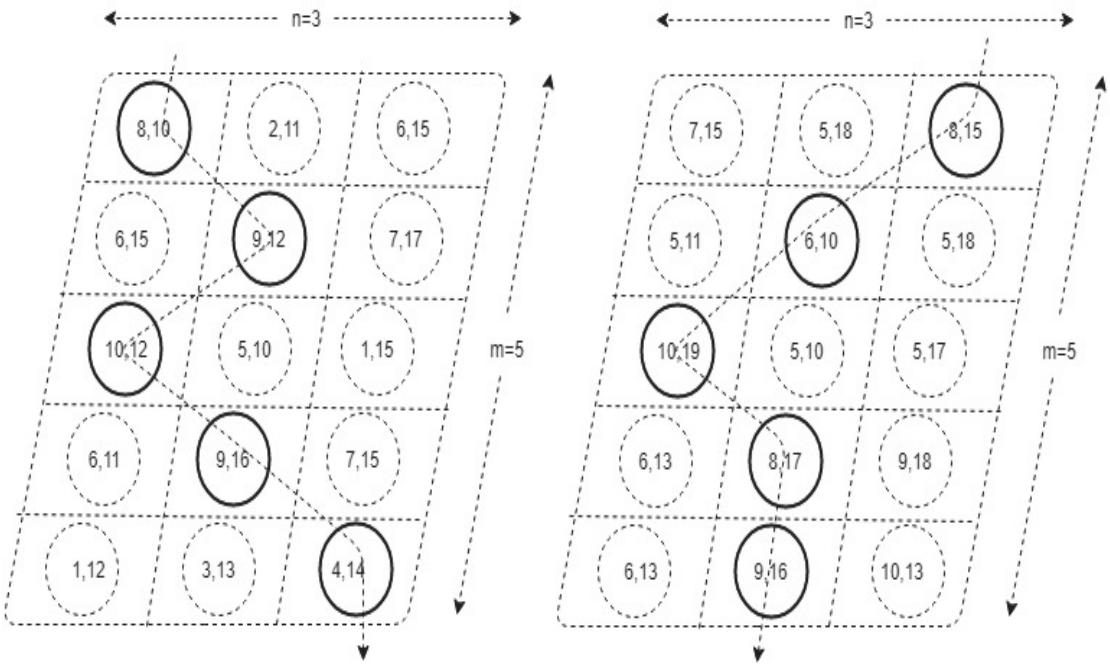

FIGURE 7.5: Optimum sensor placement for throughput maximisation where the parameters of unit region A_{ij} are $\Lambda_{ij},\ \lambda_{ij},\ \mu_{ij} = 0.1\Lambda_{ij},\ \gamma_{ij} = v_{ij} + \mu_{ij} - \Lambda_{ij}$.

7.6 Impacts of Modelling Assumptions on the Results

In this chapter, it has been assumed that a sensor can only sense DPs from the unit region where it is placed. In reality, however, a sensor node is able to collect data from a circular region where the sensor is located in the centre. Thus, a sensor node needs to occupy with not only the traffic from the unit region it is placed but also the traffic from the neighbouring units. In this case, energy consumption for the transmission would increase along with the increasing total data arrival rate. Furthermore, the additional traffic from the other units would lower the reliability of the information collected by the monitoring devices. One reasonable approach to re-evaluate this assumption is that the circular sensing range covers the possible maximum area that stays inside the unit region. In this case, the integrity problem still remains since a small fraction of the unit regions can not be covered by the sensing range of a sensor node. However, this model dramatically reduces the effect of the interference and the total energy consumption of the system.

7.7 Conclusion

This chapter focused on the optimum sensor placement for different transmission schemes and different optimisation objectives. The importance of sensor localisation for WSNs

was briefly mentioned and a summary of the different factors that have an impact upon initial node placement (e.g. deployment methodologies, optimisation objectives and node functionality) have been provided. The region where WSNs operate is composed of unit regions. The data and energy arrivals, at each unit region, were assumed to follow a Poisson process with different rates. While sensor nodes placed in a unit region can share the traffic load, they are all able to capture the full amount of energy (e.g. from a photovoltaic source). First, a model was investigated wherein the sensor nodes can directly communicate with the base station or the cluster head. For this model, the network objective is to provide the area coverage while minimising the total average backlog of data in the node buffers. In addition, fairness among sensor nodes was considered so that the objective function was changed to a sum of squared values of each DP backlog instead of their direct sum. Moreover, an additional model was studied wherein sensor nodes constitute a multi-hop cascade network to communicate with the base station. The network objective of this model was the placement of sensor nodes in the unit regions such that the final throughput of the cascaded network was maximised. Numerical examples were provided to illustrate the optimum node placement for single-hop transmission with and without fairness concern. Furthermore, examples of optimum path selection for a multi-hop transmission case have been provided.

Chapter 8

Conclusion and Future Work

8.1 Conclusion

This thesis has investigated recent work on mathematical models of digital devices where energy and data are in discrete packet units abstraction based on the EPN paradigm. While EPNs examine the task service times for both energy consumption and job processing, the EN paradigm considers devices with zero service time. Particularly in EHWSN, the DP transmission usually takes place on a scale of microseconds or nanoseconds, while the packet sensing and processing in the node may take many milliseconds such that the EN paradigm is applicable. EHWSNs studied in this thesis receive data from other devices or through sensing, and gather energy through harvesting from photovoltaic or other ambient energy sources. Buffers for DPs and EPs have been assumed to have limited capacities of D and E.

An EHWSN requires energy not only for packet transmission but also for node electronics. For example, packet sensing, processing and storing. Therefore, the harvested energy consumption in a sensor node was divided into two parts: K_e and K_t EPs for node electronics and for DP transmission. Whenever a sensor node stores less than K_e EPs, it cannot sense and store the data. Consequently, the information will be lost. However, if a node stores more than K_e EPs, the data arrival can be sensed, processed, and stored immediately by consuming K_e EPs. Moreover, if the remaining EPs are greater than K_t EPs, they can also be transmitted in zero time by consuming all the K_t EPs. Thus, successful sensing and transmission of a DP requires exactly $K = K_e + K_t$ EPs.

In Chapter 3, it was assumed that a successful DP transmission can occur by consuming a single EP through a perfect transmitter, i.e. $K_t = 1$ and $K_e = 0$. In addition, the energy and data leakage caused by the standby and time-out operations of the node

into the system have been introduced. These leakages have been modelled as Poisson processes. These systems led to a one-dimensional random walk diagram to model the behaviour of the state transitions. Following modelling the system, closed-form formulas for the stationary probability distributions were obtained. Excessive packets resulting from finite buffer capacities and obtained formulas for EP and DP loss rates were also investigated. Moreover, the question of system stability was analysed by considering infinite buffer sizes. Analysis revealed that systems with unlimited buffer capacity exhibit stable behaviour only when certain conditions have been satisfied. Furthermore, DP retransmission was studied by introducing the error probabilities π and p. It was shown that closed-form formulas for stationary probability distributions can be found under certain conditions according to new transition rates. In addition, the relation between the correctly receiving probability and the error probabilities π and p was investigated. Second, data transmission with K EPs through a perfect transmitter was studied. The motivation lies in the fact that a sensor node may vary the transmission power level to decrease the probability of unsuccessful transmissions or prevent energy waste in some cases. This system led us to a two-dimensional random walk for modelling its state behaviours. Closed-form formulas were obtained by modifying the system where a state can be represented with a single index, not with integer pairs. The effect of noise and interference on sensor node transmitting among a set of identical sensor nodes was also investigated.

In Chapter 4, a more practical model that considered a packet transmission through an imperfect transmitter was studied. First, we studied an imperfect transmitter that consumes a single EP for node electronics and another EP for transmission. As a consequence of this energy consumption model, the DP buffer could be either empty or can only store a single DP. Thus, it may be expected that there would be a great number of excessive DPs; however, this can be prevented for certain ratios of data and energy flows. A closed-form formula was obtained for the stationary distributions and it was shown that the system is always stable for the data queue and unstable for the energy queue. Next, a generalised energy consumption model was investigated. This contained an imperfect transmitter which consumes an arbitrary number of EPs such that $K_e > 1$ and $K_t > 1$ for both the node electronics and the transmission. A solution method was proposed to reduce the computational complexity of the system by introducing companion matrices and using linear algebra.

In Chapter 5, a network model in which N EHWSNs constitute a cascaded structure was investigated. EHWSNs with a perfect transmitter were considered. It was assumed that one EP consumption is sufficient for successful transmission. In addition, it was assumed an EHWSN can forward its data to the immediate neighbour in zero time scale when energy is available. However, if DPs must wait some time in the buffers for new

energy arrivals, the buffers suffer from information loss. In this chapter, a new PFS was developed for N-node tandem systems. In these systems external data arrives via the first node, and the other nodes operate as relays to forward the data to the last node without any other external information flow. It was shown that there must be a link between data and energy flows to obtain PFS for such systems. It was also illustrated using numerical results how the average backlog of DPs and the system throughput vary with different system parameters thanks to computational convenience that the PFS provides.

In Chapter 6, a modelling approach was proposed to evaluate effects of simple battery attacks on battery life-time of EHWSNs for two cases: where ambient and intermittent energy is used as energy source such that there is no need for battery replacement, and the case of a replaceable battery without energy harvesting. First, a brief summary of attacks was presented. Moreover, the effects of two attacks were considered in the study: attacks that create additional redundant traffic and attacks that cause packet errors and require packet retransmissions. Numerical examples reveal that these attacks significantly impact on EHWSNs and they can reduce battery life-time from months to days. Therefore, a mitigation method was proposed. This method forces the traffic arrival rate to remain below a certain threshold with the sacrifice of some information loss. Furthermore, the analysis revealed that using replaceable batteries is more stable than using the renewable energy sources, even though it requires human intervention.

In Chapter 7, optimum sensor placement was investigated by considering two different transmission schemes: the single-hop transmission, which can occur in small indoor WSNs or in many network clusters, and the multi-hop transmission where N EHWSNs constitute a cascade network. The study focused on several different network objectives such as full area coverage, while minimising the backlog of traffic in the data buffers and network connectivity, while maximising the final average throughput of the system. A single node analysis studied in Chapter 3 was used, in which data and energy that flow into the node are independent Poisson processes and a successful transmission can occur with $K_e = 0$ and $K_t = 1$ values. Furthermore, it was shown that an N layered cascade network has PFS for its joint probability, i.e, joint probability equals to the multiplication of marginal probabilities, which provides enormous computation simplifications to analyse the system.

8.2 Future Work

Several points have been raised in this thesis that can be expanded. This section discusses the open issues and possible future directions.

In Chapter 3 and Chapter 4, the work focused on single node analysis where different energy consumption models were studied by considering different energy uses by the node electronics (K_e) and the transmission sub-system (K_t). A linear algebra technique was proposed to reduce computation complexity for the systems with generalised K_e and K_t values. For future work, further analysis can be made to obtain a closed-form formula for the stationary probability distribution of states while considering independent energy and data arrivals as well as independent energy and data losses. Furthermore, one possible direction is to consider dependent traffic and energy arrivals and re-analyse the system.

In Chapter 5, an N layered cascade network was studied where only the first node can sense the external traffic, and the other nodes relayed the information to the destination point. Each relay node is capable of harvesting energy, storing data and energy in its own buffers, but cannot sense data from external sources. It was assumed that each layer has one node in this model. A re-analysis of the model could be carried out when increasing the number of nodes for each layer, such that forwarding the data to a node in the next layer can happen with a certain probability. The optimum values of these probabilities can be investigated to maximise the throughput of the system. Moreover, nodes in this model were assumed to consume single EP just for DP transmission but not node electronics. Similar network models can be studied by considering different K_e and K_t values.

In Chapter 6, basic energy attacks were modelled to evaluate their impact on sensor life-time. Moreover, a simple mitigation technique that maintains the life-time above a certain threshold was proposed. This system can be improved by adding other attacks into the model. Moreover, several results in this section assumed that the attack traffic was proportional to the ongoing normal traffic. This may not be realistic as attackers may inject a fixed traffic rate of attack traffic so that the proportion of attack traffic is reduced when the normal traffic rate increases. Thus, future work will need to delve deeper into mitigation techniques and their evaluation in order to propose new methods to mitigate against battery attacks.

In Chapter 7, the optimum placement of sensor nodes for different transmission schemes and objectives were investigated. It was assumed that sensors placed in the same unit region can share the spatial traffic flow into that region while they all can take advantage of capturing the full amount of available spatial energy on arrival (eg. from photovoltaic

sources). This model can be changed so that sensor nodes also have to share the accessible energy. Moreover, the effect of possible data capturing from neighbour unit regions by limiting the sensing rage of nodes within an unit region have not been considered. Future work can consider this effect to show more practical results. Furthermore, a multi-hop communication of a cascade network where each node is capable of sensing data and capturing energy from the ambient environment has been investigated. This pre-defined routing model can be improved by studying the general network case where the network objective can be optimised by choosing the best possible routing according to data and energy availabilities of sensor nodes constituting the network.

Appendix A

Proof of Product-form Solution Of Cascade Networks

Let:

$$v_1 = \lambda_1,\ v_{i+1} = \frac{v_i \Lambda_i}{\Lambda_i + \gamma_i} = \lambda_1 \prod_{l=1}^{i} \frac{\Lambda_i}{\Lambda_i + \gamma_i}. \tag{A.1}$$

and assume that the following EDF equilibrium conditions are satisfied, i.e.:

$$v_i + \mu_i = \Lambda_i + \gamma_i, \tag{A.2}$$

$$\mu_i^0 = v_i + 2\mu_i, \tag{A.3}$$

$$\gamma_i^0 = \Lambda_i + 2\gamma_i. \tag{A.4}$$

Then the steady-state probability distribution for the system $\pi(\bar{n}) = \lim_{t\to\infty} p(\bar{n}, t)$ is given by:

$$\pi(\bar{n}) = \prod_{i=1}^{N} \pi_i(n_i), \tag{A.5}$$

where

$$\pi_i(n_i) = \begin{cases} C_i, & \text{if } n_i = 0 \\ C_i . \frac{v_i}{\Lambda_i + \gamma_i^0} (\frac{v_i}{\Lambda_i + \gamma_i})^{n_i - 1}, & \text{if } n_i \geq 1 \\ C_i . \frac{\Lambda_i}{v_i + \mu_i^0} (\frac{\Lambda_i}{v_i + \mu_i})^{-n_i - 1}, & \text{if } n_i \leq -1 \end{cases} \tag{A.6}$$

where the normalising constants C_i are :

$$C_i = (1 + \frac{\frac{v_i}{\Lambda_i + \gamma_i^0}}{1 - \frac{v_i}{\Lambda_i + \gamma_i}} + \frac{\frac{\Lambda_i}{v_k + \mu_i^0}}{1 - \frac{\Lambda_i}{v_i + \mu_i}})^{-1}. \tag{A.7}$$

Therefore, we may calculate the followings:

$$\frac{\pi_i(n_i+1)}{\pi_i(n_i)} \triangleq G_i^+ = \begin{cases} \frac{v_i+\mu_i}{\Lambda_i}, & \text{if } n_i < -1 \\ \frac{v_i+\mu_i^0}{\Lambda_i}, & \text{if } n_i = -1 \\ \frac{v_i}{\Lambda_i+\gamma_i^0}, & \text{if } n_i = 0 \\ \frac{v_i}{\Lambda_i+\gamma_i}, & \text{if } n_i > 0 \end{cases} \qquad \frac{\pi_i(n_i-1)}{\pi_i(n_i)} \triangleq G_i^- = \begin{cases} \frac{\Lambda_i+\gamma_i}{v_i}, & \text{if } n_i > 1 \\ \frac{\Lambda_i+\gamma_i^0}{v_i}, & \text{if } n_i = 1 \\ \frac{\Lambda_i}{v_i+\mu_i^0}, & \text{if } n_i = 0 \\ \frac{\Lambda_i}{v_i+\mu_i}, & \text{if } n_i < 0 \end{cases}$$

The equilibrium equation is:

$$\pi(\bar{n})\ [\lambda_1 + \sum_{i=1}^{N} (\Lambda_i + \gamma_i 1_{n_i>1} + \gamma_i^0 1_{n_i=1} + \mu_i 1_{n_i<-1} + \mu_i^0 1_{n_i=-1})] \tag{A.8}$$

$$= \sum_{i=1}^{N} [\pi(\bar{n}+e_i)(\gamma_i 1_{n_i>0} + \gamma_i^0 1_{n_i=0} + \Lambda_i 1_{n_i<0} 1_{i\neq N} + \Lambda_N 1_{i=N})] \tag{A.9}$$

$$+ \sum_{i=1}^{N} [\pi(\bar{n}-e_i)(\mu_i 1_{n_i<0} + \mu_i^0 1_{n_i=0} + \lambda_1 1_{n_1>0} 1_{i=1})] \tag{A.10}$$

$$+ \sum_{j=1}^{N-1} [\pi(\bar{n} - \sum_{i=1}^{j+1} e_i)\lambda_1 \prod_{i=1}^{j} 1_{n_i\leq 0}\ (1_{n_{1+j=N}} + 1_{n_{j+1}\geq 1} 1_{n_{1+j\neq N}})] \tag{A.11}$$

$$+ \sum_{j=1}^{N-1} \sum_{i=1}^{j} [\pi(\bar{n} + e_i - \sum_{k=1}^{N-j} e_{i+k})\Lambda_i 1_{n_i\geq 0}(1_{N-j\leq 1} + 1_{N-j\geq 2} \prod_{k=1}^{N-j-1} 1_{n_{i+k}\leq 0})(1_{i=j} + 1_{n_{N+i-j}\geq 1} 1_{i\neq j})] \tag{A.12}$$

Dividing both sides of the equilibrium equation by $\pi(\bar{n})$ we have:

$$[\lambda_1 + \sum_{i=1}^{N} (\Lambda_i + \gamma_i 1_{n_i>1} + \gamma_i^0 1_{n_i=1} + \mu_i 1_{n_i<-1} + \mu_i^0 1_{n_i=-1})] \tag{A.13}$$

$$= \sum_{i=1}^{N} [G_i^+(\gamma_i 1_{n_i>0} + \gamma_i^0 1_{n_i=0} + \Lambda_i 1_{n_i<0} 1_{i\neq N} + \Lambda_N 1_{i=N})] \tag{A.14}$$

$$+ \sum_{i=1}^{N} [G_i^-(\mu_i 1_{n_i<0} + \mu_i^0 1_{n_i=0} + \lambda_1 1_{n_1>0} 1_{i=1})] \tag{A.15}$$

$$+ \sum_{j=1}^{N-1} [\prod_{i=1}^{j+1} G_i^- \lambda_1 \prod_{i=1}^{j} 1_{n_i\leq 0}\ (1_{1+j=N} + 1_{n_{j+1}\geq 1} 1_{1+j\neq N})] \tag{A.16}$$

$$+ \sum_{j=1}^{N-1} \sum_{i=1}^{j} [G_i^+ \prod_{k=1}^{N-j} G_{k+i}^-(\Lambda_i 1_{n_i\geq 0}(1_{N-j\leq 1} + 1_{N-j\geq 2} \prod_{k=1}^{N-j-1} 1_{n_{i+k}\leq 0})(1_{i=j} + 1_{n_{N+i-j}\geq 1} 1_{i\neq j}))] \tag{A.17}$$

Consider the line (A.14) so that we have the following:

$$\sum_{i=1}^{N}[G_i^+(\gamma_i 1_{n_i>0}+\gamma_i^0 1_{n_i=0}+\Lambda_i 1_{n_i<0}1_{i\neq N}+\Lambda_N 1_{i=N})]= \tag{A.18}$$

$$G_N^+\Lambda_N 1_{n_N\geq 0}+\sum_{i=1}^{N}[\frac{v_i\gamma_i}{\Lambda_i+\gamma_i}1_{n_i>0}+\frac{v_i\gamma_i^0}{\Lambda_i+\gamma_i^0}1_{n_i=0}+(v_i+u_i^0)1_{n_i=-1}+(v_i+u_i)1_{n_i<-1}] \tag{A.19}$$

Consider the line (A.15) so that we have the following:

$$\sum_{i=1}^{N}[(G_i^-)(\mu_i 1_{n_i<0}+\mu_i^0 1_{n_i=0}+\lambda_1 1_{n_1>0}1_{i=1})]= \tag{A.20}$$

$$G_1^-\lambda_1 1_{n_1>0}+\sum_{i=1}^{N}[\frac{\Lambda_i\mu_i}{v_i+\mu_i}1_{n_i<0}+\frac{\Lambda_i\mu_i^0}{v_i+\mu_i^0}1_{n_i=0}]. \tag{A.21}$$

The summation of the lines (A.19) and (A.21):

$$=G_1^-\lambda_1 1_{n_1>0}+G_N^+\Lambda_N 1_{n_N\geq 0} \tag{A.22}$$

$$+\sum_{i=1}^{N}[\frac{v_i\gamma_i}{\Lambda_i+\gamma_i}1_{n_i>0}+(\frac{v_i\gamma_i^0}{\Lambda_i+\gamma_i^0}+\frac{\Lambda_i\mu_i^0}{v_i+\mu_i^0})1_{n_i=0}+.$$

$$.(v_i+u_i^0+\frac{\Lambda_i\mu_i}{v_i+\mu_i})1_{n_i=-1}+(v_i+u_i+\frac{\Lambda_i\mu_i}{v_i+\mu_i})1_{n_i<-1}],$$

where

$$\frac{v_i\gamma_i^0}{\Lambda_i+\gamma_i^0}+\frac{\Lambda_i\mu_i^0}{v_i+\mu_i^0}=\frac{v_i(\Lambda_i+2\gamma_i)+\Lambda_i(v_i+2\mu_i)}{2(\Lambda_i+\gamma_i)}=v_i+\frac{\Lambda_i\mu_i}{\Lambda_i+\gamma_i}, \tag{A.23}$$

and

$$\frac{v_i\gamma_i}{\Lambda_i+\gamma_i}=v_i+\frac{\Lambda_i\mu_i}{\Lambda_i+\gamma_i}+\frac{v_i\gamma_i}{\Lambda_i+\gamma_i}-v_i-\frac{\Lambda_i\mu_i}{\Lambda_i+\gamma_i} \tag{A.24}$$

$$=v_i+\frac{\Lambda_i\mu_i}{\Lambda_i+\gamma_i}+\frac{v_i\gamma_i-v_i\Lambda_i-v_i\gamma_i-\Lambda_i\mu_i}{\Lambda_i+\gamma_i} \tag{A.25}$$

$$=v_i-\Lambda_i+\frac{\Lambda_i\mu_i}{\Lambda_i+\gamma_i}. \tag{A.26}$$

When we use the lines (A.23) and (A.26) into (A.22) we have:

$$= G_1^- \lambda_1 1_{n_1>0} + G_N^+ \Lambda_N 1_{n_N \geq 0} \tag{A.27}$$

$$+ \sum_{i=1}^{N} [v_i + \frac{\Lambda_i \mu_i}{\Lambda_i + \gamma_i} + \mu_i^0 1_{n_i=-1} + \mu_i 1_{n_i<-1} - \Lambda_i 1_{n_i>0}] \tag{A.28}$$

$$= G_1^- \lambda_1 1_{n_1>0} + G_N^+ \Lambda_N 1_{n_N \geq 0} \tag{A.29}$$

$$+ \sum_{i=1}^{N} [\Lambda_i + \frac{v_i \gamma_i}{\Lambda_i + \gamma_i} + \mu_i^0 1_{n_i=-1} + \mu_i 1_{n_i<-1} - \Lambda_i 1_{n_i>0}] \tag{A.30}$$

Thus, up to this point the equilibrium equation is simplified to the following:

$$\lambda_1 + \sum_{i=1}^{N} [\gamma_i 1_{n_i>1} + \gamma_i^0 1_{n_i=1}] \tag{A.31}$$

$$= G_1^- \lambda_1 1_{n_1>0} + G_N^+ \Lambda_N 1_{n_N \geq 0} + \sum_{i=1}^{N} [\frac{v_i \gamma_i}{\Lambda_i + \gamma_i} - \Lambda_i 1_{n_i>0}] \tag{A.32}$$

$$+ \sum_{j=1}^{N-1} [\prod_{i=1}^{j+1} G_i^- \lambda_1 \prod_{i=1}^{j} 1_{n_i \leq 0} \ (1_{1+j=N} + 1_{n_{j+1} \geq 1} 1_{1+j \neq N})] \tag{A.33}$$

$$+ \sum_{j=1}^{N-1} \sum_{i=1}^{j} [G_i^+ \prod_{k=1}^{N-j} G_{k+i}^- \Lambda_i 1_{n_i \geq 0} (1_{N-j \leq 1} + 1_{N-j \geq 2} \prod_{k=1}^{N-j-1} 1_{n_{i+k} \leq 0}). \tag{A.34}$$

Now consider the line (A.33):

$$\sum_{j=1}^{N-1}[\prod_{i=1}^{j+1}G_i^-\lambda_1\prod_{i=1}^{j}1_{n_i\leq 0}\,(1_{1+j=N}+1_{n_{j+1}\geq 1}1_{1+j\neq N})] \tag{A.35}$$

$$=\lambda_1 G_N^-\prod_{i=1}^{N-1}G_i^-1_{n_i\leq 0} \tag{A.36}$$

$$+\sum_{j=1}^{N-2}[\lambda_1 G_{j+1}^-1_{n_{j+1}\geq 1}\prod_{i=1}^{j}G_i^-1_{n_i\leq 0}] \tag{A.37}$$

$$=\lambda_1 G_N^-\prod_{i=1}^{N-1}[\frac{\Lambda_i}{v_i+\mu_i^0}1_{n_i=0}+\frac{\Lambda_i}{v_i+\mu_i}1_{n_i<0}] \tag{A.38}$$

$$+\sum_{j=1}^{N-2}[\lambda_1(\frac{\Lambda_{1+j}+\gamma_{1+j}}{v_{1+j}}1_{n_{1+j}>1}+\frac{\Lambda_{1+j}+\gamma_{1+j}^0}{v_{1+j}}1_{n_{1+j}=1})\prod_{i=1}^{j}\frac{\Lambda_i}{v_i+\mu_i^0}1_{n_i=0}+\frac{\Lambda_i}{v_i+\mu_i}1_{n_i<0}] \tag{A.39}$$

$$=[\lambda_1 G_N^-\prod_{i=1}^{N-1}(\frac{v_{i+1}}{v_i})(\frac{1_{n_i=0}}{2}+1_{n_i<0})] \tag{A.40}$$

$$+\sum_{j=1}^{N-2}[\frac{\lambda_1}{v_{1+j}}((\Lambda_{1+j}+\gamma_{1+j})1_{n_{1+j}>1}+(\Lambda_{1+j}+\gamma_{1+j}^0)1_{n_{1+j}=1})\prod_{i=1}^{j}(\frac{v_{i+1}}{v_i})(\frac{1_{n_i=0}}{2}+1_{n_i<0})] \tag{A.41}$$

$$=v_N G_N^-\prod_{i=1}^{N-1}(\frac{1_{n_i=0}}{2}+1_{n_i<0})] \tag{A.42}$$

$$+\sum_{j=1}^{N-2}[\big((\Lambda_{1+j}+\gamma_{1+j})1_{n_{1+j}>1}+(\Lambda_{1+j}+\gamma_{1+j}^0)1_{n_{1+j}=1}\big)\prod_{i=1}^{j}(\frac{1_{n_i=0}}{2}+1_{n_i<0})] \tag{A.43}$$

$$=v_N G_N^-\prod_{i=1}^{N-1}f(n_i) \tag{A.44}$$

$$+\sum_{j=1}^{N-2}[G_{j+1}^-v_{j+1}1_{n_{j+1}\geq 1}\prod_{i=1}^{j}f(n_i)]. \tag{A.45}$$

where $\frac{v_{i+1}}{v_i}=\frac{\Lambda_i}{\Lambda_i+\gamma_i}$ and $f(n_i)\triangleq\frac{1_{n_i=0}}{2}+1_{n_i<0}$.

When we consider the line (A.34):

$$+\sum_{j=1}^{N-1}\sum_{i=1}^{j}[G_i^+\prod_{k=1}^{N-j}G_{k+i}^-\Lambda_i 1_{n_i\geq 0}(1_{N-j\leq 1}+1_{N-j\geq 2}\prod_{k=1}^{N-j-1}1_{n_{i+k}\leq 0})(1_{i=j}+1_{n_{N+i-j}\geq 1}1_{i\neq j})] \tag{A.46}$$

$$=G_{N-1}^+\,G_N^-\,\Lambda_{N-1}1_{N-1\geq 0} \tag{A.47}$$

$$+\sum_{i=1}^{N-2}[G_i^+\,G_{i+1}^-\,\Lambda_i 1_{i\geq 0}1_{i+1\geq 1}] \tag{A.48}$$

$$+\sum_{j=2}^{N-2}\sum_{i=1}^{j-1}[G_i^+\prod_{k=1}^{N-j}G_{k+i}^-\Lambda_i 1_{n_i\geq 0}\prod_{k=1}^{N-j-1}l_{n_{i+k}\leq 0}\,1_{n_{N+i-j}\geq 1}\,] \tag{A.49}$$

$$+\sum_{j=1}^{N-2}[G_j^+\prod_{k=1}^{N-j}G_{k+j}^-\Lambda_j 1_{n_j\geq 0}\prod_{k=1}^{N-j-1}l_{n_{j+k}\leq 0}] \tag{A.50}$$

$$=v_N\,G_N^-\,h(n_{N-1}) \tag{A.51}$$

$$+\sum_{i=1}^{N-2}v_{i+1}\,G_{i+1}^-\,1_{n_{i+1}\geq 1}\,h(n_i) \tag{A.52}$$

$$+\sum_{j=2}^{N-2}\sum_{i=1}^{j-1}[G_i^+\Lambda_i 1_{n_i\geq 0}\,G_{N-j+i}^-1_{n_N-j+i\geq 1}\prod_{k=1}^{N-j-1}G_{k+i}^-1_{n_k+i\leq 0}] \tag{A.53}$$

$$+\sum_{j=1}^{N-2}[G_N^-G_j^+\Lambda_j 1_{n_j\geq 0}\prod_{k=1}^{N-j-1}G_{k+j}^-l_{n_{j+k}\leq 0}] \tag{A.54}$$

$$=v_N\,G_N^-\,h(n_{N-1})) \tag{A.55}$$

$$+\sum_{i=1}^{N-2}[v_{i+1}\,G_{i+1}^-\,1_{n_{i+1}\geq 1}\,h(n_i)] \tag{A.56}$$

$$+\sum_{j=2}^{N-2}\sum_{i=1}^{j-1}[v_{i+1}h(n_i)\,G_{N-j+i}^-1_{n_{N-j+i}\geq 1}\,\frac{v_{N-j+i}}{v_{i+1}}\prod_{k=1}^{N-j-1}f(n_{k+i})] \tag{A.57}$$

$$+\sum_{j=1}^{N-2}[G_N^-\,v_{j+1}h(n_j)\frac{v_N}{v_{j+1}}\prod_{k=1}^{N-j-1}f(n_{k+j})] \tag{A.58}$$

$$=v_N\,G_N^-\,h(n_{N-1}) \tag{A.59}$$

$$+\sum_{i=1}^{N-2}[v_{i+1}\,G_{i+1}^-\,1_{n_{i+1}\geq 1}\,h(n_i)] \tag{A.60}$$

$$+\sum_{j=2}^{N-2}\sum_{i=1}^{j-1}[v_{N-j+i}G_{N-j+i}^-1_{n_{N-j+i}\geq 1}h(n_i)\prod_{k=1}^{N-j-1}f(n_{k+i})] \tag{A.61}$$

$$+v_NG_N^-\sum_{j=1}^{N-2}[h(n_j)\prod_{k=1}^{N-j-1}f(n_{k+j})]. \tag{A.62}$$

where $\prod_{i=1}^{M} G_i^- \delta_{n_i \leq 0} = \frac{v_{M+1}}{v_1} \prod_{i=1}^{M} f(n_i)$, $G_i^+ \Lambda_i \delta_{n_i \geq 0} = v_{i+1} h(n_i)$ and $h(n_i) \triangleq \frac{1_{n_i=0}}{2} + 1_{n_i>0}$.

The summation of the lines (A.59) and (A.62):

$$v_N \; G_N^- \; h(n_{N-1}) + v_N G_N^- \sum_{j=1}^{N-2} [h(n_j) \prod_{k=1}^{N-j-1} f(n_{k+j})] \tag{A.63}$$

$$= v_N G_N^- \sum_{j=1}^{N-1} [h(n_j) \prod_{k=1}^{N-j-1} f(n_{k+j})] \tag{A.64}$$

$$= v_N G_N^- \sum_{j=1}^{N-1} [(1 - f(n_j)) \prod_{k=1}^{N-j-1} f(n_{k+j})] \tag{A.65}$$

$$= v_N G_N^- \sum_{j=1}^{N-1} [\prod_{k=1}^{N-j-1} f(n_{k+j}) - f(n_j) \prod_{k=1}^{N-j-1} f(n_{k+j})] \tag{A.66}$$

$$= v_N G_N^- \sum_{j=1}^{N-1} [\prod_{k=j+1}^{N-1} f(n_k) - f(n_j) \prod_{k=j+1}^{N-1} f(n_k)] \tag{A.67}$$

$$= v_N G_N^- (1 - \prod_{k=1}^{N-1} f(n_k)). \tag{A.68}$$

The summation of the lines (A.44) and (A.68):

$$v_N G_N^- \prod_{i=1}^{N-1} f(n_i) + v_N G_N^- (1 - \prod_{k=1}^{N-1} f(n_k)) = v_N G_N^-. \tag{A.69}$$

After these simplifications, we may re-write the equilibrium equation as the following:

$$\lambda_1 + \sum_{i=1}^{N} (\gamma_i 1_{n_i>1} + \gamma_i^0 1_{n_i=1}) \tag{A.70}$$

$$= G_1^- \lambda_1 1_{n_1>0} + G_N^+ \Lambda_N 1_{n_N \geq 0} + \sum_{i=1}^{N} [\frac{v_i \gamma_i}{\Lambda_i + \gamma_i} - \Lambda_i 1_{n_i>0}] \tag{A.71}$$

$$+ \sum_{j=1}^{N-2} [G_{j+1}^- v_{j+1} 1_{n_{j+1} \geq 1} \prod_{i=1}^{j} f(n_i)] \tag{A.72}$$

$$+ v_N G_N^- \tag{A.73}$$

$$+ \sum_{i=1}^{N-2} [v_{i+1} \; G_{i+1}^- \; 1_{n_{i+1} \geq 1} \; h(n_i)] \tag{A.74}$$

$$+ \sum_{j=2}^{N-2} \sum_{i=1}^{j-1} [v_{N-j+i} G_{N-j+i}^- 1_{n_{N-j+i} \geq 1} h(n_i) \prod_{k=1}^{N-j-1} f(n_{k+i})]. \tag{A.75}$$

When we consider the summation of the lines (A.71) and (A.73):

$$= G_1^- \lambda_1 1_{n_1>0} + G_N^+ \Lambda_N 1_{n_N \geq 0} + \sum_{i=1}^{N} \frac{v_i \gamma_i}{\Lambda_i + \gamma_i} - \sum_{i=1}^{N} \Lambda_i 1_{n_i>0} \tag{A.76}$$
$$+ v_N G_N^- 1_{n_N>0} + v_N G_N^- 1_{n_N \leq 0},$$

where

$$G_N^+ \Lambda_N 1_{n_N \geq 0} + v_N G_N^- 1_{n_N \leq 0} = \frac{v_N \Lambda_N}{\Lambda_N + \gamma_N}, \tag{A.77}$$

and

$$\frac{v_N \Lambda_N}{\Lambda_N + \gamma_N} + \sum_{i=1}^{N} \frac{v_i \gamma_i}{\Lambda_i + \gamma_i} = \lambda_1. \tag{A.78}$$

Thus the equilibrium equation has been simplified to:

$$\sum_{i=1}^{N} [\gamma_i 1_{n_i>1} + \gamma_i^0 1_{n_i=1} + \Lambda_i 1_{n_i>0}] - G_1^- \lambda_1 1_{n_1>0} - G_N^- v_N 1_{n_N>0} \tag{A.79}$$
$$= \sum_{j=1}^{N-2} G_{j+1}^- v_{j+1} 1_{n_{j+1} \geq 1} \prod_{i=1}^{j} f(n_i) \tag{A.80}$$
$$+ \sum_{i=1}^{N-2} v_{i+1} \; G_{i+1}^- \; 1_{n_{i+1} \geq 1} \; h(n_i) \tag{A.81}$$
$$+ \sum_{j=2}^{N-2} \sum_{i=1}^{j-1} v_{N-j+i} G_{N-j+i}^- 1_{n_{N-j+i} \geq 1} h(n_i) \prod_{k=1}^{N-j-1} f(n_{k+i}) \tag{A.82}$$

Define $\Theta_i \triangleq G_i^- \; v_i \; 1_{n_i \geq 1}$ so that (A.82) becomes:

$$\sum_{j=2}^{N-2} \sum_{i=1}^{j-1} v_{N-j+i} G_{N-j+i}^- 1_{n_{N-j+i} \geq 1} h(n_i) \prod_{k=1}^{N-j-1} f(n_{k+i}) \tag{A.83}$$

$$= \Theta_{N-1} h(n_1) f(n_2) f(n_3) \cdots f(n_{N-2}) \tag{A.84}$$

$$+\Theta_{N-1} h(n_2) f(n_3) f(n_4) \cdots f(n_{N-2}) \tag{A.85}$$

$$\vdots$$

$$+\Theta_{N-1} h(n_N - 4) f(n_{N-3}) f(n_{N-2}) \tag{A.86}$$

$$+\Theta_{N-1} h(n_N - 3) f(n_{N-2}) \tag{A.87}$$

$$+\Theta_{N-2} h(n_1) f(n_2) f(n_3) \cdots f(n_{N-3}) \tag{A.88}$$

$$+\Theta_{N-2} h(n_2) f(n_3) f(n_4) \cdots f(n_{N-3}) \tag{A.89}$$

$$\vdots$$

$$+\Theta_{N-2} h(n_N - 5) f(n_{N-4}) f(n_{N-3}) \tag{A.90}$$

$$+\Theta_{N-2} h(n_N - 4) f(n_{N-3}) \tag{A.91}$$

$$\vdots$$

$$+\Theta_5 h(n_1) f(n_2) f(n_3) f(n4) \tag{A.92}$$

$$+\Theta_5 h(n_2) f(n_3) f(n_4) \tag{A.93}$$

$$+\Theta_5 h(n_3) f(n_4) \tag{A.94}$$

$$+\Theta_4 h(n_1) f(n_2) f(n_3) \tag{A.95}$$

$$+\Theta_4 h(n_2) f(n_3) \tag{A.96}$$

$$+\Theta_3 h(n_1) f(n_2). \tag{A.97}$$

Since $h(n_i) = 1 - f(n_i)$ we may re-write from (A.84) to (A.87) as:

$$\Theta_{N-1} f(n_2) f(n_3) \cdots f(n_{N-2}) - \Theta_{N-1} f(n_1) f(n_2) f(n_3) \cdots f(n_{N-2}) \tag{A.98}$$

$$+\Theta_{N-1} f(n_3) f(n_4) \cdots f(n_{N-2}) - \Theta_{N-1} f(n_2) f(n_3) f(n_4) \cdots f(n_{N-2}) \tag{A.99}$$

$$\vdots$$

$$+\Theta_{N-1} f(n_{N-3}) f(n_{N-2}) - \Theta_{N-1} f(n_N - 4) f(n_{N-3}) f(n_{N-2}) \tag{A.100}$$

$$+\Theta_{N-1} f(n_{N-2}) - \Theta_{N-1} f(n_N - 3) f(n_{N-2}) \tag{A.101}$$

$$= \Theta_{N-1} f(n_{N-2}) - \Theta_{N-1} \prod_{k=1}^{N-2} f(n_i). \tag{A.102}$$

Similarly, we consider the Θ_i's for $i \in \{3, \cdots, N-1\}$ and have:

$$\sum_{j=2}^{N-2} \sum_{i=1}^{j-1} [v_{N-j+i} G^-_{N-j+i} 1_{n_{N-j+i} \geq 1} h(n_i) \prod_{k=1}^{N-j-1} f(n_{k+i})] \tag{A.103}$$

$$= \sum_{j=3}^{N-1} [\Theta_j f(n_{j-1})] - \sum_{j=3}^{N-1} [\Theta_j \prod_{k=1}^{j-1} f(n_k)]. \tag{A.104}$$

Thus, the equilibrium equation has now been reduced to:

$$\sum_{i=1}^{N} [G^-_i v_i 1_{n_i \geq 1}] - G^-_1 \lambda_1 1_{n_1 > 0} - G^-_N v_N 1_{n_N > 0} \tag{A.105}$$

$$= \sum_{j=1}^{N-2} [G^-_{j+1} v_{j+1} 1_{n_{j+1} \geq 1} \prod_{i=1}^{j} f(n_i)] \tag{A.106}$$

$$+ \sum_{i=1}^{N-2} [v_{i+1} \; G^-_{i+1} \; 1_{n_{i+1} \geq 1} \; h(n_i)] \tag{A.107}$$

$$+ \sum_{j=3}^{N-1} [\Theta_j f(n_{j-1})] - \sum_{j=3}^{N-1} [\Theta_j \prod_{k=1}^{j-1} f(n_k)], \tag{A.108}$$

where $\gamma_i 1_{n_i > 1} + \gamma^0_i 1_{n_i = 1} + \Lambda_i 1_{n_i > 0} = G^-_i v_i 1_{n_i \geq 1}$ so that we may write:

$$\sum_{i=2}^{N-1} \Theta_i \tag{A.109}$$

$$= \sum_{j=3}^{N-1} [\Theta_j \prod_{i=1}^{j-1} f(n_i)] + \Theta_2 f(n_1) \tag{A.110}$$

$$+ \sum_{i=3}^{N-1} [\Theta_i h(n_{i-1})] + \Theta_2 h(n_1) \tag{A.111}$$

$$+ \sum_{j=3}^{N-1} [\Theta_j f(n_{j-1})] - \sum_{j=3}^{N-1} [\Theta_j \prod_{k=1}^{j-1} f(n_k)], \tag{A.112}$$

where

$$\sum_{i=3}^{N-1} [\Theta_i h(n_{i-1})] + \sum_{j=3}^{N-1} [\Theta_j f(n_{j-1})] = \sum_{i=3}^{N-1} \Theta_i, \tag{A.113}$$

and

$$\Theta_2 f(n_1) + \Theta_2 h(n_1) = \Theta_2. \tag{A.114}$$

So finally we see that the left and right hand sides of the equilibrium equation cancel each other. Also, C_i values can be calculated by using the fact that summation of the

probabilities is 1:

$$1 \tag{A.115}$$

$$= \sum_{n_i=-\infty}^{\infty} \pi_i(n_i) \tag{A.116}$$

$$= \sum_{n_i=-\infty}^{-1} C_i . \frac{\Lambda_i}{v_i + \mu_i^0} (\frac{\Lambda_i}{v_i + \mu_i})^{-n_i - 1} + \sum_{n_i=1}^{\infty} C_i . \frac{v_i}{\Lambda_i + \gamma_i^0} (\frac{v_i}{\Lambda_i + \gamma_i})^{n_i - 1} + C_i \tag{A.117}$$

Thus,

$$C_i = (1 + \frac{\frac{v_i}{\Lambda_i + \gamma_i^0}}{1 - \frac{v_i}{\Lambda_i + \gamma_i}} + \frac{\frac{\Lambda_i}{v_i + \mu_i^0}}{1 - \frac{\Lambda_i}{v_i + \mu_i}})^{-1}. \tag{A.118}$$

completing the proof.

Appendix B

Proof of Product-form Solution of Multi-Hop Transmission Scheme

Let:

$$v_1 = \lambda_1,\ v_{i+1} = \lambda_{i+1} + \sum_{j=1}^{i} \lambda_j \prod_{k=j}^{i} \frac{\Lambda_k}{\Lambda_k + \gamma_k}. \tag{B.1}$$

and the conditions

$$v_i + \mu_i = \Lambda_i + \gamma_i, \tag{B.2}$$

$$\mu_i^0 = v_i + 2\mu_i, \tag{B.3}$$

$$\gamma_i^0 = \Lambda_i + 2\gamma_i. \tag{B.4}$$

are satisfied, then the steady state probability distribution:

$$\pi(\bar{n}) = P \prod_{i=1}^{N} \pi_i(n_i), \tag{B.5}$$

where $\bar{n} = (n_1, n_2, \cdots, n_N)$ and

$$\pi_i(n_i) = \begin{cases} 1, & \text{if } n_i = 0 \\ \frac{1}{2}(\frac{v_i}{\Lambda_i+\gamma_i})^{n_i}, & \text{if } n_i \geq 1 \\ \frac{1}{2}(\frac{\Lambda_i}{v_i+\mu_i})^{-n_i}, & \text{if } n_i \leq -1 \end{cases} \tag{B.6}$$

where the normalising constants P is:

$$P = \prod_{k=1}^{N} (1 + \frac{v_k}{2\mu_k} + \frac{\Lambda_k}{2\gamma_k})^{-1}, \tag{B.7}$$

and

$$\frac{\pi_i(n_i+1)}{\pi_i(n_i)} \triangleq G_i^+ = \begin{cases} \frac{v_i+\mu_i}{\Lambda_i}, & \text{if } n_i < -1 \\ \frac{v_i+\mu_i^0}{\Lambda_i}, & \text{if } n_i = -1 \\ \frac{v_i}{\Lambda_i+\gamma_i^0}, & \text{if } n_i = 0 \\ \frac{v_i}{\Lambda_i+\gamma_i}, & \text{if } n_i > 0 \end{cases} \qquad \frac{\pi_i(n_i-1)}{\pi_i(n_i)} \triangleq G_i^- = \begin{cases} \frac{\Lambda_i+\gamma_i}{v_i}, & \text{if } n_i > 1 \\ \frac{\Lambda_i+\gamma_i^0}{v_i}, & \text{if } n_i = 1 \\ \frac{\Lambda_i}{v_i+\mu_i^0}, & \text{if } n_i = 0 \\ \frac{\Lambda_i}{v_i+\mu_i}, & \text{if } n_i < 0 \end{cases}$$

The equilibrium equation is the following:

$$\pi(\bar{n}) \sum_{i=1}^{N} [\lambda_i + \Lambda_i + \gamma_i \delta_{n_i>1} + \gamma_i^0 \delta_{n_i=1} + \mu_i \delta_{n_i<-1} + \mu_i^0 \delta_{n_i=-1}] \tag{B.8}$$

$$= \sum_{i=1}^{N} [\pi(\bar{n}+e_i)(\gamma_i \delta_{n_i>0} + \gamma_i^0 \delta_{n_i=0} + \Lambda_i \delta_{n_i<0} \delta_{i\neq N} + \Lambda_N \delta_{i=N})] \tag{B.9}$$

$$+ \sum_{i=1}^{N} [\pi(\bar{n}-e_i)(\mu_i \delta_{n_i<0} + \mu_i^0 \delta_{n_i=0} + \lambda_i \delta_{n_i>0} \delta_{i\neq N} + \lambda_N \delta_{i=N})] \tag{B.10}$$

$$+ \sum_{j=1}^{N-1} \sum_{i=j}^{N-1} [\pi(\bar{n} - \sum_{k=j}^{i+1} e_k) \lambda_j \prod_{k=j}^{i} \delta_{n_k \leq 0} \ (\delta_{1+i=N} + \delta_{n_{i+1}\geq 1} \delta_{1+i\neq N})] \tag{B.11}$$

$$+ \sum_{j=1}^{N-1} \sum_{i=1}^{j} [\pi(\bar{n} + e_i - \sum_{k=1}^{N-j} e_{i+k}) \Lambda_i \delta_{n_i \geq 0} \ (\delta_{N-j\leq 1} + \delta_{N-j\geq 2} \prod_{k=1}^{N-j-1} \delta n_{i+k} \leq 0) \ (\delta_{i=j} + \delta_{n_{N+i-j}\geq 1} \delta_{i\neq j})] \tag{B.12}$$

$\Rightarrow$ Dividing both sides by $\pi(\bar{n})$

$$\sum_{i=1}^{N} [\lambda_i + \Lambda_i + \gamma_i \delta_{n_i>1} + \gamma_i^0 \delta_{n_i=1} + \mu_i \delta_{n_i<-1} + \mu_i^0 \delta_{n_i=-1}] \tag{B.13}$$

$$= \sum_{i=1}^{N} [(G_i^+)(\gamma_i \delta_{n_i>0} + \gamma_i^0 \delta_{n_i=0} + \Lambda_i \delta_{n_i<0} \delta_{i\neq N} + \Lambda_N \delta_{i=N})] \tag{B.14}$$

$$+ \sum_{i=1}^{N} [(G_i^-)(\mu_i \delta_{n_i<0} + \mu_i^0 \delta_{n_i=0} + \lambda_i \delta_{n_i>0} \delta_{i\neq N} + \lambda_N \delta_{i=N})] \tag{B.15}$$

$$+ \sum_{j=1}^{N-1} \sum_{i=j}^{N-1} [\prod_{k=j}^{i+1} (G_k^-) \lambda_j \prod_{k=j}^{i} \delta_{n_k \leq 0} \ (\delta_{1+i=N} + \delta_{n_{i+1}\geq 1} \delta_{1+i\neq N})] \tag{B.16}$$

$$+ \sum_{j=1}^{N-1} \sum_{i=1}^{j} [G_i^+ \prod_{k=1}^{N-j} (G_{k+i}^-) \Lambda_i \delta_{n_i \geq 0} (\delta_{N-j\leq 1} + \delta_{N-j\geq 2} \prod_{k=1}^{N-j-1} (\delta n_{i+k} \leq 0)) \ (\delta_{i=j} + \delta_{n_{N+i-j}\geq 1} \delta_{i\neq j})] \tag{B.17}$$

$\Rightarrow$ Consider the line (B.14)

$$= \sum_{i=1}^{N} [(G_i^+)(\gamma_i \delta_{n_i>0} + \gamma_i^0 \delta_{n_i=0} + \Lambda_i \delta_{n_i<0} \delta_{i\neq N} + \Lambda_N \delta_{i=N})] \tag{B.18}$$

$$= G_N^+ \Lambda_N \delta_{n_N \geq 0} + \sum_{i=1}^{N} [\frac{v_i \gamma_i}{\Lambda_i + \gamma_i} \delta_{n_i>0} + \frac{v_i \gamma_i^0}{\Lambda_i + \gamma_i^0} \delta_{n_i=0} + (v_i + u_i^0)\delta_{n_i=-1} + (v_i + u_i)\delta_{n_i<-1}] \tag{B.19}$$

$\Rightarrow$ Consider the line (B.15)

$$= \sum_{i=1}^{N} [(G_i^-)(\mu_i \delta_{n_i<0} + \mu_i^0 \delta_{n_i=0} + \lambda_i \delta_{n_i>0} \delta_{i\neq N} + \lambda_N \delta_{i=N})] \tag{B.20}$$

$$= G_N^- \lambda_N \delta_{n_N \leq 0} + \sum_{i=1}^{N} [\frac{\Lambda_i \mu_i}{v_i + \mu_i} \delta_{n_i<0} + \frac{\Lambda_i \mu_i^0}{v_i + \mu_i^0} \delta_{n_i=0} + \frac{\lambda_i}{v_i}(\Lambda_i + \gamma_i^0)\delta_{n_i=1} + \frac{\lambda_i}{v_i}(\Lambda_i + \gamma_i)\delta_{n_i>1}] \tag{B.21}$$

$\Rightarrow$ Consider the summation (B.19)+(B.21)

$$= G_N^+ \Lambda_N \delta_{n_N \geq 0} + G_N^- \lambda_N \delta_{n_N \leq 0} \tag{B.22}$$

$$+ \sum_{i=1}^{N} [(v_i + u_i + \frac{\Lambda_i \mu_i}{v_i + \mu_i})\delta_{n_i<-1} + (v_i + u_i^0 + \frac{\Lambda_i \mu_i}{v_i + \mu_i})\delta_{n_i=-1} + (v_i + \frac{\Lambda_i \mu_i}{v_i + \mu_i})\delta_{n_i=0}] \tag{B.23}$$

$$+ \sum_{i=1}^{N} [\frac{\lambda_i}{v_i}(\Lambda_i + \gamma_i^0)\delta_{n_i=1} + \frac{\lambda_i}{v_i}(\Lambda_i + \gamma_i)\delta_{n_i>1} + \frac{v_i \gamma_i}{\Lambda_i + \gamma_i}\delta_{n_i>0}] \tag{B.24}$$

where

$$v_i + \frac{\Lambda_i \mu_i}{v_i + \mu_i} = \Lambda_i + \frac{v_i \gamma_i}{v_i + \mu_i} \tag{B.25}$$

$\Rightarrow$ So that the equilibrium equation reduces :

$$\sum_{i=1}^{N}[\lambda_i + (1-\frac{\lambda_i}{v_i})(\Lambda_i\delta_{n_i>0} + \gamma_i\delta_{n_i>1} + \gamma_i^0\delta_{n_i=1})] \tag{B.26}$$

$$= G_N^+\Lambda_N\delta_{n_N\geq 0} + G_N^-\lambda_N\delta_{n_N\leq 0} \tag{B.27}$$

$$+ \sum_{i=1}^{N}[\frac{v_i\gamma_i}{v_i+\mu_i}] \tag{B.28}$$

$$+ \sum_{j=1}^{N-1}\sum_{i=j}^{N-1}[\prod_{k=j}^{i+1}(G_k^-)\lambda_j\prod_{k=j}^{i}\delta_{n_k\leq 0}\ (\delta_{1+i=N} + \delta_{n_{i+1}\geq 1}\delta_{1+i\neq N})] \tag{B.29}$$

$$+ \sum_{j=1}^{N-1}\sum_{i=1}^{j}[G_i^+\prod_{k=1}^{N-j}(G_{k+i}^-)\Lambda_i\delta_{n_i\geq 0}(\delta_{N-j\leq 1} + \delta_{N-j\geq 2}\prod_{k=1}^{N-j-1}(\delta n_{i+k}\leq 0))\ (\delta_{i=j} + \delta_{n_{N+i-j}\geq 1}\delta_{i\neq j})] \tag{B.30}$$

where

$$\sum_{i=1}^{N}[\frac{v_i\gamma_i}{\Lambda_i+\gamma_i}] = \sum_{i=1}^{N}[(v_i - \Lambda_i + \frac{\Lambda_i\mu_i}{\Lambda_i+\gamma_i})] = \sum_{i=1}^{N-1}[(v_i - v_{i+1} + \lambda_{i+1})] + \frac{v_N\gamma_N}{\Lambda_N+\gamma_N} \tag{B.31}$$

$$= \sum_{i=1}^{N}[\lambda_i] - \frac{v_N\Lambda_N}{\Lambda_N+\gamma_N} \tag{B.32}$$

$\Rightarrow$ After further simplification, the equilibrium equation:

$$\sum_{i=1}^{N}[(1-\frac{\lambda_i}{v_i})(\Lambda_i\delta_{n_i>0} + \gamma_i\delta_{n_i>1} + \gamma_i^0\delta_{n_i=1})] \tag{B.33}$$

$$= G_N^+\Lambda_N\delta_{n_N\geq 0} + G_N^-\lambda_N\delta_{n_N\leq 0} - \frac{v_N\Lambda_N}{\Lambda_N+\gamma_N} \tag{B.34}$$

$$+ \sum_{j=1}^{N-1}\sum_{i=j}^{N-1}[\prod_{k=j}^{i+1}(G_k^-)\lambda_j\prod_{k=j}^{i}\delta_{n_k\leq 0}\ (\delta_{1+i=N} + \delta_{n_{i+1}\geq 1}\delta_{1+i\neq N})] \tag{B.35}$$

$$+ \sum_{j=1}^{N-1}\sum_{i=1}^{j}[G_i^+\prod_{k=1}^{N-j}(G_{k+i}^-)\Lambda_i\delta_{n_i\geq 0}(\delta_{N-j\leq 1} + \delta_{N-j\geq 2}\prod_{k=1}^{N-j-1}(\delta n_{i+k}\leq 0))\ (\delta_{i=j} + \delta_{n_{N+i-j}\geq 1}\delta_{i\neq j})] \tag{B.36}$$

where

$$G_N^+\Lambda_N\delta_{n_N\geq 0} + G_N^-\lambda_N\delta_{n_N\leq 0} - \frac{v_N\Lambda_N}{\Lambda_N+\gamma_N} \tag{B.37}$$

$$= (\lambda_N - v_N)G_N^-\delta_{n_N\leq 0} \tag{B.38}$$

⇒ Thus, it has been simplified so far as the following:

$$\sum_{i=1}^{N}[(1-\frac{\lambda_i}{v_i})(\Lambda_i\delta_{n_i>0}+\gamma_i\delta_{n_i>1}+\gamma_i^0\delta_{n_i=1})]+(v_N-\lambda_N)G_N^-\delta_{n_N\leq 0} \tag{B.39}$$

$$+\sum_{j=1}^{N-1}\sum_{i=j}^{N-1}[\prod_{k=j}^{i+1}(G_k^-)\lambda_j\prod_{k=j}^{i}\delta_{n_k\leq 0}\ (\delta_{1+i=N}+\delta_{n_{i+1}\geq 1}\delta_{1+i\neq N})] \tag{B.40}$$

$$+\sum_{j=1}^{N-1}\sum_{i=1}^{j}[G_i^+\prod_{k=1}^{N-j}(G_{k+i}^-)\Lambda_i\delta_{n_i\geq 0}(\delta_{N-j\leq 1}+\delta_{N-j\geq 2}\prod_{k=1}^{N-j-1}(\delta n_{i+k}\leq 0))\ (\delta_{i=j}+\delta_{n_{N+i-j}\geq 1}\delta_{i\neq j})] \tag{B.41}$$

$\Rightarrow$ Consider the line (B.40)

$$\sum_{j=1}^{N-1}\sum_{i=j}^{N-1}[\prod_{k=j}^{i+1}(G_k^-)\lambda_j\prod_{k=j}^{i}\delta_{n_k\leq 0}\ (\delta_{1+i=N}+\delta_{n_{i+1}\geq 1}\delta_{1+i\neq N})] \tag{B.42}$$

$$=\sum_{j=1}^{N-1}[\prod_{k=j}^{N}(G_k^-)\lambda_j\prod_{k=j}^{N-1}\delta_{n_k\leq 0}] \tag{B.43}$$

$$+\sum_{j=1}^{N-2}\sum_{i=j}^{N-2}[\prod_{k=j}^{i+1}(G_k^-)\lambda_j\prod_{k=j}^{i}\delta_{n_k\leq 0}\ \delta_{n_{i+1}\geq 1}] \tag{B.44}$$

$$=G_N^-\sum_{j=1}^{N-1}[\lambda_j\prod_{k=j}^{N-1}G_k^-\delta_{n_k\leq 0}] \tag{B.45}$$

$$+\sum_{j=1}^{N-2}\sum_{i=j}^{N-2}[\lambda_j G_{i+1}^-\delta_{n_{i+1}\geq 1}\prod_{k=j}^{i}G_k^-\delta_{n_k\leq 0}] \tag{B.46}$$

$$=G_N^-\sum_{j=1}^{N-1}[\lambda_j\prod_{k=j}^{N-1}\frac{\Lambda_k}{\Lambda_k+\gamma_k}f(n_k)] \tag{B.47}$$

$$+\sum_{j=1}^{N-2}\sum_{i=j}^{N-2}[\lambda_j G_{i+1}^-\delta_{n_{i+1}\geq 1}\prod_{k=j}^{i}\frac{\Lambda_k}{\Lambda_k+\gamma_k}f(n_k)] \tag{B.48}$$

$$=G_N^-(v_N-\lambda_N)\sum_{j=1}^{N-1}[\frac{\lambda_j}{v_j}f(n_j)\prod_{k=j+1}^{N-1}(1-\frac{\lambda_k}{v_k})f(n_k)] \tag{B.49}$$

$$+\sum_{j=1}^{N-2}\sum_{i=j}^{N-2}[\frac{\lambda_j}{v_j}G_{i+1}^-(v_{i+1}-\lambda_{i+1})\delta_{n_{i+1}\geq 1}f(n_j)\prod_{k=j+1}^{i}(1-\frac{\lambda_k}{v_k})f(n_k)] \tag{B.50}$$

$$=G_N^-(v_N-\lambda_N)\sum_{j=1}^{N-1}[\frac{\lambda_j}{v_j}f(n_j)\prod_{k=j+1}^{N-1}(1-\frac{\lambda_k}{v_k})f(n_k)] \tag{B.51}$$

$$+\sum_{j=1}^{N-2}\sum_{i=j+1}^{N-2}[\frac{\lambda_j}{v_j}G_{i+1}^-(v_{i+1}-\lambda_{i+1})\delta_{n_{i+1}\geq 1}f(n_j)\prod_{k=j+1}^{i}(1-\frac{\lambda_k}{v_k})f(n_k)] \tag{B.52}$$

$$+\sum_{j=1}^{N-2}[\frac{\lambda_j}{v_j}G_{j+1}^-(v_{j+1}-\lambda_{j+1})\delta_{n_{j+1}\geq 1}f(n_j)] \tag{B.53}$$

$\Rightarrow$ Consider the line (B.41)

$$\sum_{j=1}^{N-1}\sum_{i=1}^{j}[G_i^+\prod_{k=1}^{N-j}(G_{k+i}^-)\Lambda_i\delta_{n_i\geq 0}(\delta_{N-j\leq 1}+\delta_{N-j\geq 2}\prod_{k=1}^{N-j-1}(\delta n_{i+k}\leq 0))\ (\delta_{i=j}+\delta_{n_{N+i-j}\geq 1}\delta_{i\neq j})] \tag{B.54}$$

$$= G_{N-1}^+\ G_N^-\ \Lambda_{N-1}\delta_{N-1\geq 0} \tag{B.55}$$

$$+\sum_{i=1}^{N-2}[G_i^+\ G_{i+1}^-\ \Lambda_i\delta_{i\geq 0}\delta_{i+1\geq 1}] \tag{B.56}$$

$$+\sum_{j=1}^{N-2}\sum_{i=1}^{j}[G_i^+\prod_{k=1}^{N-j}(G_{k+i}^-)(\Lambda_i\delta_{n_i\geq 0}\prod_{k=1}^{N-j-1}(\delta n_{i+k}\leq 0)\ (\delta_{i=j}+\delta_{n_{N+i-j}\geq 1}\delta_{i\neq j})] \tag{B.57}$$

$$= G_{N-1}^+\ \Lambda_{N-1}\delta_{N-1\geq 0}\ G_N^- \tag{B.58}$$

$$+\sum_{i=1}^{N-2}[G_i^+\ \Lambda_i\delta_{i\geq 0}\ G_{i+1}^-\ \delta_{i+1\geq 1}] \tag{B.59}$$

$$+\sum_{j=2}^{N-2}\sum_{i=1}^{j-1}[G_i^+\prod_{k=1}^{N-j}(G_{k+i}^-)(\Lambda_i\delta_{n_i\geq 0}\prod_{k=1}^{N-j-1}(\delta n_{i+k}\leq 0)\ \delta_{n_{N+i-j}\geq 1}] \tag{B.60}$$

$$+\sum_{j=1}^{N-2}[G_j^+\prod_{k=1}^{N-j}(G_{k+j}^-)(\Lambda_j\delta_{n_j\geq 0}\prod_{k=1}^{N-j-1}(\delta n_{j+k}\leq 0)] \tag{B.61}$$

$$= (v_N-\lambda_N)\ G_N^-\ h(n_{N-1}) \tag{B.62}$$

$$+\sum_{i=1}^{N-2}[(v_{i+1}-\lambda_{i+1})\ G_{i+1}^-\ \delta_{n_{i+1}\geq 1}\ h(n_i)] \tag{B.63}$$

$$+\sum_{j=2}^{N-2}\sum_{i=1}^{j-1}[G_i^+\Lambda_i\delta_{n_i\geq 0}\ G_{N-j+i}^-\delta_{n_N-j+i\geq 1}\prod_{k=1}^{N-j-1}(G_{k+i}^-\delta_{n_k+i\leq 0})] \tag{B.64}$$

$$+\sum_{j=1}^{N-2}[G_N^-G_j^+\Lambda_j\delta_{n_j\geq 0}\prod_{k=1}^{N-j-1}(G_{k+j}^-\delta n_{j+k}\leq 0)] \tag{B.65}$$

$$= (v_N-\lambda_N)\ G_N^-\ h(n_{N-1}) \tag{B.66}$$

$$+\sum_{i=1}^{N-2}[(v_{i+1}-\lambda_{i+1})\ G_{i+1}^-\ \delta_{n_{i+1}\geq 1}\ h(n_i)] \tag{B.67}$$

$$+\sum_{j=2}^{N-2}\sum_{i=1}^{j-1}[(v_{i+1}-\lambda_{i+1})h(n_i)\ G_{N-j+i}^-\delta_{n_{N-j+i}\geq 1}\frac{1}{v_{i+1}}(v_{N-j+i}-\lambda_{N-j+i}). \tag{B.68}$$

$$.f(n_{1+i})\prod_{k=2}^{N-j-1}(1-\frac{\lambda_{k+i}}{v_{k+i}})f(n_{k+i})]$$

$$+(v_N-\lambda_N)G_N^-\sum_{j=1}^{N-2}[(v_{j+1}-\lambda_{j+1})h(n_j)\frac{1}{v_{j+1}}f(n_{1+j})\prod_{k=2}^{N-j-1}(1-\frac{\lambda_{k+j}}{v_{k+j}})f(n_{k+j})] \tag{B.69}$$

$$= (v_N - \lambda_N)\ G_N^-\ h(n_{N-1}) \tag{B.70}$$

$$+ \sum_{i=1}^{N-2} (v_{i+1} - \lambda_{i+1})\ G_{i+1}^-\ \delta_{n_{i+1}\geq 1}\ h(n_i) \tag{B.71}$$

$$+ \sum_{j=2}^{N-2} \sum_{i=1}^{j-1} h(n_i)\ G_{N-j+i}^- \delta_{n_{N-j+i}\geq 1} (v_{N-j+i} - \lambda_{N-j+i}) \prod_{k=1}^{N-j-1} (1 - \frac{\lambda_{k+i}}{v_{k+i}}) f(n_{k+i}) \tag{B.72}$$

$$+ (v_N - \lambda_N) G_N^- \sum_{j=1}^{N-2} h(n_j) \prod_{k=1}^{N-j-1} (1 - \frac{\lambda_{k+j}}{v_{k+j}}) f(n_{k+j}) \tag{B.73}$$

⇒ Consider the summation (B.70)+(B.73)

$$(v_N - \lambda_N)\ G_N^-\ h(n_{N-1}) + (v_N - \lambda_N) G_N^- \sum_{j=1}^{N-2} h(n_j) \prod_{k=1}^{N-j-1} (1 - \frac{\lambda_{k+j}}{v_{k+j}}) f(n_{k+j}) \tag{B.74}$$

$$= (v_N - \lambda_N) G_N^- \sum_{j=1}^{N-1} h(n_j) \prod_{k=1+j}^{N-1} (1 - \frac{\lambda_k}{v_k}) f(n_k) \tag{B.75}$$

⇒ Consider the summation (B.51)+(B.75)

$$= G_N^-(v_N - \lambda_N)(\sum_{j=1}^{N-1} [(\frac{\lambda_j}{v_j} f(n_j) + h(n_j)) \prod_{k=j+1}^{N-1} (1 - \frac{\lambda_k}{v_k}) f(n_k)]) \tag{B.76}$$

$$= G_N^-(v_N - \lambda_N)(\sum_{j=1}^{N-1} [\prod_{k=j+1}^{N-1} (1 - \frac{\lambda_k}{v_k}) f(n_k) - f(n_j)(1 - \frac{\lambda_j}{v_j}) \prod_{k=j+1}^{N-1} (1 - \frac{\lambda_k}{v_k}) f(n_k)]) \tag{B.77}$$

$$= G_N^-(v_N - \lambda_N)(\sum_{j=1}^{N-1} [\prod_{k=j+1}^{N-1} (1 - \frac{\lambda_k}{v_k}) f(n_k) - \prod_{k=j}^{N-1} (1 - \frac{\lambda_k}{v_k}) f(n_k)]) \tag{B.78}$$

$$= G_N^-(v_N - \lambda_N)(1 - \prod_{k=1}^{N-1} (1 - \frac{\lambda_k}{v_k}) f(n_k)) \tag{B.79}$$

$$= G_N^-(v_N - \lambda_N) \tag{B.80}$$

⇒ Consider the summation (B.53)+(B.71)

$$\sum_{j=1}^{N-2}[\frac{\lambda_j}{v_j}G_{j+1}^{-}(v_{j+1}-\lambda_{j+1})\delta_{n_{j+1}\geq 1}f(n_j)]+\sum_{i=1}^{N-2}(v_{i+1}-\lambda_{i+1})\ G_{i+1}^{-}\ \delta_{n_{i+1}\geq 1}\ h(n_i) \tag{B.81}$$

$$=\sum_{j=1}^{N-2}[G_{j+1}^{-}(v_{j+1}-\lambda_{j+1})\delta_{n_{j+1}\geq 1}]-\sum_{j=1}^{N-2}[(1-\frac{\lambda_j}{v_j})f(n_j)G_{j+1}^{-}(v_{j+1}-\lambda_{j+1})\delta_{n_{j+1}\geq 1}] \tag{B.82}$$

$$=\sum_{j=2}^{N-1}[(1-\frac{\lambda_j}{v_j})(\Lambda_j\delta_{n_j>0}+\gamma_j\delta_{n_j>1}+\gamma_j^0\delta_{n_j=1})]-\sum_{j=2}^{N-2}[(1-\frac{\lambda_j}{v_j})f(n_j)G_{j+1}^{-}(v_{j+1}-\lambda_{j+1})\delta_{n_{j+1}\geq 1}] \tag{B.83}$$

⇒ Thus, the equilibrium equation reduces:

$$\sum_{i=1}^{N}[(1-\frac{\lambda_i}{v_i})(\Lambda_i\delta_{n_i>0}+\gamma_i\delta_{n_i>1}+\gamma_i^0\delta_{n_i=1})]+(v_N-\lambda_N)G_N^{-}\delta_{n_N\leq 0}-G_N^{-}(v_N-\lambda_N) \tag{B.84}$$

$$+\sum_{j=1}^{N-2}\sum_{i=j+1}^{N-2}[\frac{\lambda_j}{v_j}G_{i+1}^{-}(v_{i+1}-\lambda_{i+1})\delta_{n_{i+1}\geq 1}f(n_j)\prod_{k=j+1}^{i}(1-\frac{\lambda_k}{v_k})f(n_k)] \tag{B.85}$$

$$+\sum_{j=2}^{N-2}\sum_{i=1}^{j-1}h(n_i)\ G_{N-j+i}^{-}\delta_{n_{N-j+i}\geq 1}(v_{N-j+i}-\lambda_{N-j+i})\prod_{k=1}^{N-j-1}(1-\frac{\lambda_{k+i}}{v_{k+i}})f(n_{k+i}) \tag{B.86}$$

$$+\sum_{j=2}^{N-1}[(1-\frac{\lambda_j}{v_j})(\Lambda_j\delta_{n_j>0}+\gamma_j\delta_{n_j>1}+\gamma_j^0\delta_{n_j=1})]-\sum_{j=2}^{N-2}[(1-\frac{\lambda_j}{v_j})f(n_j)G_{j+1}^{-}(v_{j+1}-\lambda_{j+1})\delta_{n_{j+1}\geq 1}] \tag{B.87}$$

⇒ After further simplifications:

$$(1-\frac{\lambda_N}{v_N})(\Lambda_N\delta_{n_N>0}+\gamma_N\delta_{n_N>1}+\gamma_N^0\delta_{n_N=1})-(v_N-\lambda_N)G_N^{-}\delta_{n_N>0} \tag{B.88}$$

$$=\sum_{j=1}^{N-2}\sum_{i=j+1}^{N-2}[\frac{\lambda_j}{v_j}G_{i+1}^{-}(v_{i+1}-\lambda_{i+1})\delta_{n_{i+1}\geq 1}f(n_j)\prod_{k=j+1}^{i}(1-\frac{\lambda_k}{v_k})f(n_k)] \tag{B.89}$$

$$+\sum_{j=2}^{N-2}\sum_{i=1}^{j-1}h(n_i)\ G_{N-j+i}^{-}\delta_{n_{N-j+i}\geq 1}(v_{N-j+i}-\lambda_{N-j+i})\prod_{k=1}^{N-j-1}(1-\frac{\lambda_{k+i}}{v_{k+i}})f(n_{k+i}) \tag{B.90}$$

$$-\sum_{j=2}^{N-2}[(1-\frac{\lambda_j}{v_j})f(n_j)G_{j+1}^{-}(v_{j+1}-\lambda_{j+1})\delta_{n_{j+1}\geq 1}] \tag{B.91}$$

where

$$(1-\frac{\lambda_N}{v_N})(\Lambda_N\delta_{n_N>0}+\gamma_N\delta_{n_N>1}+\gamma_N^0\delta_{n_N=1})=(v_N-\lambda_N)G_n^-\delta_{n_N>0} \tag{B.92}$$

⇒ Thus, the equilibrium equation has became as the following:

$$\sum_{j=2}^{N-2}[(1-\frac{\lambda_j}{v_j})f(n_j)G_{j+1}^-(v_{j+1}-\lambda_{j+1})\delta_{n_{j+1}\geq 1}] \tag{B.93}$$

$$=\sum_{j=1}^{N-2}\sum_{i=j+1}^{N-2}[\frac{\lambda_j}{v_j}G_{i+1}^-(v_{i+1}-\lambda_{i+1})\delta_{n_{i+1}\geq 1}f(n_j)\prod_{k=j+1}^{i}(1-\frac{\lambda_k}{v_k})f(n_k)] \tag{B.94}$$

$$+\sum_{j=2}^{N-2}\sum_{i=1}^{j-1}h(n_i)\ G_{N-j+i}^-\delta_{n_{N-j+i}\geq 1}(v_{N-j+i}-\lambda_{N-j+i})\prod_{k=1}^{N-j-1}(1-\frac{\lambda_{k+i}}{v_{k+i}})f(n_{k+i}) \tag{B.95}$$

⇒ Summation of (B.94) and (B.95) reduces:

$$\sum_{j=2}^{N-2}(1-\frac{\lambda_j}{v_j})f(n_j)G_{j+1}^-(v_{j+1}-\lambda_{j+1})\delta_{n_{j+1}\geq 1}-\sum_{j=2}^{N-2}G_{j+1}^-(v_{j+1}-\lambda_{j+1})\delta_{n_{j+1}\geq 1}\prod_{k=1}^{j}(1-\frac{\lambda_k}{v_k})f(n_k)$$

where

$$\sum_{j=2}^{N-2}G_{j+1}^-(v_{j+1}-\lambda_{j+1})\delta_{n_{j+1}\geq 1}\prod_{k=1}^{j}(1-\frac{\lambda_k}{v_k})f(n_k)=0$$

since, $v_1=\lambda_1$ and $\prod_{k=1}^{j}(1-\frac{\lambda_k}{v_k})f(n_k)=0$.
⇒ So finally the left and right hand sides of the equilibrium equation cancel each other.

Also, P value can be calculated by using the fact that summation of the probabilities is 1:

$$1 \tag{B.96}$$

$$=\sum_{n_i=-\infty}^{\infty}\pi_i(n_i) \tag{B.97}$$

$$=P\ (\sum_{n_i=-\infty}^{-1}(\frac{\Lambda_i}{2(v_i+\mu_i)})^{-n_i}+\sum_{n_i=1}^{\infty}(\frac{v_i}{2(\Lambda_i+\gamma_i)})^{n_i}+1) \tag{B.98}$$

Thus,

$$P=\prod_{k=1}^{N}(1+\frac{v_k}{2\mu_k}+\frac{\Lambda_k}{2\gamma_k})^{-1}, \tag{B.99}$$

completing the proof.

Bibliography

[1] L. Da Xu, W. He, and S. Li, "Internet of things in industries: A survey," *IEEE Transactions on industrial informatics*, vol. 10, no. 4, pp. 2233–2243, 2014.

[2] A. Whitmore, A. Agarwal, and L. Da Xu, "The internet of things: A survey of topics and trends," *Information Systems Frontiers*, vol. 17, no. 2, pp. 261–274, 2015.

[3] C. Perera, C. H. Liu, S. Jayawardena, and M. Chen, "A survey on internet of things from industrial market perspective," *IEEE Access*, vol. 2, pp. 1660–1679, 2014.

[4] F. K. Shaikh, S. Zeadally, and E. Exposito, "Enabling technologies for green internet of things," *IEEE Systems Journal*, vol. 11, no. 2, pp. 983–994, June 2017.

[5] D. Gunduz, K. Stamatiou, N. Michelusi, and M. Zorzi, "Designing intelligent energy harvesting communication systems," *IEEE Communications Magazine*, vol. 52, no. 1, pp. 210–216, 2014.

[6] S. Ulukus, A. Yener, E. Erkip, O. Simeone, M. Zorzi, P. Grover, and K. Huang, "Energy harvesting wireless communications: A review of recent advances," *IEEE Journal on Selected Areas in Communications*, vol. 33, no. 3, pp. 360–381, 2015.

[7] J. R. Jackson, "Jobshop-like queueing systems," *Management Science*, vol. 10, no. 1, p. 131–142, 1963.

[8] F. Baskett, K. M. Chandy, R. R. Muntz, and F. G. Palacios, "Open, closed, and mixed networks of queues with different classes of customers," *Journal of the ACM (JACM)*, vol. 22, no. 2, pp. 248–260, 1975.

[9] E. Uysal-Biyikoglu, B. Prabhakar, and A. El Gamal, "Energy-efficient packet transmission over a wireless link," *IEEE/ACM Transactions on Networking (TON)*, vol. 10, no. 4, pp. 487–499, 2002.

[10] L. Schor, P. Sommer, and R. Wattenhofer, "Towards a zero-configuration wireless sensor network architecture for smart buildings," in *Proceedings of the First ACM Workshop on Embedded Sensing Systems for Energy-Efficiency in Buildings*, ser.

BuildSys '09. New York, NY, USA: ACM, 2009, pp. 31–36. [Online]. Available: http://doi.acm.org/10.1145/1810279.1810287

[11] R. R. P. Jackson, "Random queueing with phase-type service," *Journal of the Royal Statistical Society*, vol. 18, pp. 129–132, 1956.

[12] C. Kim and A. Agrawala, "Analysis of the fork-join queue," *IEEE Transactions on Computers*, vol. 38, no. 2, pp. 250–255, 1989.

[13] P. Konstantopoulos and J. Walrand, "Stationary and stability of fork-join networks," *Journal of Applied Probability*, vol. 26, pp. 604–614, 1989.

[14] E. Varki, "Mean value technique for closed fork-join networks," in *Proc. ACM SIGMETRICS Iinternational Conference on Measurement and Modeling of Computer Systems*, 1999, pp. 103–112.

[15] S. Balsamo, P. G. Harrison, and A. Marin, "Methodological construction of product-form stochastic Petri nets for performance evaluation," *Journal of Systems and Software*, vol. 85, no. 7, pp. 1520–1539, 2012.

[16] E. Gelenbe, "G-networks with triggered customer movement," *Journal of Applied Probability*, vol. 30, no. 3, pp. 742–748, 1993.

[17] A. Marin, S. Balsamo, and P. G. Harrison, "Analysis of stochastic petri nets with signals," *Performance Evaluation*, vol. 69, no. 11, pp. 551–572, 2012.

[18] E. Gelenbe, "Steady-state solution of probabilistic gene regulatory networks," *Physical Review E*, vol. 76, no. 3, p. 031903, 2007.

[19] ——, "Energy packet networks: adaptive energy management for the cloud," in *CloudCP '12 Proceedings of the 2nd International Workshop on Cloud Computing Platforms*. ACM New York, NY, USA, April 2012.

[20] S. Sarma, D. L. Brock, and K. Ashton, "The networked physical world," *Auto-ID Center White Paper MIT-AUTOID-WH-001*, 2000.

[21] S. Meloan, "Toward a global "internet of things"," *Sun Developer Network*, vol. 6, no. 11, pp. 32–35, 2003.

[22] F. Tao, Y. Wang, Y. Zuo, H. Yang, and M. Zhang, "Internet of things in product life-cycle energy management," *Journal of Industrial Information Integration*, vol. 1, no. Supplement C, pp. 26 – 39, 2016. [Online]. Available: http://www.sciencedirect.com/science/article/pii/S2452414X16000030

[23] O. Said and M. Masud, "Towards internet of things: Survey and future vision," *International Journal of Computer Networks*, vol. 5, no. 1, pp. 1–17, 2013.

[24] J. Gubbi, R. Buyya, S. Marusic, and M. Palaniswami, "Internet of things (iot): A vision, architectural elements, and future directions," *Future generation computer systems*, vol. 29, no. 7, pp. 1645–1660, 2013.

[25] I. Lee and K. Lee, "The internet of things (iot): Applications, investments, and challenges for enterprises," *Business Horizons*, vol. 58, no. 4, pp. 431–440, 2015.

[26] L. Atzori, A. Iera, and G. Morabito, "The internet of things: A survey," *Computer networks*, vol. 54, no. 15, pp. 2787–2805, 2010.

[27] S. Li, H. Wang, T. Xu, and G. Zhou, "Application study on internet of things in environment protection field," in *Informatics in Control, Automation and Robotics*. Springer, 2011, pp. 99–106.

[28] A. Gluhak, S. Krco, M. Nati, D. Pfisterer, N. Mitton, and T. Razafindralambo, "A survey on facilities for experimental internet of things research," *IEEE Communications Magazine*, vol. 49, no. 11, 2011.

[29] S. Severi, F. Sottile, G. Abreu, C. Pastrone, M. Spirito, and F. Berens, "M2m technologies: Enablers for a pervasive internet of things," in *Networks and Communications (EuCNC), 2014 European Conference on*. IEEE, 2014, pp. 1–5.

[30] J. Lee, "E-manufacturing—fundamental, tools, and transformation," *Robotics and Computer-Integrated Manufacturing*, vol. 19, no. 6, pp. 501–507, 2003.

[31] J.-c. Zhao, J.-f. Zhang, Y. Feng, and J.-x. Guo, "The study and application of the iot technology in agriculture," in *Computer Science and Information Technology (ICCSIT), 2010 3rd IEEE International Conference on*, vol. 2. IEEE, 2010, pp. 462–465.

[32] F. Shrouf and G. Miragliotta, "Energy management based on internet of things: practices and framework for adoption in production management," *Journal of Cleaner Production*, vol. 100, pp. 235–246, 2015.

[33] M. Swan, "Sensor mania! the internet of things, wearable computing, objective metrics, and the quantified self 2.0," *Journal of Sensor and Actuator Networks*, vol. 1, no. 3, pp. 217–253, 2012.

[34] W. He, G. Yan, and L. Da Xu, "Developing vehicular data cloud services in the iot environment," *IEEE Transactions on Industrial Informatics*, vol. 10, no. 2, pp. 1587–1595, 2014.

[35] I. F. Akyildiz, W. Su, Y. Sankarasubramaniam, and E. Cayirci, "Wireless sensor networks: A survey," *Comput. Netw.*, vol. 38, no. 4, pp. 393–422, Mar. 2002. [Online]. Available: http://dx.doi.org/10.1016/S1389-1286(01)00302-4

[36] M. P. Durisic, Z. Tafa, G. Dimic, and V. Milutinovic, "A survey of military applications of wireless sensor networks," in *2012 Mediterranean Conference on Embedded Computing (MECO)*, June 2012, pp. 196–199.

[37] A. Cerpa, J. Elson, D. Estrin, L. Girod, M. Hamilton, and J. Zhao, "Habitat monitoring: Application driver for wireless communications technology," *ACM SIGCOMM Computer Communication Review*, vol. 31, no. 2 supplement, pp. 20–41, 2001.

[38] W. R. Heinzelman, J. Kulik, and H. Balakrishnan, "Adaptive protocols for information dissemination in wireless sensor networks," in *Proceedings of the 5th annual ACM/IEEE international conference on Mobile computing and networking.* ACM, 1999, pp. 174–185.

[39] P. Bonnet, J. Gehrke, and P. Seshadri, "Querying the physical world," *IEEE personal Communications*, vol. 7, no. 5, pp. 10–15, 2000.

[40] B. Sibbald, "Use computerized systems to cut adverse drug events: report," 2001.

[41] N. Noury, T. Hervé, V. Rialle, G. Virone, E. Mercier, G. Morey, A. Moro, and T. Porcheron, "Monitoring behavior in home using a smart fall sensor and position sensors," in *Microtechnologies in Medicine and Biology, 1st Annual International, Conference On. 2000.* IEEE, 2000, pp. 607–610.

[42] E. M. Petriu, N. D. Georganas, D. C. Petriu, D. Makrakis, and V. Z. Groza, "Sensor-based information appliances," *IEEE Instrumentation & Measurement Magazine*, vol. 3, no. 4, pp. 31–35, 2000.

[43] M. Hatler, "Industrial wireless sensor networks: Trends and developments," *Retrieved*, vol. 11, no. 14, p. 2013, 2013.

[44] P. Harrop and R. Das, "Wireless sensor networks 2010-2020," *Networks*, vol. 2010, p. 2020, 2010.

[45] F. K. Shaikh, S. Zeadally, and E. Exposito, "Enabling technologies for green internet of things," *IEEE Systems Journal*, vol. 11, no. 2, pp. 983–994, 2017.

[46] N. A. Pantazis and D. D. Vergados, "A survey on power control issues in wireless sensor networks," *IEEE Communications Surveys & Tutorials*, vol. 9, no. 4, pp. 86–107, 2007.

[47] W. Ye, J. Heidemann, and D. Estrin, "An energy-efficient mac protocol for wireless sensor networks," in *INFOCOM 2002. Twenty-First Annual Joint Conference of the IEEE Computer and Communications Societies. Proceedings. IEEE*, vol. 3, 2002, pp. 1567–1576 vol.3.

[48] W. Heinzelman, A. Chandrakasan, and H. Balakrishnan, "Energy-efficient communication protocol for wireless microsensor networks," in *System Sciences, 2000. Proceedings of the 33rd Annual Hawaii International Conference on*, Jan 2000, pp. 10 pp. vol.2–.

[49] H. Liu, A. Chandra, and J. Srivastava, "esense: energy efficient stochastic sensing framework scheme for wireless sensor platforms," in *Proceedings of the 5th international conference on Information processing in sensor networks*. ACM, 2006, pp. 235–242.

[50] F. Ingelrest, G. Barrenetxea, G. Schaefer, M. Vetterli, O. Couach, and M. Parlange, "Sensorscope: Application-specific sensor network for environmental monitoring," *ACM Transactions on Sensor Networks (TOSN)*, vol. 6, no. 2, p. 17, 2010.

[51] V. Rodoplu and T. H. Meng, "Bits-per-joule capacity of energy-limited wireless networks," *Wireless Communications, IEEE Transactions on*, vol. 6, no. 3, pp. 857–865, 2007.

[52] F. Meshkati, H. V. Poor, S. C. Schwartz, and N. B. Mandayam, "An energy-efficient approach to power control and receiver design in wireless data networks," *Communications, IEEE Transactions on*, vol. 53, no. 11, pp. 1885–1894, 2005.

[53] C. Alippi and C. Galperti, "An adaptive system for optimal solar energy harvesting in wireless sensor network nodes," *Circuits and Systems I: Regular Papers, IEEE Transactions on*, vol. 55, no. 6, pp. 1742–1750, 2008.

[54] W. K. Seah, Z. A. Eu, and H.-P. Tan, "Wireless sensor networks powered by ambient energy harvesting (wsn-heap)-survey and challenges," in *Wireless Communication, Vehicular Technology, Information Theory and Aerospace & Electronic Systems Technology, 2009. Wireless VITAE 2009. 1st International Conference on*. IEEE, 2009, pp. 1–5.

[55] E. Gelenbe, K. Hussain, and V. Kaptan, "Simulating autonomous agents in augmented reality," *Journal of Systems and Software*, vol. 74, no. 3, pp. 255–268, February 2005.

[56] A. Rahimi, O. Zorlu, and H. Külah, "A fully self-powered electromagnetic energy harvesting system with highly efficient dual rail output," *IEEE Sensours Journal*, vol. 12, pp. 2287–2298, 2012.

[57] J. Yang and S. Ulukuş, "Optimal packet scheduling in an energy harvesting communication system," *IEEE Trans. Commun.*, vol. 60, pp. 220–230, 2012.

[58] E. Gelenbe, D. Gesbert, D. Gündüz, H. Külah, and E. Uysal-Biyikoglu, "Energy harvesting communication networks: ptimization and demonstration: The e-crops project," in *Proc. 24th Tyrrhenian International Workshop 2013 on Digital Communications—Green ICT (TIWDC)*. Genoa, Italy: IEEE, 23–25 September 2013, pp. 1–6.

[59] E. Gelenbe and D. Gündüz, "Optimum power level for communications with interference," in *24th TIWDC, Tyrrhenian International Workshop 2013 on Digital Communications: Green ICT*. IEEE Xplore, 2013.

[60] M. Gatzianas, L. Georgiadis, and L. Tassiulas, "Control of wireless networks with rechargeable batteries," *IEEE Transactions on Wireless Communications*, vol. 9, no. 2, pp. 581–593, February 2010.

[61] S. Sarkar, M. H. R. Khouzani, and K. Kar, "Optimal routing and scheduling in multihop wireless renewable energy networks," *IEEE Transactions on Automatic Control*, vol. 58, no. 7, pp. 1792–1798, July 2013.

[62] Z. Mao, C. E. Koksal, and N. B. Shroff, "Near optimal power and rate control of multi-hop sensor networks with energy replenishment: Basic limitations with finite energy and data storage," *IEEE Transactions on Automatic Control*, vol. 57, no. 4, pp. 815–829, April 2012.

[63] E. Gelenbe, "Synchronising energy harvesting and data packets in a wireless sensor," *Energies*, vol. 8, no. 1, pp. 356–369, January 2015. [Online]. Available: www.mdpi.com/journal/energies

[64] Y. M. Kadioglu, "Finite capacity energy packet networks," *Probability in the Engineering and Informational Sciences*, pp. 1–28, 2017.

[65] E. Gelenbe and A. Marin, "Interconnected wireless sensors with energy harvesting," in *Analytical and Stochastic Modelling Techniques and Applications*. Springer, 2015, pp. 87–99.

[66] Y. M. Kadioglu and E. Gelenbe, "Packet transmission with k energy packets in an energy harvesting sensor," in *Proceedings of the 2nd International Workshop on Energy-Aware Simulation*, ser. ENERGY-SIM '16. New York, NY, USA: ACM, 2016, pp. 1:1–1:6. [Online]. Available: http://doi.acm.org/10.1145/2939948.2939949

[67] Y. M. Kadioglu, "Energy consumption model for data processing and transmission in energy harvesting wireless sensors," in *Computer and Information Sciences - 31st International Symposium, ISCIS 2016, Kraków, Poland, October 27-28, 2016, Proceedings*, 2016, pp. 117–125.

[68] Y. M. Kadioglu and E. Gelenbe, "Wireless sensor with data and energy packets," in *Communications Workshops (ICC Workshops), 2017 IEEE International Conference on*. IEEE, 2017, pp. 564–569.

[69] E. Gelenbe and Y. M. Kadioglu, "Energy loss through standby and leakage in energy harvesting wireless sensors," in *20th IEEE International Workshop on Computer Aided Modelling and Design of Communication Links and Networks,*, 2015.

[70] ——, "Performance of an autonomous energy harvesting wireless sensor," in *Information Sciences and Systems 2015*. Springer, 2016, pp. 35–43.

[71] O. Brun, Y. Yin, E. Gelenbe, Y. Kadioglu, J. Augusto-Gonzalez, and M. Ramos, "Deep learning with dense random neural networks for detecting attacks against iot-connected home environments," in *Gelenbe, E., Campegiani, P., Czachorski, T., Katsikas, S., Komnios, I., Romano, L., Tzovaras, D. (eds.) Recent Cybersecurity Research in Europe: Proceedings of the 2018 ISCIS Security Workshop, Imperial College London*. Lecture Notes CCIS No. 821, Springer Verlag, 2018.

[72] E. Gelenbe and Y. M. Kadioglu, "Battery attacks on sensors," in *International Symposium on Computer and Information Sciences, Security Workshop. Springer International Publishing*, 2018.

[73] ——, "Energy life-time of wireless nodes with network attacks and mitigation," in *2018 IEEE International Conference on Communications Workshops, Kansas City, IEEE*, 2018.

[74] Y. M. Kadioglu and E. Gelenbe, "Product form solution to cascade networks with intermittent energy," in *IEEE Systems Journal*, 2018.

[75] Y. M. Kadioglu, "Tandem networks with intermittent energy," *International Symposium on Computer and Information Sciences*, 2018.

[76] J. Sztrik, "Basic queueing theory," *University of Debrecen, Faculty of Informatics*, vol. 193, 2012.

[77] W. L. Winston and J. B. Goldberg, *Operations research: applications and algorithms*. Thomson/Brooks/Cole Belmont, 2004, vol. 3.

[78] L. Kleinrock, *Queueing Systems: Volune 2, Computer Applications*. John Wiley Interscience, 1976.

[79] S. Tucci and C. H. Sauer, "The tree MVA algorithm," *Perform. Eval.*, vol. 5, no. 3, pp. 187–196, 1985.

[80] E. Gelenbe, "G-networks: An unifying model for queuing networks and neural networks," pp. 433–461, 1994.

[81] ——, "Random neural networks with negative and positive signals and product form solution," *Neural computation*, vol. 1, no. 4, pp. 502–510, 1989.

[82] ——, "Product-form queueing networks with negative and positive customers," *Journal of applied probability*, vol. 28, no. 3, pp. 656–663, 1991.

[83] ——, "Energy packet networks: Ict based energy allocation and storage - (invited paper)," in *GreeNets*, 2011, pp. 186–195.

[84] ——, "G-networks by triggered customer movement," *Journal of applied probability*, vol. 30, no. 03, pp. 742–748, 1993.

[85] ——, "G-networks with signals and batch removal," *Probability in the Engineering and Informational Sciences*, vol. 7, pp. 335–342, 1993.

[86] E. Gelenbe and J.-M. Fourneau, "G-networks with resets," *Performance Evaluation*, vol. 49, no. 1, pp. 179–191, 2002.

[87] E. Gelenbe and A. Labed, "G-networks with multiple classes of signals and positive customers," *European journal of operational research*, vol. 108, no. 2, pp. 293–305, 1998.

[88] E. Gelenbe, "Adaptive management of energy packets," in *Computer Software and Applications Conference Workshops (COMPSACW), 2014 IEEE 38th International*. IEEE, 2014, pp. 1–6.

[89] T. Takuno, M. Koyama, and T. Hikihara, "In-home power distribution systems by circuit switching and power packet dispatching," in *Smart Grid Communications (SmartGridComm), 2010 First IEEE International Conference on*. IEEE, 2010, pp. 427–430.

[90] K. Tashiro, R. Takahashi, and T. Hikihara, "Feasibility of power packet dispatching at in-home dc distribution network," in *Smart Grid Communications (SmartGridComm), 2012 IEEE Third International Conference on*. IEEE, 2012, pp. 401–405.

[91] E. Gelenbe, "Energy packet networks: smart electricity storage to meet surges in demand," in *Proceedings of the 5th International ICST Conference on Simulation Tools and Techniques*. ICST (Institute for Computer Sciences, Social-Informatics and Telecommunications Engineering), 2012, pp. 1–7.

[92] ——, "Energy packet networks: adaptive energy management for the cloud," in *Proceeding CloudCP '12, Proceedings of the 2nd International Workshop on Cloud Computing Platforms*. ACM, 2012.

[93] E. T. Ceran and E. Gelenbe, "Energy packet model optimisation with approximate matrix inversion," in *Proceedings of the 2nd International Workshop on Energy-Aware Simulation*. ACM, 2016, p. 4.

[94] E. Gelenbe and E. T. Ceran, "Energy packet networks with energy harvesting," *IEEE Access*, vol. 4, pp. 1321–1331, 2016.

[95] ——, "Central or distributed energy storage for processors with energy harvesting," in *Sustainable Internet and ICT for Sustainability (SustainIT), 2015*. IEEE, 2015, pp. 1–3.

[96] E. Gelenbe, "A sensor node with energy harvesting," *ACM SIGMETRICS Performance Evaluation Review*, vol. 42, no. 2, pp. 37–39, 2014.

[97] W. R. Heinzelman, A. Chandrakasan, and H. Balakrishnan, "Energy-efficient communication protocol for wireless microsensor networks," in *System sciences, 2000. Proceedings of the 33rd annual Hawaii international conference on*. IEEE, 2000, pp. 10–pp.

[98] T. Crompton, "Battery reference book (third edition)," in *Battery Reference Book (Third Edition)*. Newnes, 2000.

[99] A. Goldsmith, *Wireless communications*. Cambridge University Press, 2005.

[100] B. Anderson, J. Jackson, and M. Sitharam, "Descartes' rule of signs revisited," *The American Mathematical Monthly*, vol. 105, no. 5, pp. 447–451, 1998.

[101] H. Żołądek, "The topological proof of abel–ruffini theorem," *Topol. Methods Nonlinear Anal*, vol. 16, pp. 253–265, 2000.

[102] J. Dong and W. Whitt, "Using a birth-and-death process to estimate the steady-state distribution of a periodic queue," *Naval Research Logistics (NRL)*, vol. 62, no. 8, pp. 664–685, 2015.

[103] I. Shams, S. Ajorlou, and K. Yang, "Modeling clustered non-stationary poisson processes for stochastic simulation inputs," *Computers & Industrial Engineering*, vol. 64, no. 4, pp. 1074–1083, 2013.

[104] M. E. Kuhl, J. R. Wilson, and M. A. Johnson, "Estimating and simulating poisson processes having trends or multiple periodicities," *IIE transactions*, vol. 29, no. 3, pp. 201–211, 1997.

[105] M. Calle and J. Kabara, "Measuring energy consumption in wireless sensor networks using gsp," in *Personal, Indoor and Mobile Radio Communications, 2006 IEEE 17th International Symposium on*, Sept 2006, pp. 1–5.

[106] F. Baskett, K. M. Chandy, R. R. Muntz, and F. G. Palacios, "Open, closed, and mixed networks of queues with different classes of customers," *Journal of the ACM (JACM)*, vol. 22, no. 2, pp. 248–260, 1975.

[107] A. Dubey, V. Jain, and A. Kumar, "A survey in energy drain attacks and their countermeasures in wireless sensor networks," *Int. J. Eng. Res. Technol*, vol. 3, no. 2, pp. 1206–1210, 2014.

[108] F. François, O. H. Abdelrahman, and E. Gelenbe, "Impact of signaling storms on energy consumption and latency of LTE user equipment," in *17th IEEE International Conference on High Performance Computing and Communications, HPCC 2015, 7th IEEE International Symposium on Cyberspace Safety and Security, CSS 2015, and 12th IEEE International Conference on Embedded Software and Systems, ICESS 2015, New York, NY, USA, August 24-26, 2015*, 2015, pp. 1248–1255. [Online]. Available: https://doi.org/10.1109/HPCC-CSS-ICESS.2015.84

[109] ——, "Towards assessment of energy consumption and latency of LTE ues during signaling storms," in *Information Sciences and Systems 2015 - 30th International Symposium on Computer and Information Sciences, ISCIS 2015, London, UK, 21-24 September 2015*, 2015, pp. 45–55.

[110] V. V. Shakhov, "Protecting wireless sensor networks from energy exhausting attacks," in *International Conference on Computational Science and Its Applications*. Springer, 2013, pp. 184–193.

[111] D. N. Geethanjali and E. Gayathri, "A survey on energy depletion attacks in wireless sensor network," *International Journal of Science and Researchl*, vol. 3, pp. 2070–2074, 2014.

[112] S. R. Singh, "Improving the performance of energy attack detection in wireless sensor networks by secure forward mechanism," *International Journal of Scientific and Research Publications*, p. 367.

[113] E. Y. Vasserman and N. Hopper, "Vampire attacks: draining life from wireless ad hoc sensor networks," *IEEE transactions on mobile computing*, vol. 12, no. 2, pp. 318–332, 2013.

[114] Y.-C. Hu, A. Perrig, and D. B. Johnson, "Ariadne: A secure on-demand routing protocol for ad hoc networks," *Wireless networks*, vol. 11, no. 1-2, pp. 21–38, 2005.

[115] A. Kröller, S. P. Fekete, D. Pfisterer, and S. Fischer, "Deterministic boundary recognition and topology extraction for large sensor networks," in *Proceedings of the seventeenth annual ACM-SIAM symposium on Discrete algorithm*. Society for Industrial and Applied Mathematics, 2006, pp. 1000–1009.

[116] Y. Wang, J. Gao, and J. S. Mitchell, "Boundary recognition in sensor networks by topological methods," in *Proceedings of the 12th annual international conference on Mobile computing and networking.* ACm, 2006, pp. 122–133.

[117] B. Umakanth and J. Damodhar, "Detection of energy draining attack using ewma in wireless ad hoc sensor networks," *International Journal of Engineering Trends and Technology (IJETT)*, vol. 4, no. 8, 2013.

[118] M. Soni and B. Pahadiya, "Detection and removal of vampire attack in wireless sensor network," *International Journal of Computer Applications*, vol. 126, no. 7, 2015.

[119] E. Gelenbe and R. Lent, "Power-aware ad hoc cognitive packet networks," *Ad Hoc Networks*, vol. 2, pp. 205–2016, 2004.

[120] E. Gelenbe and T. Mahmoodi, "Energy-aware routing in the cognitive packet network," *Energy*, pp. 7–12, 2011.

[121] D. E. Boubiche and A. Bilami, "A defense strategy against energy exhausting attacks in wireless sensor networks," *Journal Of Emerging Technologies In Web Intelligence*, vol. 5, no. 1.

[122] R. Falk and H.-J. Hof, "Fighting insomnia: A secure wake-up scheme for wireless sensor networks," in *Emerging Security Information, Systems and Technologies, 2009. SECURWARE'09. Third International Conference on.* IEEE, 2009, pp. 191–196.

[123] F. Stajano, "The resurrecting duckling," in *International workshop on security protocols.* Springer, 1999, pp. 183–194.

[124] M. Pirretti, S. Zhu, N. Vijaykrishnan, P. McDaniel, M. Kandemir, and R. Brooks, "The sleep deprivation attack in sensor networks: Analysis and methods of defense," *International Journal of Distributed Sensor Networks*, vol. 2, no. 3, pp. 267–287, 2006.

[125] X. Lu, M. Spear, K. Levitt, N. S. Matloff, and S. F. Wu, "A synchronization attack and defense in energy-efficient listen-sleep slotted mac protocols," in *Emerging Security Information, Systems and Technologies, 2008. SECURWARE'08. Second International Conference on.* IEEE, 2008, pp. 403–411.

[126] A. Di Mauro, X. Fafoutis, S. Mödersheim, and N. Dragoni, "Detecting and preventing beacon replay attacks in receiver-initiated mac protocols for energy efficient wsns," in *Nordic Conference on Secure IT Systems.* Springer, 2013, pp. 1–16.

[127] V. Sharma and M. Hussain, "Mitigating replay attack in wireless sensor network through assortment of packets," in *Proceedings of the First International Conference on Computational Intelligence and Informatics*. Springer, 2017, pp. 221–230.

[128] M. Brownfield, Y. Gupta, and N. Davis, "Wireless sensor network denial of sleep attack," in *Information Assurance Workshop, 2005. IAW'05. Proceedings from the Sixth Annual IEEE SMC*. IEEE, 2005, pp. 356–364.

[129] Y. W. Law, M. Palaniswami, L. V. Hoesel, J. Doumen, P. Hartel, and P. Havinga, "Energy-efficient link-layer jamming attacks against wireless sensor network MAC protocols," *ACM Trans. Sen. Netw.*, vol. 5, no. 1, pp. 6:1–6:38, Feb. 2009. [Online]. Available: http://doi.acm.org/10.1145/1464420.1464426

[130] H. Chaudhari and L. Kadam, "Wireless sensor networks: security, attacks and challenges," *International Journal of Networking*, vol. 1, no. 1, pp. 4–16, 2011.

[131] L. Buttyan and L. Csik, "Security analysis of reliable transport layer protocols for wireless sensor networks," in *Pervasive Computing and Communications Workshops (PERCOM Workshops), 2010 8th IEEE International Conference on*. IEEE, 2010, pp. 419–424.

[132] C.-T. Hsueh, C.-Y. Wen, and Y.-C. Ouyang, "A secure scheme against power exhausting attacks in hierarchical wireless sensor networks," *IEEE Sensors journal*, vol. 15, no. 6, pp. 3590–3602, 2015.

[133] S. Wei, J. H. Ahnn, and M. Potkonjak, "Energy attacks and defense techniques for wireless systems," in *Proceedings of the sixth ACM conference on Security and privacy in wireless and mobile networks*. ACM, 2013, pp. 185–194.

[134] K. Akkaya and M. Younis, "A survey on routing protocols for wireless sensor networks," *Ad hoc networks*, vol. 3, no. 3, pp. 325–349, 2005.

[135] I. F. Akyildiz, W. Su, Y. Sankarasubramaniam, and E. Cayirci, "Wireless sensor networks: a survey," *Computer networks*, vol. 38, no. 4, pp. 393–422, 2002.

[136] P. Naik and K. M. Sivalingam, "A survey of MAC protocols for sensor networks," in *Wireless sensor networks*. Springer, 2004, pp. 93–107.

[137] N. Sadagopan, B. Krishnamachari, and A. Helmy, "Active query forwarding in sensor networks," *Ad Hoc Networks*, vol. 3, no. 1, pp. 91–113, 2005.

[138] G. Gorbil and E. Gelenbe, "Opportunistic communications for emergency support systems," *Procedia Computer Science*, vol. 5, pp. 39–47, 2011.

[139] M. Younis and K. Akkaya, "Strategies and techniques for node placement in wireless sensor networks: A survey," *Ad Hoc Networks*, vol. 6, no. 4, pp. 621–655, 2008.

[140] X. Cheng, D.-Z. Du, L. Wang, and B. Xu, "Relay sensor placement in wireless sensor networks," *Wireless Networks*, vol. 14, no. 3, pp. 347–355, 2008.

[141] S. Poduri, S. Pattem, B. Krishnamachari, and G. S. Sukhatme, "Sensor network configuration and the curse of dimensionality," in *Proc. Third Workshop on Embedded Networked Sensors (EmNets 2006), Cambridge, MA, USA*. Citeseer, 2006.

[142] J. Pan, L. Cai, Y. T. Hou, Y. Shi, and S. X. Shen, "Optimal base-station locations in two-tiered wireless sensor networks," *IEEE Transactions on Mobile Computing*, vol. 4, no. 5, pp. 458–473, 2005.

[143] S. S. Dhillon and K. Chakrabarty, "Sensor placement for effective coverage and surveillance in distributed sensor networks," in *Wireless Communications and Networking, 2003. WCNC 2003. 2003 IEEE*, vol. 3. IEEE, 2003, pp. 1609–1614.

[144] K. Akkaya, M. Younis, and M. Bangad, "Sink repositioning for enhanced performance in wireless sensor networks," *Computer Networks*, vol. 49, no. 4, pp. 512–534, 2005.

[145] G. Wang, G. Cao, T. La Porta, and W. Zhang, "Sensor relocation in mobile sensor networks," in *INFOCOM 2005. 24th Annual Joint Conference of the IEEE Computer and Communications Societies. Proceedings IEEE*, vol. 4. IEEE, 2005, pp. 2302–2312.

[146] A. Brooks, A. Makarenko, T. Kaupp, S. Williams, and H. Durrant-Whyte, "Implementation of an indoor active sensor network," in *Experimental Robotics IX*. Springer, 2006, pp. 397–406.

[147] V. A. Petrushin, G. Wei, O. Shakil, D. Roqueiro, and V. Gershman, "Multiple-sensor indoor surveillance system," in *Computer and Robot Vision, 2006. The 3rd Canadian Conference on*. IEEE, 2006, pp. 40–40.

[148] J. Paek, K. Chintalapudi, R. Govindan, J. Caffrey, and S. Masri, "A wireless sensor network for structural health monitoring: Performance and experience," in *Embedded Networked Sensors, 2005. EmNetS-II. The Second IEEE Workshop on*. IEEE, 2005, pp. 1–9.

[149] J. W. Berry, L. Fleischer, W. E. Hart, C. A. Phillips, and J.-P. Watson, "Sensor placement in municipal water networks," *Journal of Water Resources Planning and Management*, vol. 131, no. 3, pp. 237–243, 2005.

[150] I. F. Akyildiz, D. Pompili, and T. Melodia, "Underwater acoustic sensor networks: research challenges," *Ad hoc networks*, vol. 3, no. 3, pp. 257–279, 2005.

[151] M. Ishizuka and M. Aida, "Performance study of node placement in sensor networks," in *Distributed Computing Systems Workshops, 2004. Proceedings. 24th International Conference on.* IEEE, 2004, pp. 598–603.

[152] K. Xu, H. Hassanein, G. Takahara, and Q. Wang, "Relay node deployment strategies in heterogeneous wireless sensor networks: single-hop communication case," in *Global Telecommunications Conference, 2005. GLOBECOM'05. IEEE*, vol. 1. IEEE, 2005, pp. 5–pp.

[153] C.-F. Huang and Y.-C. Tseng, "The coverage problem in a wireless sensor network," *Mobile Networks and Applications*, vol. 10, no. 4, pp. 519–528, 2005.

[154] A. Boukerche and X. Fei, "A coverage-preserving scheme for wireless sensor network with irregular sensing range," *Ad hoc networks*, vol. 5, no. 8, pp. 1303–1316, 2007.

[155] M. Cardei and J. Wu, "Coverage problems in wireless ad hoc sensor networks," *Handbook of Sensor Networks*, 2004.

[156] K. Kar and S. Banerjee, "Node placement for connected coverage in sensor networks," in *WiOpt'03: Modeling and Optimization in Mobile, Ad Hoc and Wireless Networks*, 2003, pp. 2–pages.

[157] J. L. Bredin, E. D. Demaine, M. Hajiaghayi, and D. Rus, "Deploying sensor networks with guaranteed capacity and fault tolerance," in *Proceedings of the 6th ACM international symposium on Mobile ad hoc networking and computing.* ACM, 2005, pp. 309–319.

[158] M. Younis, M. Youssef, and K. Arisha, "Energy-aware routing in cluster-based sensor networks," in *Modeling, Analysis and Simulation of Computer and Telecommunications Systems, 2002. MASCOTS 2002. Proceedings. 10th IEEE International Symposium on.* IEEE, 2002, pp. 129–136.

[159] T. Clouqueur, V. Phipatanasuphorn, P. Ramanathan, and K. K. Saluja, "Sensor deployment strategy for target detection," in *Proceedings of the 1st ACM international workshop on Wireless sensor networks and applications.* ACM, 2002, pp. 42–48.

[160] A. A. Abbasi and M. Younis, "A survey on clustering algorithms for wireless sensor networks," *Computer communications*, vol. 30, no. 14-15, pp. 2826–2841, 2007.

[161] R. Jain, D.-M. Chiu, and W. R. Hawe, *A quantitative measure of fairness and discrimination for resource allocation in shared computer system.* Eastern Research Laboratory, Digital Equipment Corporation Hudson, MA, 1984, vol. 38.